Mykhailo Moskalets

INTRODUCTION

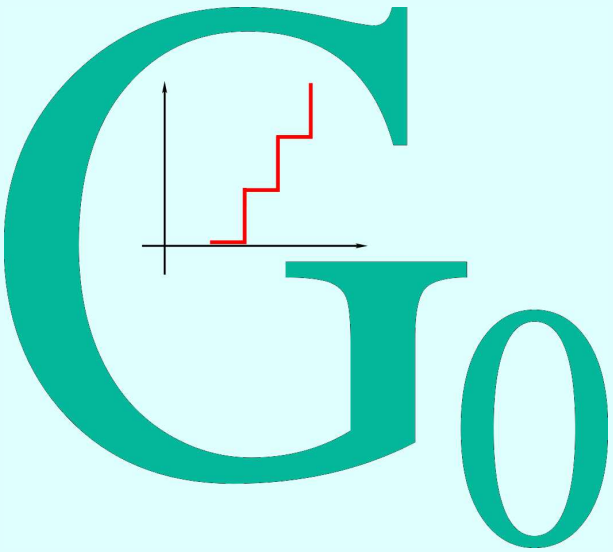

TO MESOSCOPICS

2025

Preface

Mesoscopic physics is one of those branches of modern condensed matter physics that are developing rapidly. The progress achieved in the last few decades in the manufacture of micron and sub-micron-sized samples has made it possible to discover a whole range of new physical effects that are absent in macroscopic samples and has made it possible to create solid-state devices whose operating principle is based on quantum laws.

These lecture notes contain the basics of the theory of mesoscopic systems. The presented theory allows us to describe the physics of the main phenomena and the conditions for their observation in such systems. A characteristic feature of a mesoscopic system is that its properties are determined by the behaviour of a single quantum particle. Therefore, preserving the phase coherence, spectrum quantization, and charge quantization are the components that determine the occurrence of mesoscopic effects.

The lecture notes are intended for students and postgraduates who are specializing in condensed matter physics, microelectronics, and nano physics. The knowledge of the basics of quantum mechanics and statistical physics is essential.

Contents

1. Intro

Mesoscopic physics, or mesoscopics for short, is a branch of condensed matter physics that studies the physical properties of small-sized samples at low temperatures.

Below, we will look in more detail at how small the samples should be and how low the temperature should be.

1.1. Subject of mesoscopics

Mesoscopics deals with samples whose size L is sufficiently small in one or more directions [1, 2], Fig. 1.1.

As we will see below, the characteristic length is the phase coherence length L_φ, the value of which can vary widely. At low temperatures, a rough estimate can be given as $L_\varphi \sim 10^{-6}$ m. If none of the dimensions of the sample exceeds this length $L \lesssim L_\varphi$, then such a sample is the subject of research in mesoscopics. The dimensions of a mesoscopic conducting sample are determined based on the ratio between the wavelength λ_F of an electron with the Fermi energy and the minimum size of the sample, Fig. 1.1. For a standard metal, $\lambda_F \sim 10^{-10}$ m. At the same time, for a two-dimensional electron gas of a GaAs/AlGaAs semiconductor heterostructure, this value is much larger and is $\lambda_F \sim 10^{-7}$ m.

Mesoscopics studies the same properties of samples as condensed matter physics: kinetic, magnetic, etc. However, it should be emphasized that the properties of mesoscopic and macroscopic samples are qualitatively different.

As an illustration of this difference, let us consider the flow of electric current through a sample, Fig. 1.2. It is well known that current is the directed motion of charged particles, for example, electrons. Due to collisions with defects, phonons, and other quasiparticles, the directed motion of electrons is destroyed. An electric field is necessary to maintain the current. Such a field can be created, for example, by means of a galvanic cell attached to the sample,

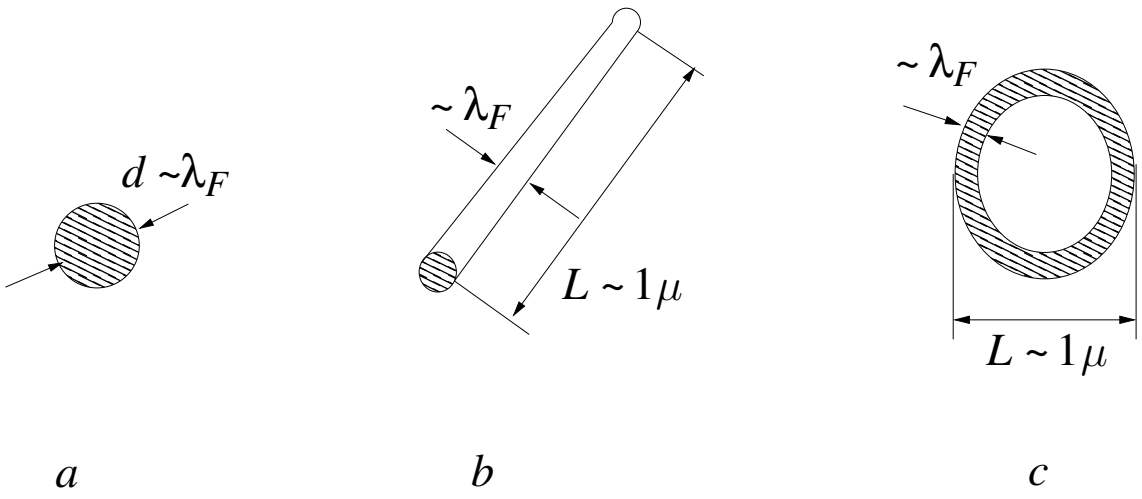

Fig. 1.1. Characteristic types of mesoscopic samples: single-connected – zero-dimensional (*a*), one-dimensional (*b*) and biconnected (*c*). λ_F – the wavelength of an electron with the Fermi energy. The characteristic length L is about one micron.

Fig. 1.2, *a*, or by means of an alternating magnetic flux $\Phi(t)$ (where t – time), that penetrates a closed circuit Fig. 1.2, *b*. Mesoscopic samples at low temperatures exhibit a qualitatively different property, namely, even a magnetic flux constant in time can induce a persistent current in the mesoscopic ring, Fig. 1.2, *c*.

Another example. The electrical conductance $G = I/V$ (here V is the applied voltage; I is the current) of a macroscopic resistor is proportional to the specific electrical conductivity σ and depends on the geometry of the sample. For a sample in the form of a parallelepiped with length L, width w, and thickness d, the electrical conductance when current flows along side L is:

$$G = \sigma \frac{dw}{L} . \tag{1.1}$$

Therefore, the dependence on the thickness d is linear, Fig. 1.3, *a*.

A mesoscopic resistor of the same shape exhibits a stepwise dependence of

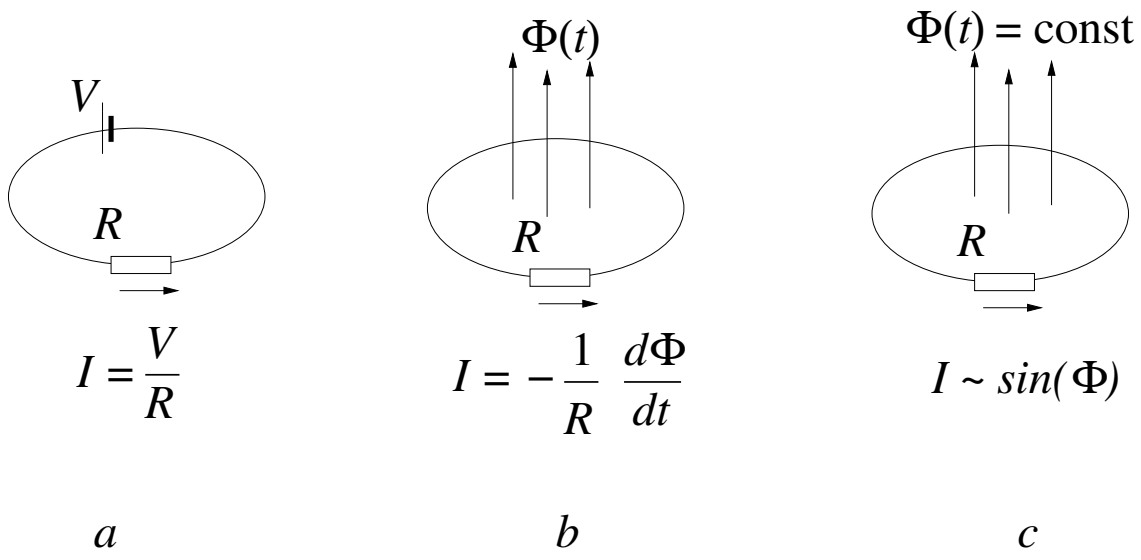

Fig. 1.2. Current I in a macroscopic ring with a battery (a) or with a time-varying magnetic flux $\Phi(t)$ (b). In a mesoscopic non-superconducting ring at low temperatures, a time-constant magnetic flux Φ = const can induce a persistent current (c)

electrical conductance on thickness, Fig. 1.3, *b*. Jump size is the following,

$$G_0 = \frac{2e^2}{h} \tag{1.2}$$

and it is called the conductance quantum $G_0 \approx (12,9 \times 10^3\,\Omega)^{-1}$. Here $e = -1,6 \times \times 10^{-19}$ C is the electron charge, $h = 6,6 \times 10^{-34}$ J·s is the Planck's constant.

Further, we will mainly focus on the electrical conductance of mesoscopic samples as the easiest to measure and most informative characteristic. The special interest in studying this characteristic is due to the fact that most of the properties of mesoscopic samples are determined by the characteristics of their electronic system. And the electrical conductance provides direct information about the electronic system of the sample. On the other hand, the study of electrical conductance also has great applied significance, since the rapid development of mesoscopics is caused by advances in the technology of manufacturing microscopic (and, one might say, nanoscopic) objects, which is due to the requirements of miniaturization in the manufacture of various types

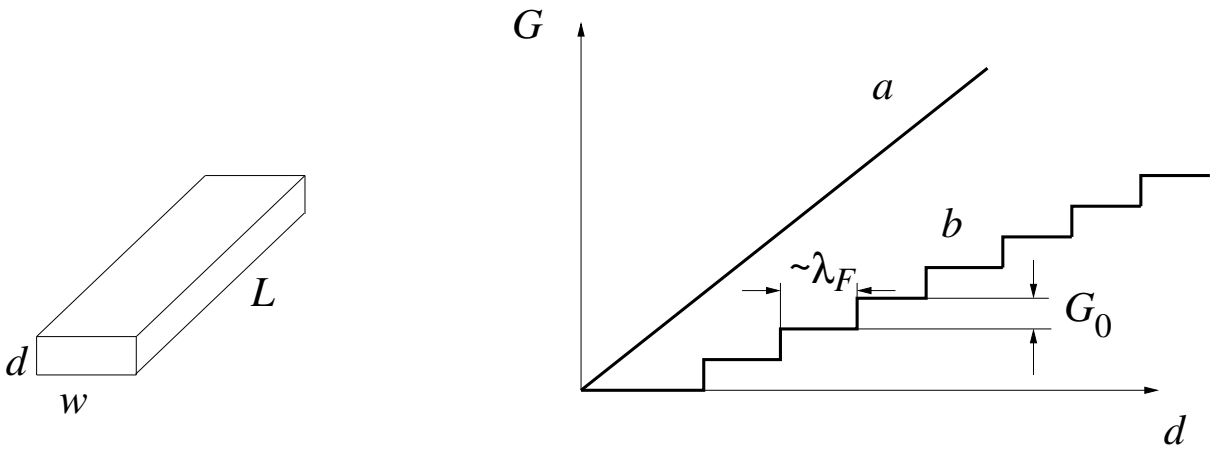

Fig. 1.3. Dependence of the conductance G on the thickness w for macroscopic (a) and mesoscopic (b) resistors

of electronic devices. This purely technical reason, in fact, led to the emergence of a new scientific direction - mesoscopics. We learned to make samples of very small sizes and manipulate such objects, for example, to bring electrical contacts to micron- and nano-sized samples. This, in turn, allowed us to apply well-developed methods of physical research used to study macroscopic samples of both artificially created objects and existing ones, for example, individual molecules and clusters. We can say that it is possible to measure the current-voltage characteristic of an individual molecule.

So, to summarize: Mesoscopics studies the macroscopic characteristics of microscopic objects.

1.2. Intermediate position of mesoscopics

The word “mesoscopics”, which was introduced into physical usage by van Kepman in 1976, [3], consists of two words: the Greek “mesos” – intermediate and the English “score” – sphere of action. Therefore, translated literally, we can say that mesoscopics studies phenomena that occupy an intermediate position. The name itself suggests comparing mesoscopic phenomena with other, already known and better studied phenomena. What is the main criterion that distinguishes mesoscopic phenomena from others?

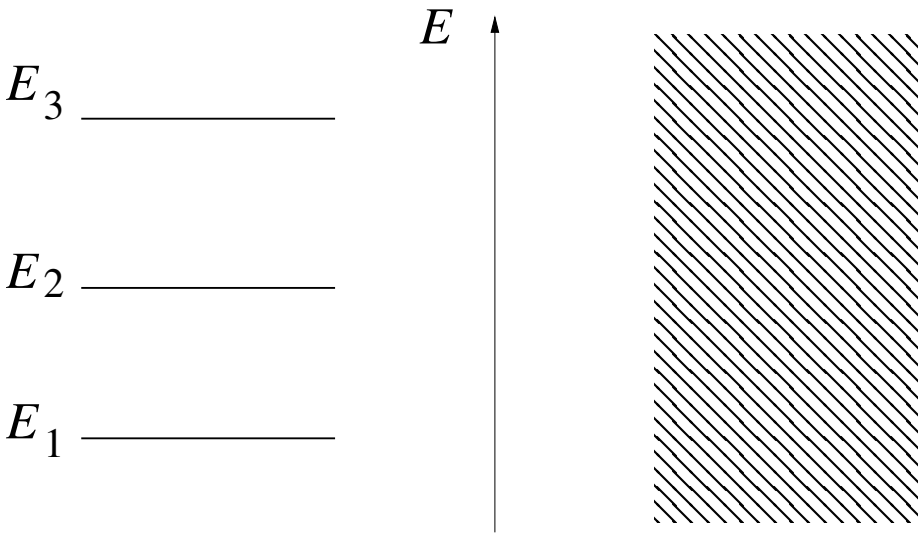

Fig. 1.4. Discrete (left part) and continuous (right part) spectra

The decisive, but far from the only, parameter is the size of the sample being studied, and therefore the number of particles that make up the sample. Therefore, we compare mesoscopics – the physics of intermediate dimensions – with microscopics – the physics of electrons and atoms and macroscopics – the physics of systems with a formally infinite number of particles.

Microscopic objects, for example, electrons in a hydrogen atom, are described by quantum mechanics. In quantum mechanics, the state of a particle is characterized by a wave function ψ, which is determined from the Schrödinger equation. In a hydrogen atom, an electron can only be in some fixed states ψ_N with a completely definite energy E_N. In this case, the electron spectrum is said to be discrete, Fig. 1.4, left part. Therefore, for the purposes of the comparison we are now making, we can assume that microscopic objects have (i) a characteristic size of about one angstrom, 10^{-10}m (the size of an atom), and (ii) a characteristic energy of about 1 eV or 10^4 K (the difference between the electron energy levels in an atom). Macroscopic bodies are characterized by (i) a large number of particles that compose them, i.e. atoms or molecules, and (ii) a continuous spectrum, for example, for electrons in a metal, Fig. 1.4, right part. It should be noted that condensed-state physics, unlike, for example, the

physics of continuous media, geophysics, or astrophysics, studies macroscopic bodies with a size of about 1 sm^3 and a number of particles close to Avogadro's number $N_A \sim 6 \times 10^{26}$ 1/kg-mol.

In addition to quantitative differences, fundamentally new characteristics also appear at the macroscopic level that are absent for microobjects. These are the so-called thermodynamic characteristics, for example, temperature, which characterizes the average energy per particle of a substance. The possibility of using a thermodynamic description is due to the fact that macroscopic bodies consist of a large number of particles.

The question naturally arises: if we remove one atom from a macroscopic body, when will the macroscopic description be replaced by the microscopic description? And how will the transition from one description to another occur? There is no final answer to this question. However, it is already well known that such a transition is not uniform, and the properties of matter on intermediate scales differ from both the properties of macrobodies and the properties of microparticles.

The above can be illustrated by the following example. Let us take several identically prepared macroscopic samples. It is assumed that their properties are the same. Let us consider, for example, two conductors and compare their electrical resistances R_1 and R_2. Strictly speaking, these two quantities will differ. However, this difference $\Delta R = R_1 - R_2$ will be small:

$$\frac{\Delta R}{R} \ll 1\,, \tag{1.3}$$

where $R = (R_1 + R_2)/2$. If the conductor sizes are small enough, the difference can reach 100 %:

$$\frac{\Delta R}{R} \sim 1\,. \tag{1.4}$$

In the second case, macrophysics no longer works, since conditions that cannot be controlled at the macroscopic level have become significant. Although both samples were manufactured under the same conditions, their measured parameters turned out to be different. For such samples, which are called mesoscopic, a change in the position of even one atom can lead to a change in the characteristics of the sample, for example, its resistance by 100%. We note

that sufficiently low temperatures are required to observe such "single-particle" effects. We will dwell on this below.

It should be emphasised that the samples we are considering are still far from the atomic scale: the number of particles in the sample is quite large. Thus, for a mesoscopic sample of about 10^{-7}m in size, the number of particles in it is about 10^8, which allows measuring contacts to be brought together to study the properties of such bodies. At the same time, the properties of mesoscopic samples are determined by the behaviour of a single microscopic particle and are therefore described by quantum laws. An important feature is that the particles that make up the mesoscopic sample interact strongly with the environment. Such interaction significantly, and sometimes decisively, affects the properties of the particles. Yes, the electron spectrum in mesoscopic samples can be discrete, but the position and width of the energy levels are very sensitive to the influence of the environment.

We note that quantum laws are manifested at the macroscopic level in many already known and not at all mesoscopic phenomena, such as superconductivity. Electrons in a metal are also a quantum system that obeys Fermi–Dirac statistics. However, in mesoscopics, and this should be emphasised, the quantum behaviour of a single micro particle is manifested at the macroscopic level. Such phenomena as interference, spectrum quantization, charge quantization, etc. are significant.

This is on the one hand. On the other hand, no other laws, except those known from quantum and classical physics, operate in mesoscopic systems.

Let us summarise the above.

Mesoscopic are macroscopic bodies whose properties are determined by the behaviour of a single microscopic particle.

Table 1.1 gives the values of some physical quantities that illustrate the difference between macro-, meso-, and micro bodies. ΔE is the distance between discrete energy levels.

It should be noted that, in fact, physics has been dealing with micron-sized particles for a long time. For example, when studying finely dispersed media or island films. However, if we consider one separately taken micron-sized sample (for example, a granule or an island), then this will be the subject of mesoscopics. From this it is clear that it is impossible to strictly delimit

Table 1.1

Particle	Size	Quantity	Temperature	Spectrum
Macro-	1 sm	10^{23}	300 K	continuous
Meso-	$< 1\,\mu$ m	$10^6 \div 10^9$	$< 0{,}1$ K	discrete, $\Delta E \sim 1\,K$
Micro-	1 Å	1	–	discrete, $\Delta E \sim 10^4\,K$

mesoscopics and other areas of solid-state physics that study the properties of small-sized samples.

The development of the technology for manufacturing solid-state low - dimensional systems (in particular, one-dimensional (1D), two-dimensional (2D) systems created by the electron-beam lithography method) has led to the emergence of a number of unique artificially created mesoscopic objects, Fig. 1.1: 0D – quantum dots, 1D – quantum wires, 2D – structures with non-trivial topology (rings), and the like.

On the one hand, it is necessary to understand the properties of such objects, and this is important from a practical point of view for the development of microelectronics and the creation of new microelectronic devices based on such systems.

On the other hand, using specially designed objects, it is possible to simulate situations when certain quantum mechanical laws are most clearly manifested.

For example, samples in the form of rings are most naturally suitable for studying the phenomenon of interference. In this case, mesoscopic objects are used to study the quantum laws themselves, and all this occurs on a completely macroscopic scale. This is significantly different from the situation with an electron, which certainly obeys quantum laws, but which cannot be “touched with hands.”

Thus, mesoscopics is not limited to solving purely applied problems, but also deals with the study of fundamental problems of physics, in particular, quantum physics.

Below we will try to understand why exactly such parameters characterising mesoscopics are given in Table 1.1, and what kind of phenomena are inherent in mesoscopic bodies. Now we will consider a simple example that illustrates the transition from macroscopic to mesoscopic bodies.

1.3. Example: from macro resistor to meso resistor

We will focus on two aspects. First, why it is possible to measure such a macroscopic characteristic as electrical conductance in a mesoscopic sample. And, second, what new features does this characteristic of a mesoscopic sample have in comparison with the analogous characteristic of a macroscopic sample.

Let us take a homogeneous conductor, Fig. 1.5, a. Let us connect a battery with a voltage V to it and measure the flowing current I. The current along the sample will be homogeneous and the magnitude of the current I= V/R is determined by the total resistance R of the sample:

$$R = \rho \frac{L}{S}, \tag{1.5}$$

where L is the length of the sample; S is the cross-sectional area; ρ is the specific electrical resistivity.

Let us separate the middle part of the sample and gradually reduce its size in this part, removing the substance. What will happen? For convenience, let us assume that all three parts, the reduced middle part and the side parts are unchanged, as before, having a rectangular shape, Fig. 1.5, b. However, the cross-section of the middle part has become much smaller. Let us compare the supports of different parts of the sample. We assume that the sizes of each part in all three directions are approximately the same: $S \ L^2$. Let us denote the supports of the left, right and middle parts by R_1, R_2 and R_3, respectively:

$$\begin{aligned} R_1 &= R_2 = \rho \frac{L_1}{S_1} \sim \rho \frac{1}{L_1}, \\ R_3 &= \rho \frac{L_3}{S_3} \sim \rho \frac{1}{L_3}. \end{aligned} \tag{1.6}$$

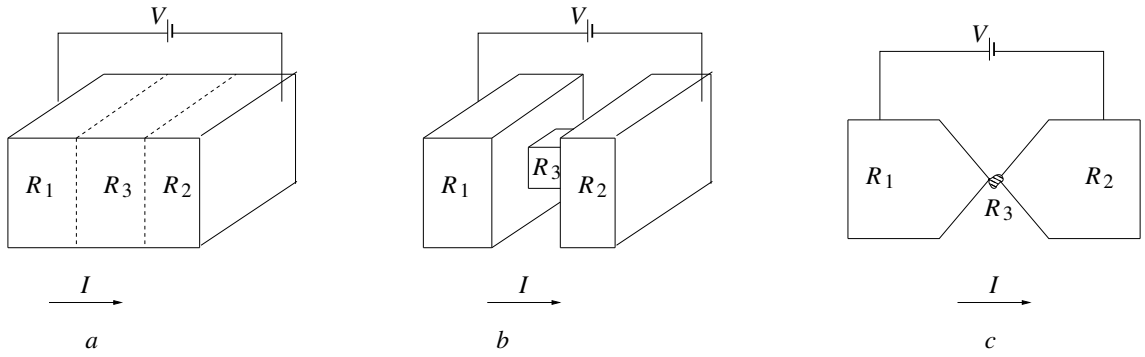

Fig. 1.5. Macroscopic conductor with uniform (a) and non-uniform (b) cross-section along its length. Mesoscopic conductor and macroscopic electrical contacts attached to it (c)

Since $L_3 \ll L_1$, then $R_3 \gg R_1$. Thus, we have obtained an obvious fact: the resistance of the entire sample is determined by the resistance of its narrowest part:

$$R = R_1 + R_2 + R_3 \approx R_3 \,. \tag{1.7}$$

And this relationship is maintained all the better, the narrower the middle part. There is nothing from mesoscopics here yet, but it is already clear that at a given voltage the current in the circuit is determined by the throughput of its narrowest part. Further, this narrow part will "transform" into the mesoscopic sample under study, and R_1 and R_2 will represent the resistances of the macroscopic electrical contacts, through which the current is supplied to the mesoscopic sample, Fig. 1.5, c. In other words, the current in the circuit is determined by the physical processes occurring in the sample under study, and does not depend on the connected contacts. The same conclusion is drawn from considering how the voltage is distributed.

$$V \;=\; V_1 \;+\; V_2 \;+\; V_3$$

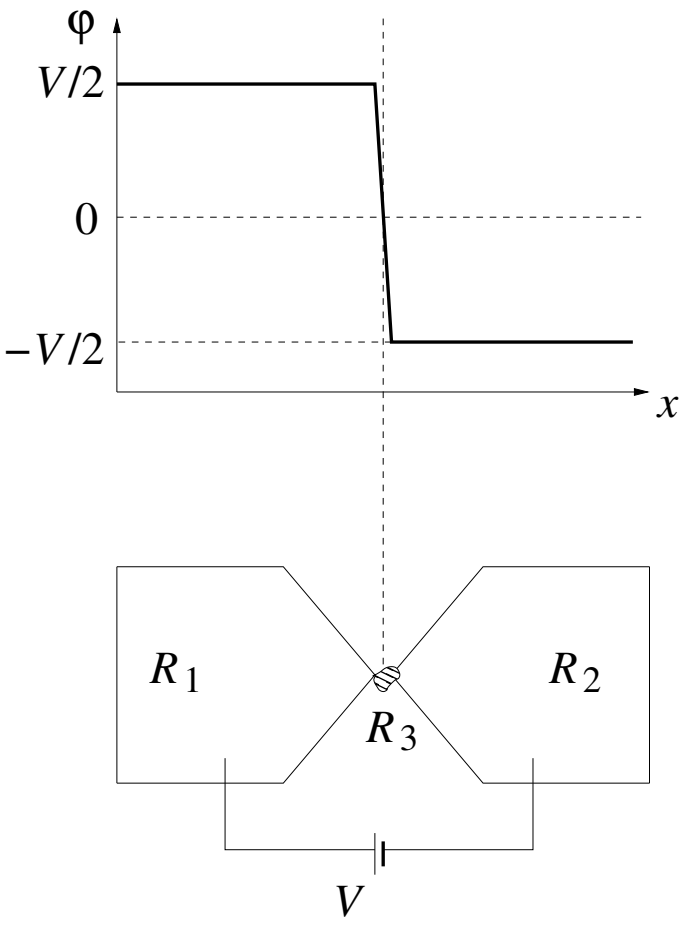

Fig. 1.6. Distribution of the electric potential φ along the length of a sample with a non-uniform cross-section

in a circuit with a non-uniform cross-sectional sample, Fig.. 1.6.. The current in each part (I1, I2 and I3, respectively) must be the same. This follows from the law of conservation of charge and the fact that charge does not accumulate inside the sample:

$$I_1 = I_2 = I_3 \equiv I\,, \qquad (1.8)$$

$$V_1 = R_1\, I, \quad V_2 = R_2\, I, \quad V_3 = R_3\, I\,.$$

Because

$$R_3 \gg R_1, R_2\,,$$

then the stress in the middle part is much higher than the stress in the massive parts. Therefore, all the stress in the circuit is applied to the narrow part of the sample:

$$V = V_1 + V_2 + V_3 \approx V_3\,. \tag{1.9}$$

Based on the obvious fact that the current in the circuit is determined by the resistance of the small-sized sample under study, we can use electrical measurements to study mesoscopic samples. The measured current I contains direct information about what is happening inside the sample under study, and not in the supply wires. By changing the voltage in the circuit, we directly change the voltage on the sample under study, since the voltage drop on the supply wires is negligibly small. Due to this, we can inject electrons with a fixed maximum excess energy, which is equal to $E_{max} = eV$, into the sample under study. When electrons collide with phonons and other quasiparticles, they lose this energy, which affects the resistance of the sample. Therefore, studying the R(V) dependence allows us, in particular, to study the interaction of electrons with other quasiparticles [4]. In this case, the voltage in the circuit plays the role of a kind of "energy probe", with the help of which it is possible to study a given sample [5].

It should be emphasised that the measurement of the current I and the application of the voltage V occurs far from the sample that we are studying. All this occurs on a macroscopic scale, and the instruments used are macroscopic: conventional ammeters and voltmeters. At the same time, a mesoscopic sample is studied, for example, an individual granule, or even a microscopic one - a separate molecule. Of course, in this case we must somehow ensure the electrical closure of the circuit, that is, bring the electrical contacts to the sample under study. The latter has become possible thanks to the achievements of modern technology.

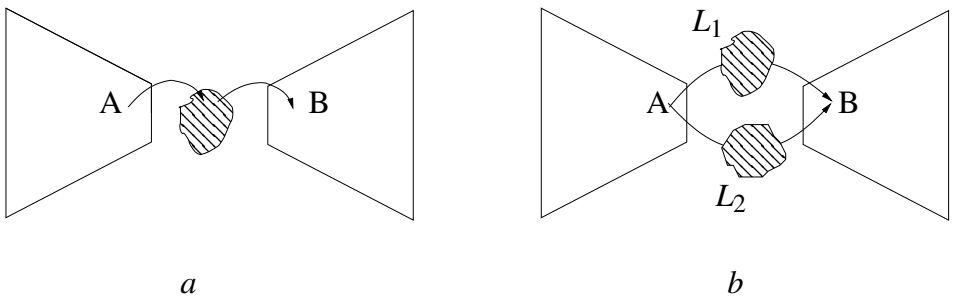

a *b*

Fig. 1.7. Mesoscopic system with one (a) or two L_1 and L_2 alternative paths for current flow (b)

So, we have considered what exactly is preserved in this example from the macro world. Now let us analyse how the micro world manifests itself. Let us consider the situation when two macroscopic parts are connected by means of a mesoscopic sample – a granule, Fig. 1.7, a. In this case, the flow of current will be determined by the processes of electron transition from the left electrode to the granule and then, from the granule to the right electrode, or in the opposite direction. What is unusual here is that the electron obeys quantum laws (exhibits wave properties) and they will determine the measured resistance. The most vivid wave properties of the electron are manifested in the case when we have not one intermediate granule, but two or more. In this case, there are several paths along which the electron can pass from the left electrode to the right one, Fig. 1.7, b.

First, let us consider what would happen if instead of the mesoscopic conductor there were macroscopic conductors. Let R_a and R_b be the resistances of these conductors, Fig. 1.8. In this case, the current I(macro) in the circuit equals the sum of the currents flowing through each of the conductors:

$$I^{(macro)} = I_a + I_b\,. \tag{1.10}$$

Neglecting the electrode resistances, we obtain that the voltage is applied only to the conductor, and we can write $I_a = V/R_a, I_b = V/R_b$. Therefore:

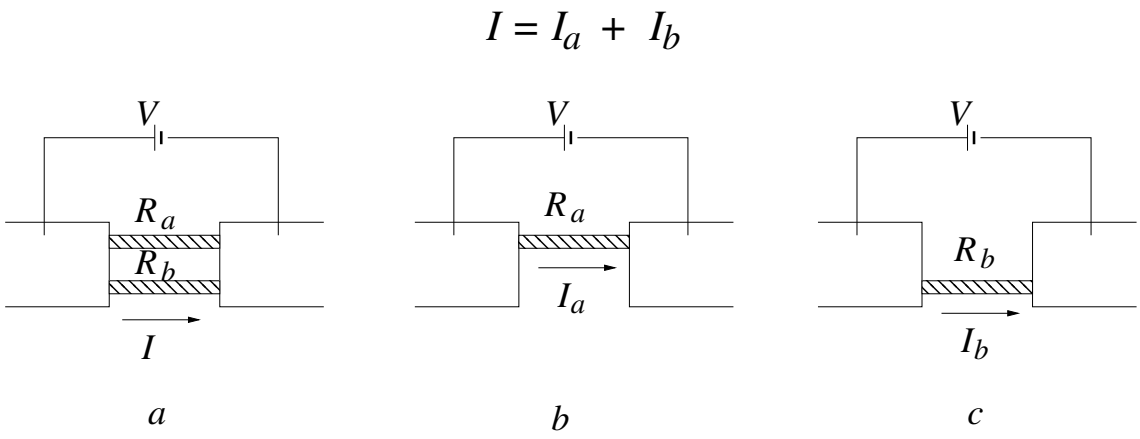

Fig. 1.8. The current $I = I^{(macro)}$, flowing through two parallel-connected macroscopic conductors R_a and R_b (a), equals the sum of the currents I_a and I_b that would flow in the same system in the absence of either conductor R_b (b) or conductor R_a (c).

$$I^{(macro)} = \frac{V}{R_a} + \frac{V}{R_b}\,. \tag{1.11}$$

Note that each term on the right-hand side is the current that would flow through a system containing only one (either a or b) conductor. In terms of the total resistance R= V/I, we obtain:

$$\frac{1}{R} = \frac{1}{R_a} + \frac{1}{R_b}\,. \tag{1.12}$$

The reciprocal of resistance is called conductance and is denoted $G = 1/R$. Thus, we have obtained the well-known fact from electrical engineering that the conductance of resistors connected in parallel equals the sum of their conductances:

$$G = G_a + G_b. \tag{1.13}$$

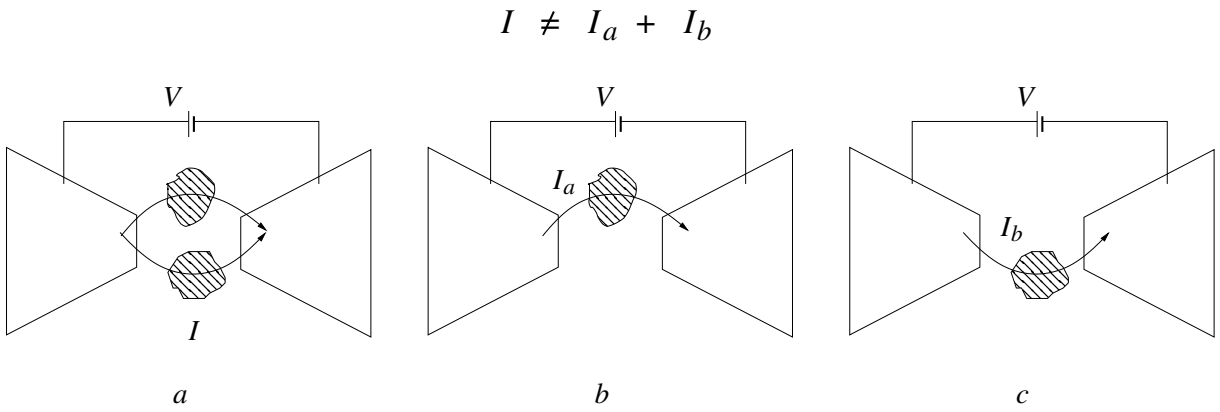

Fig. 1.9. The current $I = I^{(meso)}$, flowing through two parallel-connected granules (a), does not equal the sum of the currents I_a and I_b that would flow in the same system in the absence of either one (b) or the other (c) granule

However, for a mesoscopic conductor, the above relations for currents and conductance will not hold, Fig. 1.9. The current $I^{(meso)}$ in a circuit with two conductors, Fig. 1.9, a, does not equal the sum of the currents Ia and Ib that would flow in the same circuit if conduction were carried out either through one, Fig. 1.9, b, or through the second, Fig. 1.9, c conductor:

$$I^{(meso)} \neq I_a + I_b \,. \tag{1.14}$$

Why is the equality for currents, which is valid in the macroscopic case, violated? This occurs due to the phenomenon of interference, which leads to the fact that the probability of a quantum particle's transition from point A to point B, in the presence of several transition paths, does not equal the sum of the transition probabilities along each of the paths separately. Therefore, the above inequality for currents, written in terms of conductance:

$$G \neq G_a + G_b \,, \tag{1.15}$$

simply expresses the well-known fact that probabilities in quantum mechanics do not add up. In quantum mechanics, complex-valued transition amplitudes add up. The transition probability, which determines the conductance of a given

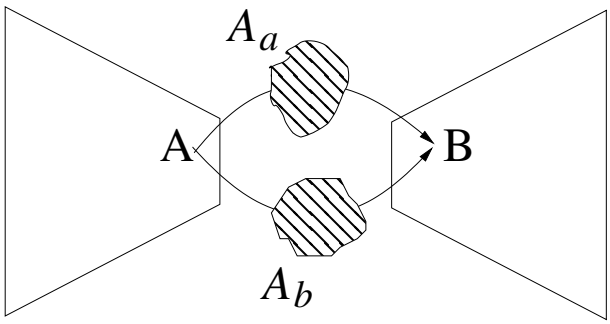

Fig. 1.10. An electron from point A to point B can pass through either one or the other granule

system, i.e., the real-valued quantity that can be measured in an experiment, is defined as the square of the amplitude.

Let us introduce the amplitudes Aa and Ab corresponding to the transitions through each of the granules, Fig. 1.10. The total amplitude of the transition A from point A to point B is:

$$\mathcal{A} = \mathcal{A}_a + \mathcal{A}_b \,. \tag{1.16}$$

Accordingly, the conductance is defined by the following equation:

$$\begin{gathered} G = g|\mathcal{A}|^2 = g|\mathcal{A}_a|^2 + g|\mathcal{A}_b|^2 + 2gRe[\mathcal{A}_a\mathcal{A}_b^*] \,, \\ G_a = g|\mathcal{A}_a|^2 \,, \quad G_b = g|\mathcal{A}_b|^2 \,, \quad G_{int} = 2gRe[\mathcal{A}_a\mathcal{A}_b^*] \,, \end{gathered} \tag{1.17}$$

where g is the coefficient of proportionality. Thus, we can write:

$$G = G_a + G_b + G_{int} \,. \tag{1.18}$$

From the above equation it is clear that there is an interference contribution G_{int} to the measured quantity. Thus, the macroscopic measured quantity, i.e., the conductance, is determined by the quantum interference effect. If the interference contribution turns out to be insignificant, $G_{int} \approx 0$, then we return to the macroscopic situation, when the parallel-connected conductivities are

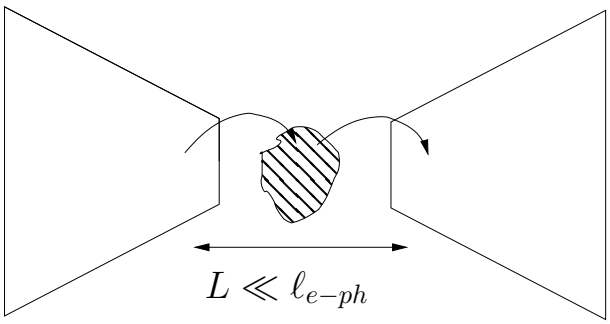

Fig. 1.11. An electron passes through a mesoscopic sample, remaining in a phase-coherent state, if the sample size L does not exceed the length over which the electron experiences inelastic collisions, for example, the electron-phonon length ℓ_{e-ph}

added. When do quantum effects begin to appear? This requires sufficiently low temperatures and sufficiently small dimensions, because the interference phenomenon will be significant only in the case when an electron passing through the system is described by a wave function with a well-defined phase. The phase-coherent state is destroyed when an electron interacts with other quasiparticles in a solid, for example, with vibrations of the crystal lattice - phonons, Fig. 1.11. When the temperature decreases, the number of phonons decreases and, accordingly, the probability of collision of electrons with them decreases. At the same time, the length of the electron path over which it retains phase coherence increases. If the sample size does not exceed this length, quantum effects will be evident.

Self-test questions

1. What does mesoscopics study?
2. What samples are considered mesoscopic?
3. What is special about the current flowing through a mesoscopic sample?
4. Is Ohm's law valid for mesoscopic samples?

5. Under what conditions does the phenomenon of interference affect electrical conductance?

2. Mesoscopic system and environment

One of the essential questions is what exactly and how determines the external conditions in which a mesoscopic sample is located.

2.1. Sample and measuring device

To study the properties of a mesoscopic sample (hereinafter referred to as a "mesoscopic system" (MS) or simply a "system"), it is necessary to connect it in one way or another with one or more macroscopic systems. For example, when measuring electrical properties, electrical contacts are such macroscopic systems, Fig. 2.1.

This problem is completely analogous to the problem of the "classical observer" in quantum mechanics. In order to obtain any information about a quantum system, it is necessary for the quantum system to interact with a classical system, which is a measuring device. However, such interaction significantly changes the state of the quantum system.

What is the peculiarity of such a situation in mesoscopics compared to microscopic systems? The peculiarity is that the MS is constantly connected to one or more macroscopic systems that play the role of an external environment for the sample under study. The macroscopic systems to which the sample is attached are much larger than the system under study. In mesoscopics, it is customary to call these macroscopic systems "reservoirs" or "contacts". These reservoirs serve as a source and/or sink of particles and energy. The reservoirs are considered so large that the exchange of energy and/or particles with the mesoscopic system does not affect their state: in any situation, the electronic systems in the reservoirs remain in an equilibrium state, characterized by a certain value of the temperature T and the chemical potential μ. In particular, the electrons in the contacts are described by the Fermi distribution function, Fig. 2.2:

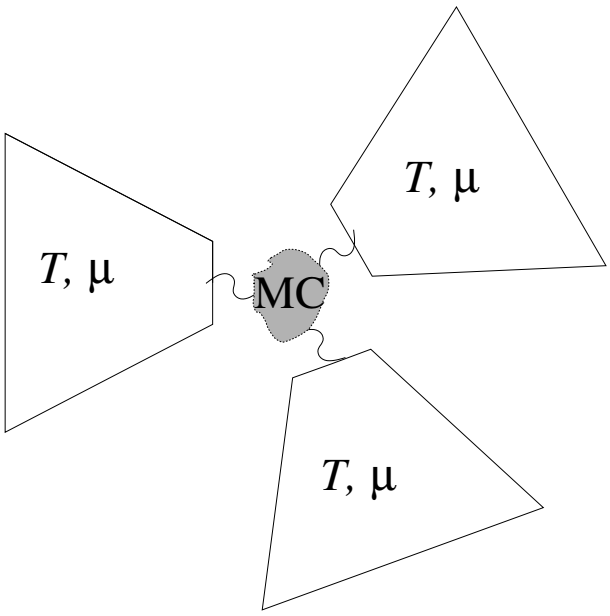

Fig. 2.1. MC is always connected to the environment. Three massive conductors are shown, having temperature T and electrochemical potential μ. These conductors play the role of electron reservoirs. The wavy lines conventionally indicate that MC can exchange energy and electrons with the reservoirs

$$f_0(\epsilon_p) = \frac{1}{1 + \exp\left(\dfrac{\epsilon_p - \mu}{k_B T}\right)}, \tag{2.1}$$

where $\epsilon_p = p^2/(2m_e)$ kinetic energy of an electron; p an electron momentum; $m_e = 9,08 \times 10^{-31}$ kg the mass of an electron; $k_B = 1,38 \times 10^{-23}$ J/K is the Boltzmann constant. The distribution function $f_0(\epsilon_p)$ shows the probability that a state with energy ϵ_p will be occupied by an electron. At zero temperature T = 0, all states with energy less than μ are occupied, $f_0 = 1$, and all states with energy greater than μ are empty, $f_0 = 0$, so the chemical potential μ is the maximum energy that an electron can have at zero temperature. This energy is called the Fermi energy.

In an equilibrium situation, when all the contacts have the same temperature T and the chemical potential μ, there is no electric current or heat flow

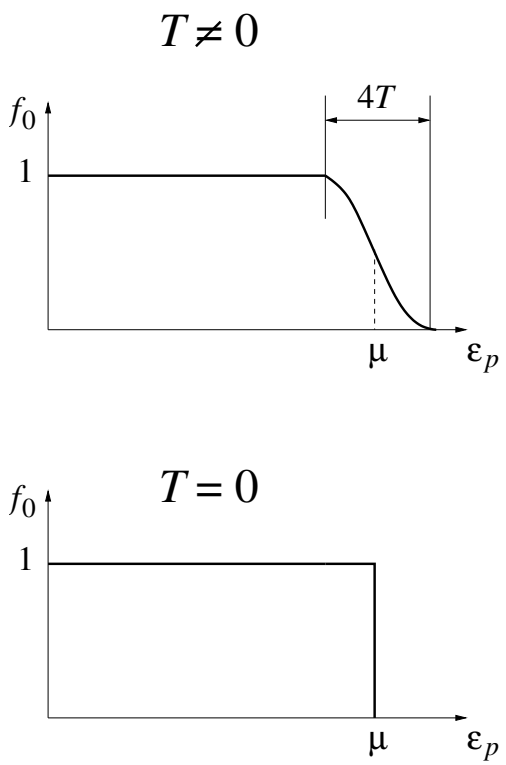

Fig. 2.2. Fermi distribution function f_0 for electrons with temperature T and chemical potential μ. ϵ_p is the kinetic energy of the electron

in the system, and the mesoscopic sample has the same temperature and the chemical potential as the contacts:

$$T_C = T\,, \quad \mu_C = \mu\,. \tag{2.2}$$

In this case, the influence of the edges is that in the mesoscopic sample, only those levels will be filled whose energy does not exceed the chemical potential μ, Fig. 2.3. Such filling is a consequence of the general physical principle according to which a closed system, in our case the reservoirs plus the MC, tends to transition to a state with a minimum total energy. Therefore, in an equilibrium situation, the distribution function for electrons in the MC is a Fermi distribution function with a temperature and a chemical potential equal

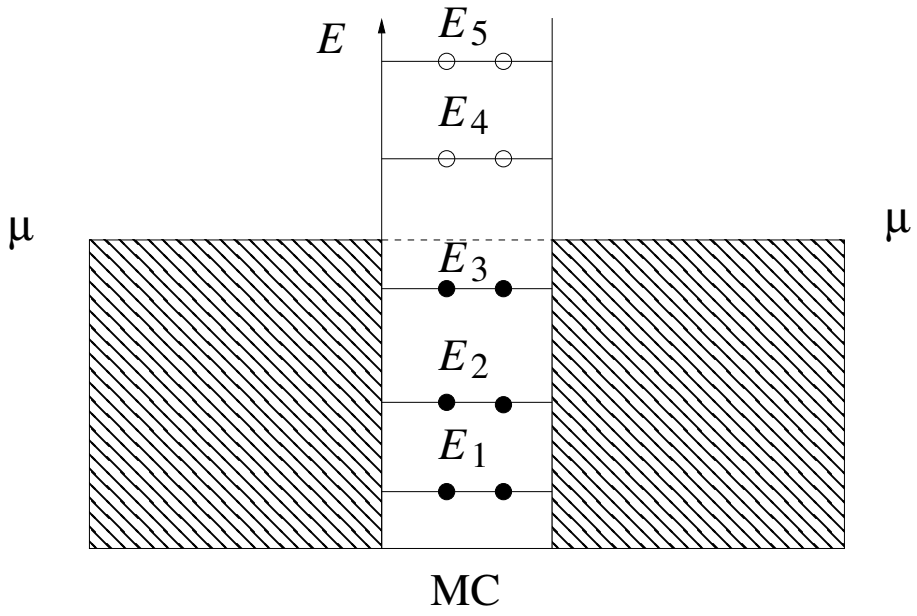

Fig. 2.3. Filling of energy levels in MC connected to reservoirs. The temperature is assumed to be zero. μ is the chemical potential of electrons in the reservoirs. Levels E_1, E_2 and E_3 are filled (black circles), and levels E_4 and E_5 are free (light circles). The double degeneracy of energy levels is due to the presence of electron spin

to the temperature and chemical potential of the edges.

If a potential difference $\Delta\varphi = \varphi_1 - \varphi_2$ is applied to the edges, then the electrochemical potentials of electrons in edges μ_1 and μ_2 are different:

$$\begin{gathered} \mu_1 \neq \mu_2 \,, \\ \mu_1 = \mu + e\varphi_1, \qquad \mu_2 = \mu + e\varphi_2 \,. \end{gathered} \tag{2.3}$$

The consequence of this is the current flowing through the sample, Fig. 2.4. In this case, the distribution function in the MS is not equilibrium and, as a rule, the chemical potential of the mesoscopic sample is not determined. A similar

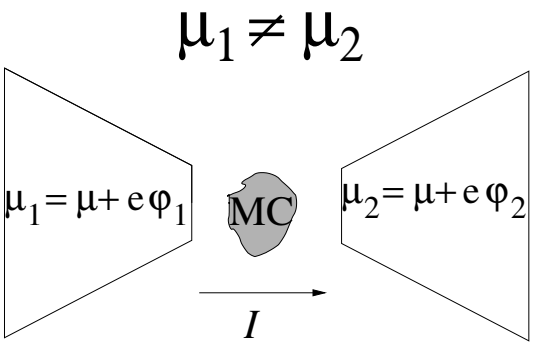

Fig. 2.4. If the electrochemical potentials μ_1 and μ_2 of the contacts are different, then a current I will flow through the sample. φ_1, φ_2 are the electric potentials applied to the left and right contacts, respectively

situation occurs when the temperatures of the edges are different and a heat flux flows through the sample. In this case, the temperature of the electrons in the mesoscopic sample is not determined. Despite the fact that in the current state the mesoscopic system is highly non-equilibrium, the contacts are in equilibrium even in this case. In particular, this follows from the fact that the entire voltage is applied to the MS. The left contact has a potential of φ_1, and the right contact has a potential of φ_2. However, if the contacts are connected to each other, a current will flow (Fig. 2.5). The non-equilibrium is concentrated in a very small region, namely, within the studied mesoscopic sample, where the potential changes from φ_1 to φ_2. Since the charge is conserved, the same current flows through the sample and through the contacts. However, the current density, which characterizes the degree of non-equilibrium, in the sample is much higher than the current density in the contacts due to the significant difference in geometric dimensions. The electron nonequilibrium of a mesoscopic sample is clearly visible when considering the energy distribution function. In contacts, this is the equilibrium, Fermi distribution function corresponding to a given

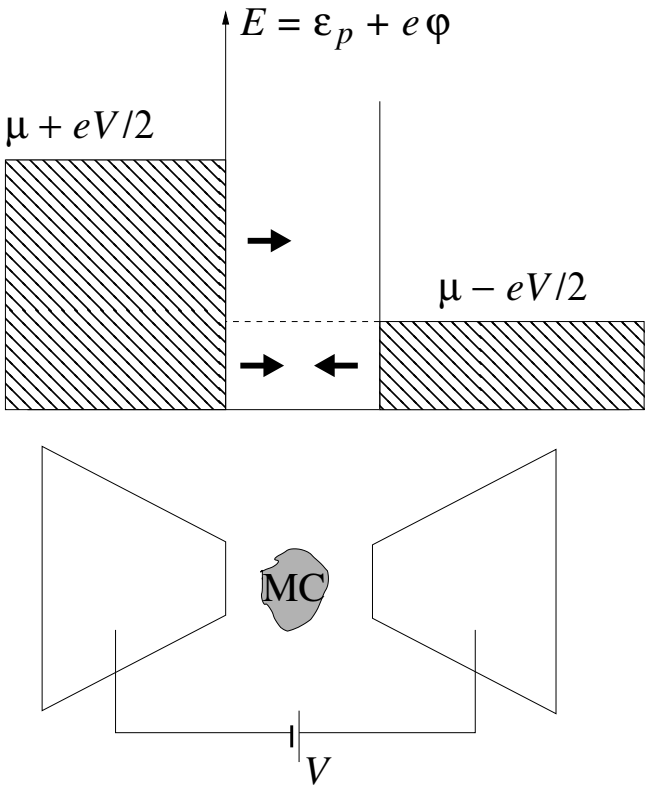

Fig. 2.5. Filling of energy levels when a potential difference V is applied to the edges. The arrows show the direction of electron motion.

electrochemical potential:

$$f_i(E) \equiv f_0(E-\varphi_i) = \frac{1}{1+\exp\left(\dfrac{E-\mu(\varphi_i)}{k_BT}\right)}\,, \qquad \mu(\varphi_i) = \mu + e\varphi_i\,, \qquad i = 1,2\,. \tag{2.4}$$

Here i = 1 corresponds to the left, and i = 2 to the right contacts. $E = \epsilon_p + e\varphi_i$ is the total energy of the electron, which includes both the kinetic ϵ_p and the potential $e\varphi$ energies. Note that in our case, with a non-uniform potential distribution $\varphi(\vec{r})$, it is more convenient to consider the total energy E

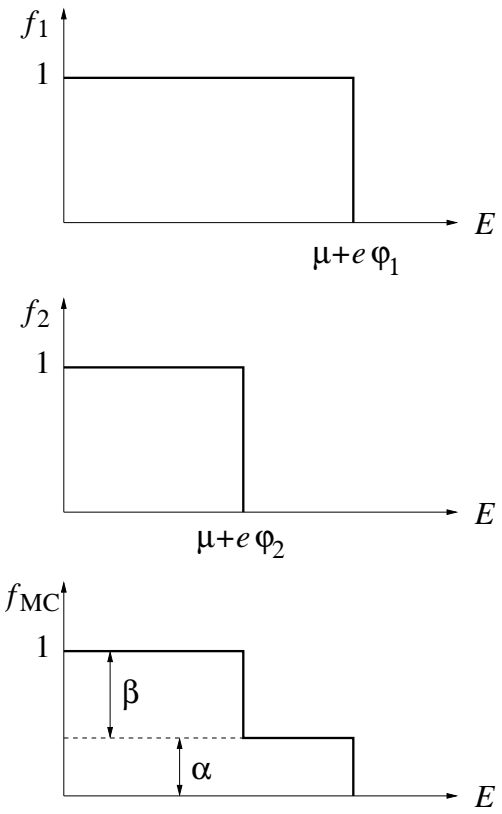

Fig. 2.6. Distribution function for electrons of the left f_1 and right f_2 reservoirs, which have different electric potentials $\varphi_1 \neq \varphi_2$. Distribution function for electrons of the MC f_{MC} in the absence of inelastic relaxation. α (β) is the probability that the electron came to the MC from the left (right) reservoir. The temperature is assumed to be zero

rather than the kinetic ϵ_p as the independent variable. In the sample, the non-equilibrium distribution function f_{MC} is expressed in terms of the functions f_i as follows, Fig. 2.6:

$$f_{\mathrm{MC}}(E) = \alpha f_1(E) + \beta f_2(E)\,, \qquad \alpha + \beta = 1\,, \tag{2.5}$$

where α (β) is the probability that an electron entered the sample from the left

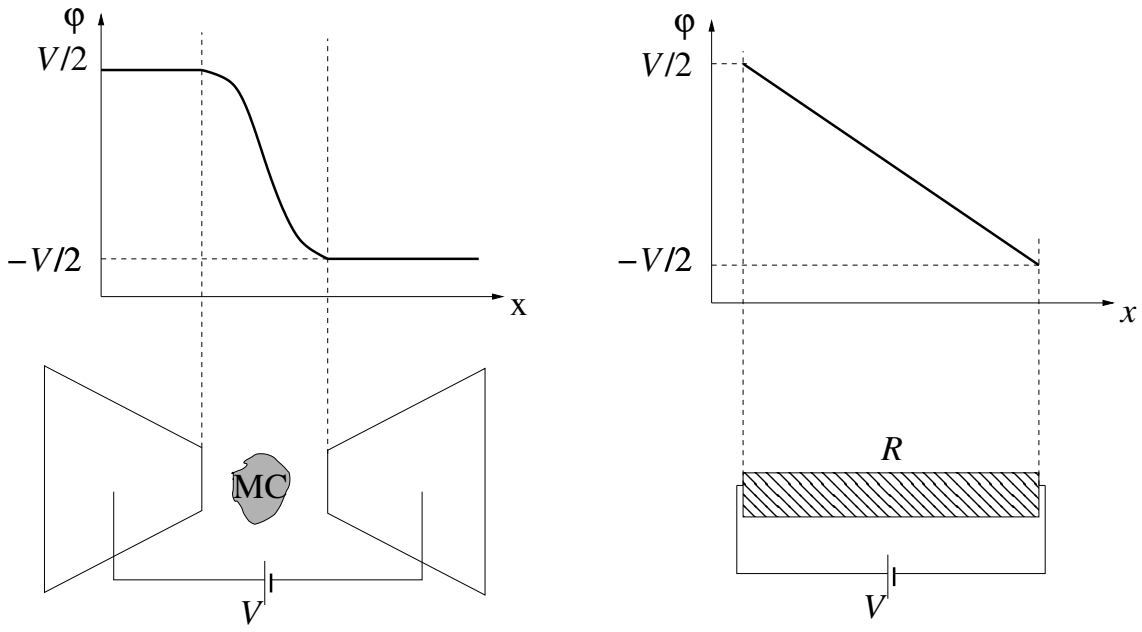

Fig. 2.7. Change in electrostatic potential when current flows through MC (left part) and through a macroscopic resistor (right part)

(right) contact. From Fig. 2.6 it is clear that f_{MC} is not a Fermi distribution function. This type of distribution function is due to the absence of inelastic processes. As a result, an electron, when moving from one contact through MC to the other contact, conserves the total energy E. The considered current state differs significantly from the current state in a macroscopic sample. In a mesoscopic sample, the current state is strongly non-equilibrium, but this non-equilibrium is concentrated in a small region of space - within the mesoscopic system. In a macroscopic resistor, the current state is characterized by a much smaller non-equilibrium due to the lower current density, which, however, captures macroscopic regions. The non-equilibrium is present where there is a change in the electrostatic potential. This is illustrated in Fig. 2.7, where the change in the electrostatic potential is schematically shown: jump-like – when current flows through a mesoscopic system (left part) and continuous – when current flows through a macroscopic resistor (right part).

Summarising the above, we can say that the reservoirs set the external con-

ditions in which the mesoscopic sample is located. The macroscopic contacts, remaining in equilibrium, inject into the mesoscopic sample a flow of particles with a fixed, equilibrium energy distribution for a given contact. In this case, we speak of the flow of current under given external conditions, i.e., at given potentials and temperatures of the contacts that are in equilibrium.

2.2. Fluctuations of thermodynamic quantities

A mesoscopic system can be considered as a subsystem of a large closed system that includes a given mesoscopic sample and its edges. It is well known that the physical quantities that characterize the subsystem fluctuate. The reason for this is the exchange of energy and particles with the environment. Let us recall that the term "fluctuation" of a certain physical quantity is understood as a spontaneous, chaotic change in time of the value of this quantity. Such a change is caused both by the chaotic motion of the particles that make up the sample and by the interaction with chaotically moving particles of the environment. It should be said that the concept of fluctuation provides the key to understanding why, when the size of bodies decreases, their properties change qualitatively long before microscopic scales are reached.

2.2.1. Fluctuations in the number of electrons

Let us consider fluctuations in the number of electrons in a small conductor connected to a macroscopic reservoir. Electrons can pass from the conductor to the reservoir and back, as a result of which the number of particles N in the sample fluctuates with time, Fig. 2.8.

To characterize the deviation of the number of particles N (t) in the sample from its mean value $\bar{N}$, the mean square of the fluctuations of the number of particles $\langle \delta N^2 \rangle$ is introduced, which is defined by the following equation:

$$\langle \delta N^2 \rangle = \lim_{\Delta t \to \infty} \frac{1}{\Delta t} \int_0^{\Delta t} dt [N(t) - \bar{N}]^2 \,. \tag{2.6}$$

For a small, but still macroscopic sample, the mean square of the fluctua-

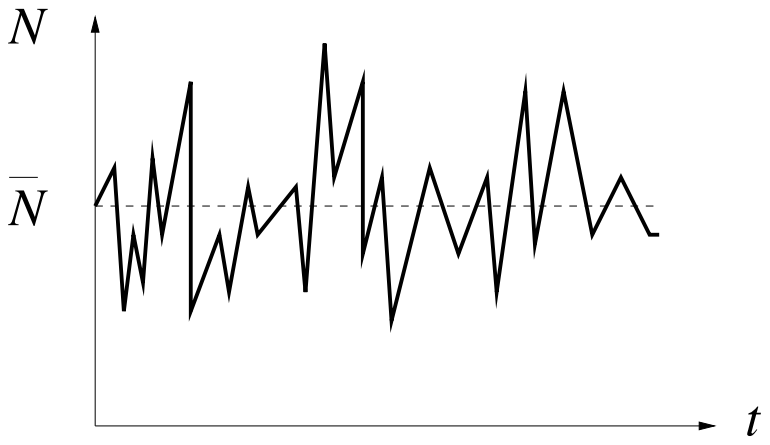

Fig. 2.8. Fluctuations of the number of particles N in the MS connected to the reservoir: t – time; $\bar{N}$ - the average number of particles in the sample

tions can be expressed in terms of $\bar{N}$ and the value of the chemical potential μ of the sample, which coincides with the chemical potential of the reservoir, as follows (see [6]):

$$\langle \delta N^2 \rangle = k_B T \left(\frac{\partial \bar{N}}{\partial \mu} \right)_T . \tag{2.7}$$

The dependence of the number of electrons $\bar{N}$ on the chemical potential μ for a three-dimensional system with a continuous spectrum:

$$\bar{N} = \frac{(2m_e\mu)^{3/2}}{3\pi^2\hbar^3} V , \tag{2.8}$$

where $\hbar = h/(2\pi)$; V - volume of the sample. Assuming the Fermi energy $\mu \sim 10^4\ K$ measuring the temperature in degrees, and the radius R in angstroms (Å), we obtain the following estimate for the fluctuations of the number of particles in a sample in the form of a sphere with radius R:

$$\langle \delta N^2 \rangle \sim 3 \times 10^{-7}\ T R^3 . \tag{2.9}$$

In a typical macroscopic situation, fluctuations are small compared to the average number of particles, but large compared to unity:

$$1 \ll \sqrt{\langle \delta N^2 \rangle} \ll N \,. \tag{2.10}$$

The right inequality allows us to speak about a well-defined number of particles in the sample, and the left inequality allows us to neglect the discrete nature of the charge.

In mesoscopic samples, the right inequality is not violated, which allows us to consider them as macroscopic bodies. However, the left inequality is violated:

$$1 \sim \sqrt{\langle \delta N^2 \rangle} \ll N \,. \tag{2.11}$$

Fluctuations in the number of particles cannot be less than one; a particle either left the sample or it did not. Therefore, if $\langle \delta N^2 \rangle$, calculated using macroscopic relations, approaches unity, then this signals that we have reached the limit of the applicability of the macroscopic approach. Therefore, it is necessary to take into account the discrete nature of matter, and therefore, the quantum laws that describe the behavior of the particles that make up the substance.

From the equation (2.9) it follows that the mean square of fluctuations becomes comparable to unity $\langle \delta N^2 \rangle \sim 1$ when the condition is satisfied:

$$\langle \delta N^2 \rangle \sim 1 \quad \Rightarrow \quad TR^3 \sim 3 \times 10^6 \,\mathrm{K}\,\mathring{\mathrm{A}}^3 \,. \tag{2.12}$$

Moreover, the lower the temperature, the more significant the discreteness becomes for larger samples. Let us emphasize that we are not talking about microscopic systems, for which $\bar{N} \sim 1$ and the discreteness account is usual, but about seemingly macroscopic samples, in which the number of particles is still large: $\bar{N} \gg 1$. Thus, assuming $T \sim 0,1\,\mathrm{K}$, we find that the condition $\langle \delta N^2 \rangle \sim 1$ is satisfied for the following sizes,

$$R \sim 300 \ \mathring{\mathrm{A}} \,. \tag{2.13}$$

In such a sample, the average number of electrons $\bar{N} \sim 1 \times 10^7$.

It should be noted that these estimates are given for the case of a standard metal with a high electron density. In fact, most mesoscopic effects are observed

in semiconductor structures with a low density and a low effective electron mass. In this case, the wavelength for electrons with an energy near the Fermi level becomes quite large. If in a metal the wavelength of a Fermi electron is about one angstrom, then in a two-dimensional electron gas of a GaAs/AlGaAs semiconductor heterostructure the wavelength of a Fermi electron is about tens of nanometers, which greatly facilitates the observation of various kinds of interference effects. In such a gas, the effective mass of the electron is small: $m^* = 0,067\, m_e$. As a consequence, the critical size of the sample at $T \sim 0,1\,\mathrm{K}$ becomes much larger and can already be of the order of 0.1μ.

Further, using the example of temperature, we will show that with a decrease in the size of the sample, a situation arises when the root mean square deviation is comparable to the value of the fluctuating physical quantity itself. In this case, such a quantity can no longer be used to characterize the properties of the mesoscopic system.

2.2.2. Temperature fluctuations

The mean square of the temperature fluctuations $\langle \Delta T^2 \rangle$ of a system of electrons, which are characterized by a continuous spectrum, is determined by the equation (see [1], [6])

$$\langle \Delta T^2 \rangle = \frac{k_B T^2}{C_v}\,, \tag{2.14}$$

де C_v – теплоємність електронного газу при постійному об'ємі. Ми розглядаємо тільки електронний внесок у теплоємність, оскільки за низьких температур решітчастим внеском можна нехтувати. Нагадаємо, електронна теплоємність є пропорційною першій степені температури, а решітчаста - T^3.

Considering that the electronic heat capacity

$$C_v = \frac{\pi^2}{3}\, k_B^2 T\, \frac{\partial \bar{N}}{\partial \mu}\,, \tag{2.15}$$

we get:

$$\frac{\langle \Delta T^2 \rangle}{T^2} = \frac{1}{T} \frac{3k_B}{\pi^2 \partial \bar{N}/\partial \mu}\,. \tag{2.16}$$

Using $\bar{N}$from (2.8), we find that the following condition

$$\sqrt{\langle \Delta T^2 \rangle} \sim T \tag{2.17}$$

is achieved with the following ratio between the temperature T and the size R of the spherical sample:

$$TR^3 \sim 1 \times 10^5 \mathrm{K}\,\mathring{\mathrm{A}}^3\,. \tag{2.18}$$

Here, the radius of the sample is expressed in angstroms Å, $\mu \sim 10^4\,\mathrm{K}$. At a temperature $T \sim 0,1\,\mathrm{K}$, from condition (2.18) we obtain the critical size $R \sim 100\,\mathring{\mathrm{A}}$, which in terms of the order of magnitude coincides with the value given in equation (2.13).

Thus, using the example of thermodynamic fluctuations, we have shown that, as the temperature decreases and the size of the sample decreases, we move to a new regime where the approach based on the laws of classical physics no longer applies. This new mesoscopic regime is characterized by the fact that for the characterization of the properties of still completely macroscopic samples, it is necessary to apply a quantum mechanical approach.

Self-test questions

1. What is the role of electron reservoirs?
2. What is the distribution function? What is the electron distribution function in a mesoscopic sample connected to reservoirs?
3. Describe the level filling in a mesoscopic sample at zero temperature.
4. How does the current state in a mesoscopic sample differ from the current state in a macroscopic sample?
5. What is the peculiarity of the fluctuations of thermodynamic quantities in mesoscopic samples?

3. Phase coherence and conductance

Below we will consider what conditions are necessary for the quantum properties of current carriers to manifest themselves in the electrical conductance of a mesoscopic sample.

3.1. Schrödinger equation and single-particle approximation

One of the main aspects of the quantum mechanical behaviour of particles is the wave nature of their motion. This is reflected in the main equation of quantum non-relativistic mechanics – the Schrödinger equation:

$$i\hbar \frac{\partial \psi(t, \mathbf{r})}{\partial t} = \mathcal{H}\psi(t, \mathbf{r}) \,, \tag{3.1}$$

where $\psi(t, \mathbf{r})$ is the wave function describing the state of a quantum particle; $\mathbf{r} = (x, y, z)$is the radius vector; and $\mathcal{H}$is the energy operator (Hamiltonian):

$$\mathcal{H} = \mathcal{H}_0 + U(t, \mathbf{r}) \,, \tag{3.2}$$

consisting of a kinetic part:

$$\begin{aligned} \mathcal{H}_0 &= -\frac{\hbar^2}{2m_e}\Delta \,, \\ \Delta &= \frac{\partial^2}{\partial x^2} + \frac{\partial^2}{\partial y^2} + \frac{\partial^2}{\partial z^2} \,, \end{aligned} \tag{3.3}$$

corresponding to the motion of the electron, and the potential part $U(t, \mathbf{r})$, which describes the interaction of the electron with the environment.

Under steady-state conditions, when potential energy does not depend on time

$$U = U(\mathbf{r}) \,, \tag{3.4}$$

The energy of the electron E is conserved in the same way as in the case of free motion, and the wave function can be represented as

$$\psi(t, \mathbf{r}) = e^{-iEt/\hbar}\psi(\mathbf{r}) \,, \tag{3.5}$$

where $\psi(\mathbf{r})$ satisfies the following Schrödinger equation:

$$\left(-\frac{\hbar^2}{2m}\Delta + U(\mathbf{r})\right)\psi(\mathbf{r}) = E\psi(\mathbf{r}) \,. \tag{3.6}$$

For an electron moving freely in empty space,

$$U = 0 \,,$$

and the wave function is

$$\psi(t, \mathbf{r}) = e^{-iEt/\hbar + i\mathbf{pr}/\hbar} \,, \tag{3.7}$$

where $\mathbf{p}$ is the electron momentum vector. This wave function corresponds to a particle (better to say, a stream of particles) moving along the direction given by the vector $\mathbf{p}$ with a velocity

$$v = p/m_e \,.$$

In the general case, to determine the wave function, it is necessary to supplement the Schrödinger equation with boundary conditions. For example,

if the boundaries of the sample are impermeable to electrons, then the wave function must vanish at the boundary surface Σ:

$$\psi(\mathbf{r} \in \Sigma) = 0\,. \tag{3.8}$$

In addition, the wave function must be appropriately normalised. Since the square of the wave function determines the probability density of detecting a particle at a given point in space, the corresponding integral over the entire part of space V accessible to the particle must be equal to unity:

$$\int_V dV|\psi(\mathbf{r})|^2 = 1\,. \tag{3.9}$$

Using equations (3.6), (3.8), and (3.9), we determine the spectrum of allowed states ψ_i, i = 1, 2... for an electron in a given system and the corresponding energies E_i. Some examples will be considered below. However, knowledge of the spectrum alone is not sufficient to describe the properties of the system.

A mesoscopic system usually contains many electrons. Electrons are Fermi particles, so no more than one particle can be in one quantum state. In this regard, it is also necessary to know which of the energy levels are occupied by electrons and which are free. The answer to this question is given by the distribution function f(E). This function shows the probability that a given energy level E is occupied.

In a state of thermodynamic equilibrium, if the mesoscopic system can exchange energy and particles with the reservoir, then the distribution function for electrons in the mesoscopic sample is the Fermi distribution function, Fig. 2.2. At zero temperature, the equilibrium filling of energy states in a mesoscopic sample in contact with the reservoirs is shown in Fig. 2.3.

The approximation based on the use of the single-particle Schrödinger equation and the Fermi distribution function for occupied states will be called the approximation of non-interacting electrons, or the single-particle approximation. In many cases, this approximation allows us to correctly describe the observed effects or, at least, allows us to give a clear physical picture and describe the phenomenon at a qualitative level.

The approximation of non-interacting electrons works quite well in macroscopic solids, despite the fact that the electron concentration is quite high and it would seem that the interaction between particles should significantly affect the properties of the system. The explanation for this is provided by the Landau Fermi-liquid theory [8].

Indeed, the interaction between electrons is important, and it leads to the fact that the electrons in a metal constitute an interacting system of particles or a quantum Fermi liquid. However, a significant simplification is that at energies small compared to the degeneracy temperature of the Fermi system (and for metals the degeneracy temperature is close to the Fermi energy and is $10^4\,K$), the many-particle spectrum of the system can be represented as a single-particle spectrum of some excitations that do not interact with each other. Such excitations are called "quasiparticles".

Quasiparticles have spin 1/2, like real electrons. However, they can have a charge either e, in which case they are called quasielectrons, or -e, in which case they are called quasiholes (or simply holes). The mass of quasiparticles m^* can differ from the mass of a free electron me. For example, in a two- dimensional electron gas existing at the GaAs/AlGaAs interface, the effective mass of the electron is $m^* = 0,067\,m_e$.

Taking this into account, we can use the Schrödinger equation (3.6) if we replace the electron mass m_e by the effective mass m^*.

3.2. Electron phase coherence length

One of the key conditions for observing mesoscopic effects is the preservation of phase coherence by an electron propagating through a mesoscopic sample. An electron is said to preserve phase coherence if its state can be described by a wave function. Then, by specifying the phase of the wave function at some point in space and using the Schrödinger equation, it is possible to uniquely determine the phase of the electron's wave function in the entire space accessible to it.

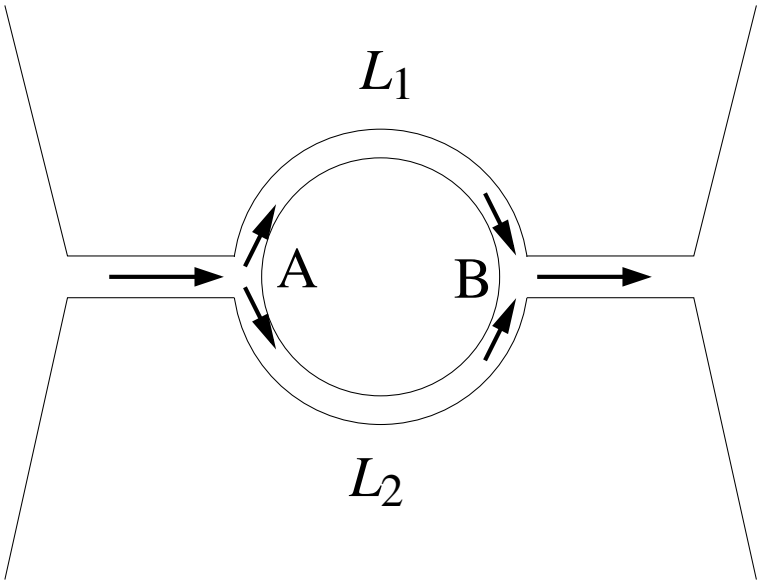

Fig. 3.1. Transfer of an electron wave through a doubly connected sample – a ring. The arrows show the direction of electron motion. At point A the electron wave splits into two waves that propagate through the upper L_1 and lower L_2 branches of the ring, respectively. At point B, these waves recombine and interfere

3.2.1. Why is the phase of the wave function important?

Consider a sample in the form of a ring, Fig. 3.1. There are two paths L_1 and L_2 for the propagation of an electron from point A to point B. Moving from the left conductor, the electron wave splits at point A into two waves, which combine and interfere at point B. The result of the interference can be determined by measuring the resistance of such a mesoscopic ring. Let $\mathcal{A}_1$ and $\mathcal{A}_2$ be the amplitudes for the propagation of an electron from point A to point B along the upper and lower paths, respectively:

$$\begin{aligned} \mathcal{A}_1 &= A_1 e^{i\varphi_1}\,, \\ \mathcal{A}_2 &= A_2 e^{i\varphi_2}\,. \end{aligned} \tag{3.10}$$

Here $A_{1(2)}$ and $\varphi_{1(2)}$ are the corresponding modulus and phase of the transition amplitude. The total transition amplitude $\mathcal{A}$ from point A to point B is the sum of the amplitudes $\mathcal{A}_\infty$ and $\mathcal{A}_\in$. In this case, the probability of an electron passing from point A to point B is equal to the square of the total transition amplitude. As we have already said, the probability of passing determines the conductance of the system $G = g|\mathcal{A}_1 + \mathcal{A}_2|^2$, which consists of three parts:

$$\begin{aligned} G &= G_1 + G_2 + G_{int}\,, \\ G_1 &= g\,A_1^2\,, \quad G_2 = g\,A_2^2\,, \\ G_{int} &= 2\,g\,A_1 A_2\,\cos(\varphi_1 - \varphi_2)\,, \end{aligned} \tag{3.11}$$

where $G_{1(2)}$ is the conductance of each of the ring branches, and G_{int} is the interference contribution to the conductance due to the doubly connected geometry.

By applying a magnetic field H perpendicular to the ring plane, the phase difference between the transition amplitudes along the paths L_1 and L_2 can be varied:

$$\Delta\varphi \equiv \varphi_1 - \varphi_2 = 2\pi\frac{\Phi}{\Phi_0} + \Delta\varphi_0\,, \tag{3.12}$$

where $\Phi = HS$ is the magnetic flux; $\Phi_0 = h/e \approx 4,14 \times 10^{-15}$Wb is the magnetic flux quantum; S is the area of the ring; $\Delta\varphi_0$ is the the phase difference in the absence of a magnetic field. Therefore, by changing the magnetic flux, one can change the interference contribution to the conductance:

$$G_{int} = 2gA_1A_2\,\cos\left(2\pi\frac{\Phi}{\Phi_0} + \Delta\varphi_0\right). \tag{3.13}$$

The dependence of conductance on the magnetic flux is shown in Fig.. 3.2.

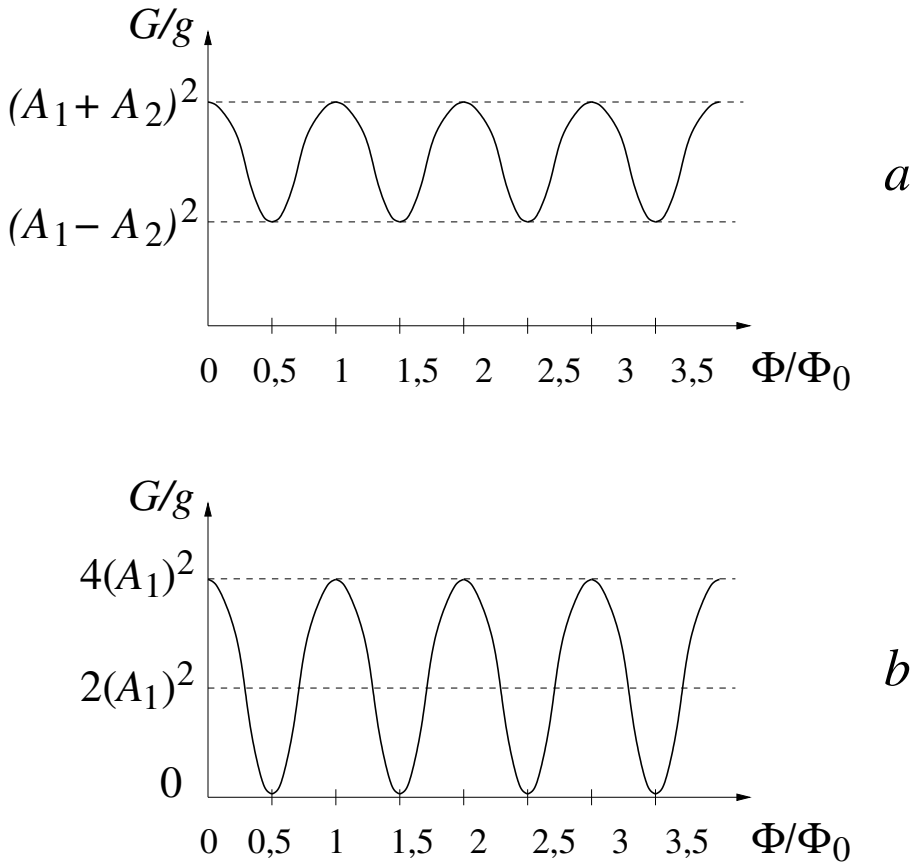

Fig. 3.2. Dependence of the conductance G of the ring on the magnetic flux Φ: a - asymmetric ring $A_1 \neq A_2$; b - symmetric ring $A_1 = A_2$

At $\Delta\varphi = \pi$, destructive interference is observed: the two waves cancel each other out, and the probability of an electron entering the right conductor is small. In this case, the conductance of the system, which is determined by the possibility of an electron passing from the left conductor to the right conductor, is small:

$$G_{\min} = g(A_1 - A_2)^2 . \tag{3.14}$$

At $\Delta\varphi = 2\pi$, constructive interference is observed: two waves reinforce

each other, which leads to an increase in the conductance of the system:

$$G_{\max} = g\left(A_1 + A_2\right)^2 . \tag{3.15}$$

This effect is most clearly manifested in the case of a symmetric ring, Fig. 3.2, b, when the amplitudes of the transfer through both branches are the same:

$$A_1 = A_2 = A\,.$$

In this case, the ratio of the minimum and maximum conductivities to the classical value

$$G_{cl} = 2gA^2 = G_1 + G_2\,,$$

which would be in the macroscopic case, when interference effects are absent, as follows:

$$\frac{G_{\min}}{G_{cl}} = 0\,, \qquad \frac{G_{\max}}{G_{cl}} = 2\,. \tag{3.16}$$

Thus, the interference phenomenon directly affects such a macroscopic characteristic as conductance, and therefore can be the subject of research in mesoscopics.

3.2.2. What breaks phase coherence?

Inelastic collisions of electrons with other quasiparticles, for example, phonons, magnons, and also with each other, violate phase coherence and thus prevent the manifestation of interference effects. Inelastic collisions change the electron energy and violate the evolution of the wave function described by the Schrödinger equation, introducing a random contribution to the electron phase. As a consequence, the phase difference becomes fluctuating in time, which leads to the suppression of the interference contribution to the measured physical quantity.

It should be emphasized that elastic processes can be described by the Schrödinger equation, so they do not destroy the interference pattern. The effect of elastic scattering is described by the potential energy $U(\mathbf{r})$ in equation (refEq2).

The probability of a scattering process, in particular inelastic scattering, can be characterized by the average time between successive scatterings of this type. In the case of inelastic electron scattering, this time is denoted by τ_φ. During the time τ_φ, an electron with Fermi energy and velocity $v_F = \sqrt{2\mu/m_e}$ will move a distance

$$L_\varphi = v_F \, \tau_\varphi \, , \tag{3.17}$$

which is called the phase braking length or the phase coherence length. We consider electrons with an energy close to the Fermi energy, because at low temperatures it is precisely such electrons that participate in the transport processes.

Let the linear size of the sample be L. Then the influence of inelastic processes on the motion of an electron through a mesoscopic sample can be neglected if the size of the sample does not exceed the phase coherence length:

$$L \ll L_\varphi(T) \, . \tag{3.18}$$

This condition is fundamental for observing mesoscopic effects.

Let us estimate the value of L_φ for metallic samples. The main sources of inelastic relaxation at low temperatures are electron-electron τ_{e-e} and electron-phonon τ_{e-ph} scattering. Let us compare the corresponding scattering times. For a three-dimensional sample, we have, in order of magnitude (see, for example, [8]):

$$\tau_{e-e} \sim \frac{\hbar \, \mu}{(k_B T)^2} \, , \qquad \tau_{e-ph} \sim \frac{\hbar^3 \, \omega_D^2}{(k_B T)^3} \, , \tag{3.19}$$

where ω_D is the Debye frequency (the limiting phonon frequency). Setting

$\mu \sim 10^4\,\mathrm{K}$ and $\omega_D \sim 100\,\mathrm{K}$, we obtain that the electron-electron interaction becomes such that it determines

$$\tau_\varphi \approx \tau_{e-e} < \tau_{e-ph}\,,$$

at temperatures

$$T < \frac{(\hbar\omega_D)^2}{k_B\,\mu} \sim 1\,\mathrm{K}\,. \tag{3.20}$$

At $T \sim 1\,\mathrm{K}$, the inelastic relaxation time $\tau_\varphi \sim 10^{-7}\,\mathrm{s}$. Taking into account the characteristic value of $v_F \sim 10^5\,\mathrm{m/s}$, we find the phase braking length $L_\varphi(T \sim 1\,\mathrm{K}) \sim 10^{-2}\,\mathrm{m}$. In real metal samples, taking into account the diffusion nature of electron motion, the value of L_φ is somewhat smaller. Usually, at $T \sim 1\,\mathrm{K}$, we have $L_\varphi \sim 10^{-6}\,\mathrm{m}$.

Self-test questions

1. Formulate the problem statement for determining the electron spectrum in a mesoscopic sample.
2. Characterize the single-particle approximation. What are its advantages and disadvantages?
3. What is the phase baking length and what is its role in electrical conductance?
4. What physical processes violate phase coherence?
5. How do the characteristic times of electron-electron and electron-phonon scattering depend on temperature?

4. Landauer formula

Let us calculate the conductance of a one-dimensional ballistic conductor containing a single scatterer, Fig. 4.1. Landauer's formula [9],

$$G = \frac{2e^2}{h}\mathcal{T} \tag{4.1}$$

reduces the calculation of the conductance $G = \lim_{V\to 0} I/V$ of a conductor to the calculation of the quantum mechanical probability of the transfer of an electron $\mathcal{T}$ through a potential barrier that represents a scatterer present in the conductor. One can say that the problem of kinetics - the calculation of the current flowing through a phase-coherent sample - is reduced to the quantum mechanical problem of scattering. In order to obtain Landauer's formula, we

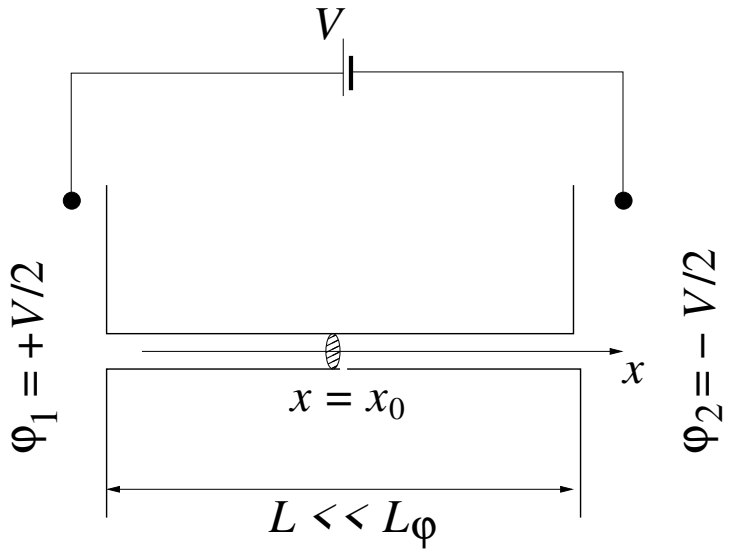

Fig. 4.1. A one-dimensional ballistic conductor with a single scatterer located at a point with coordinate $x = x_0$ connects two macroscopic electron reservoirs with different potentials $\varphi_1 \neq \varphi_2$

calculate the current I flowing through the conductor if a potential difference

V is applied to the contacts (see Fig. 4.1). The left contact has a potential $\varphi_1 = V/2$, and the right contact has a potential $\varphi_2 = -V/2$.

First, we will show how to calculate the current I carried by electrons in a ballistic sample. It is necessary to calculate the current I_p carried by an electron in some quantum state ψ_p, and then sum over all states, taking into account their occupancy:

$$I = \sum_p I_p \, f(p) \, . \tag{4.2}$$

Here, the index p numbers the allowed quantum states, and the distribution function $f(p)$ takes into account the contribution of only occupied states.

In a one-dimensional ballistic conductor, the wave function satisfies the Schrödinger equation for a free particle:

$$i\hbar \frac{\partial \psi(t,x)}{\partial t} = -\frac{\hbar^2}{2m_e} \frac{\partial^2 \psi(t,x)}{\partial x^2} \, . \tag{4.3}$$

The solution to this equation is the following,

$$\psi_p(t,x) = \frac{1}{\sqrt{L}} e^{-i\epsilon_p t/\hbar + p\,x/\hbar} \, , \tag{4.4}$$

where p is the electron momentum, $\epsilon_p = p^2/(2m_e)$ is the electron energy, L is the conductor size. The electron momentum p numbers the quantum states. We assume that the conductor has an infinite length, $L \to \infty$, and therefore we do not impose any boundary conditions. As a result, the momentum p, and therefore the energy ϵ_p, can take any values. In such a case, we say that the spectrum is continuous. In the presence of a continuous spectrum, the summation over quantum states is replaced by integration:

$$\sum_p \to \frac{L}{h} \int_{-\infty}^{\infty} dp \, . \tag{4.5}$$

4.1. General equation for current

Using (4.4) in a general quantum-mechanical equation for current,

$$\begin{aligned} I[\psi] &= i\frac{e\hbar}{2m_e}\left(\psi\frac{\partial\psi^*}{\partial x} - \psi\frac{\partial\psi^*}{\partial x}\right) \\ &\equiv -\frac{e\hbar}{m_e}\mathrm{Im}\left[\psi\frac{\partial\psi^*}{\partial x}\right] \end{aligned} \tag{4.6}$$

we obtain for $I_p \equiv I[\psi_p]$ the following,

$$I_p = \frac{e\,\mathrm{v}}{L}\,, \tag{4.7}$$

where $\mathrm{v} = p/m_e$ is a velocity of an electron in the state ψ_p. Note that we choose a positive direction for both x and current to be the same.

Then the total current that flows through 1D ballistic conductor is

$$I = \frac{2e}{h}\int\limits_{-\infty}^{\infty} dp\,\mathrm{v}\,f(p)\,. \tag{4.8}$$

The factor of 2 takes into account spin degeneracy of an electron gas.

It is convenient to go over from the interrogation over momentum to the integration over the kinetic energy. For this we write, $(p > 0)$:

$$dp = d\epsilon_p\frac{1}{d\epsilon_p/dp} = d\epsilon_p\frac{1}{v}\,, \tag{4.9}$$

where $v = |\mathrm{v}|$ is the absolute value of an electron velocity. Using Eq.(4.9) in Eq.(4.8), we get:

$$I = \frac{2e}{h}\int\limits_{0}^{\infty} d\epsilon_p[f(\epsilon_p, p>0) - f(\epsilon_p, p<0)]\,. \tag{4.10}$$

Here $f(\epsilon_p, p > 0)$ is the distribution function for right moving electrons, and $f(\epsilon_p, p < 0)$ is the distribution function for left moving electrons.

The simplification achieved by switching to integration over energy is that in the one-dimensional case the electron velocity follows from the equation for the current

4.2. Electron distribution function

Before finding the distribution function, let us note: if the problem involves a non-uniformly distributed electric potential, then it is convenient to perform the calculation by choosing the total energy $E = \epsilon_p + e\varphi(x)$ as the independent variable. This is due to the fact that during the motion of an electron, its total energy E is conserved, while the kinetic energy ϵ_p changes. In our case, such a change occurs only at the point of contact of the conductor with the reservoirs. In the conductor itself, the electric potential φ is constant and does not depend on the coordinate x along the channel, so we did not take it into account when solving the Schrödinger equation.

Let us calculate the electron distribution function to the right of the barrier $x > x_0$, denoting it by $f_{\mathcal{R}}$. Electrons coming from the right reservoir move towards the scatterer p < 0, Fig. 4.3. Such electrons are described by the distribution function for the right reservoir f_2. Electrons moving from the scatterer $p > 0$ can be divided into two groups. The first group includes electrons that initially moved from the right reservoir and were reflected by the scatterer. Such electrons are described by the distribution function Rf_2, where $R = 1 - \mathcal{T}$ is the probability of electron reflection from the potential barrier. The second group includes electrons that moved from the left reservoir and tunneled through the potential barrier. Such electrons are described by the distribution function $\mathcal{T}f_1$, where f_1 is the distribution function of electrons in the left reservoir.

Thus, the distribution function on the right from the scatterer is

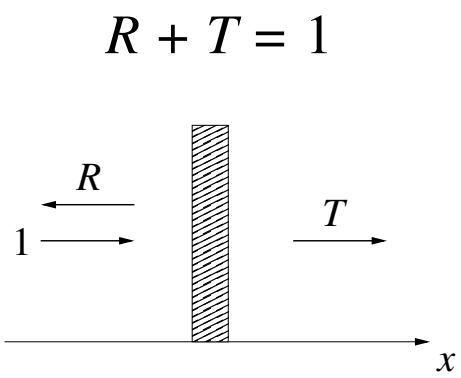

Fig. 4.2. Distribution of electron flux near a potential barrier: 1 - flux with unit intensity incident on the potential barrier; T - flux tunneling through the barrier; R - flux reflected from the barrier. Based on the law of conservation of particle number, $1 = T + R$

$$f_{\mathcal{R}}(E) = \begin{cases} f_2(E)\,, & p < 0\,, \\ Rf_2(E) + \mathcal{T}f_1(E)\,, & p > 0\,. \end{cases} \tag{4.11}$$

To calculate the current, it is necessary to substitute the distribution function $f \equiv f_{\mathcal{R}}$ into equation (4.10), expressed in terms of the kinetic energy of the electron ϵ_p at the point $x = x_2 > x_0$, where the current is calculated. Let $\varphi_{\mathcal{R}}$ be the electric potential at the point $x = x_2$, then, substituting $\epsilon_p = E - e\varphi_{\mathcal{R}}$ into (4.11) and taking into account the equation (2.4) for the electron distribution functions in the reservoirs, we obtain:

$$f_{\mathcal{R}}(\epsilon_p) = \begin{cases} f_0(\epsilon_p + e[\varphi_{\mathcal{R}} - \varphi_2])\,, & p < 0\,, \\ Rf_0(\epsilon_p + e[\varphi_{\mathcal{R}} - \varphi_2]) + \mathcal{T}f_0(\epsilon_p + e[\varphi_{\mathcal{R}} - \varphi_1])\,, & p > 0\,. \end{cases} \tag{4.12}$$

Let us analyze the given equation. It is easy to understand that the Fermi distribution functions f_0 with different arguments describe the energy distribution $f_i(\epsilon_p, \varphi)$ of particles that came from reservoirs with potentials φ_i $(i = 1, 2)$

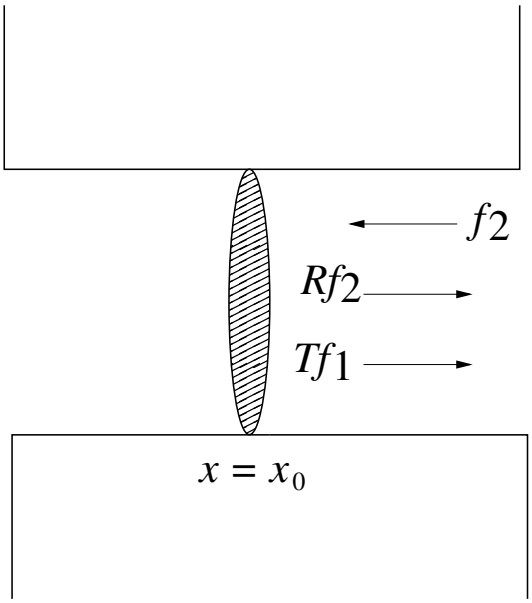

Fig. 4.3. The electron flux on one side of the scatterer. Electrons from the right contact with distribution function f_1 moves towards the scatterer. From the scatterer, there are two group of electrons. First, those that were reflected from the scatterer. Their distribution function is Rf_2. Second, those that tunnel through the scatterer. Their distribution function is Tf_1

to a point with potential φ:

$$f_i(\epsilon_p, \varphi) = \frac{1}{1 + \exp\left(\dfrac{\epsilon_p + e[\varphi - \varphi_i) - \mu}{k_B T}\right)} . \tag{4.13}$$

In the corresponding reservoir, where $\varphi = \varphi_i$, the given equation reduces to the equilibrium distribution function. At a point with a higher (lower) potential $\varphi > \varphi_i$ ($\varphi < \varphi_i$), electrons arrive accelerated (slowed down). Therefore, at zero temperature, the maximum kinetic energy of electrons is

$$\epsilon_p^{(\max)} = \mu + |e|(\varphi - \varphi_i) \tag{4.14}$$

at a point with potential φ will be greater (less) than in the corresponding

reservoir, where the maximum kinetic energy of electrons at zero temperature equals the Fermi energy μ.

4.3. Conductance of a channel with a scatterer

When determining the conductance G, we assume that the potential difference is small, $V \to 0$, so we can neglect the effect of the electric field on the electron wave function and use the equation for the current (4.10), which is valid in the case of a free electron. Substituting equations (4.12) in (4.10), we obtain:

$$I = \frac{2e}{h} \int_0^\infty d\epsilon_p \mathcal{T}(\epsilon_p) \big\{ f_1(\epsilon_p, \varphi_\mathcal{R}) - f_2(\epsilon_p, \varphi_\mathcal{R}) \big\} . \tag{4.15}$$

Here the functions $f_{1(2)}(\epsilon_p, \varphi)$ are defined in equation (4.13). This is the basic equation that relates, in the one-dimensional case, the current flowing through the sample to the probability of the transfer of an electron $\mathcal{T}$ through the sample.

Let us simplify the resulting equation by assuming that the applied voltage is small compared to the temperature and Fermi energy:

$$|eV| \ll k_B T \, , \mu \, . \tag{4.16}$$

In this case, the distribution function (4.13) can be expanded into a Taylor series in powers of the small potential difference $\varphi_\mathcal{R} - \varphi_i$. Restricting ourselves to the first-order terms, we obtain:

$$f_i(\epsilon_p, \varphi_\mathcal{R}) \approx f_0(\epsilon_p) + \frac{\partial f_0(\epsilon_p)}{\partial \epsilon_p} e \, (\varphi_\mathcal{R} - \varphi_i) \, . \tag{4.17}$$

Let us substitute this equation into (4.15) and take into account that $\varphi_1 - \varphi_2 = V$:

$$I = \frac{2e^2}{h} V \int_0^\infty d\epsilon_p \, \mathcal{T}(\epsilon_p) \left(-\frac{\partial f_0}{\partial \epsilon_p} \right) . \tag{4.18}$$

Note that the current depends only on the applied voltage V and does not depend on the potential φ at the point at which the current was calculated. The conductance $G = I/V$ is:

$$G = G_0 \int_0^\infty d\epsilon_p \, \mathcal{T}(\epsilon_p) \left(-\frac{\partial f_0}{\partial \epsilon_p} \right) , \tag{4.19}$$

where G_0 if the conductance quantum, (1.2).

The conductance G depends on the tunneling probability for electrons with an energy near the Fermi energy. This follows from the fact that the derivative of the Fermi energy distribution function

$$\frac{\partial f_0}{\partial \epsilon_p} = -\frac{1}{4k_B T} \frac{1}{\cosh^2 \left(\dfrac{\epsilon_p - \mu}{2k_B T} \right)} \tag{4.20}$$

is nonzero only in an energy interval with a width of about $4k_BT$ near $\epsilon_p = \mu$, Fig. 4.4. Therefore, for the correct calculation of the conductance of a mesoscopic conductor, the relationship between the characteristic energy interval, over which the tunneling probability changes significantly, and the temperature is important. At zero temperature, $T = 0$, the dependence (4.20) degenerates into the Dirac δ-function:

$$\frac{\partial f_0}{\partial \epsilon_p} = -\,\delta(\epsilon_p - \mu) \tag{4.21}$$

and equation (4.19) transforms into equation (4.1) with $\mathcal{T} \equiv \mathcal{T}(\mu)$.

The obtained equation can also be applied to the case when an arbitrary mesoscopic sample is connected by two one-dimensional ballistic conductors to reservoirs. In this case, the conductance of the mesoscopic sample is determined exclusively by the probability $\mathcal{T}$ of the transfer of an electron through the

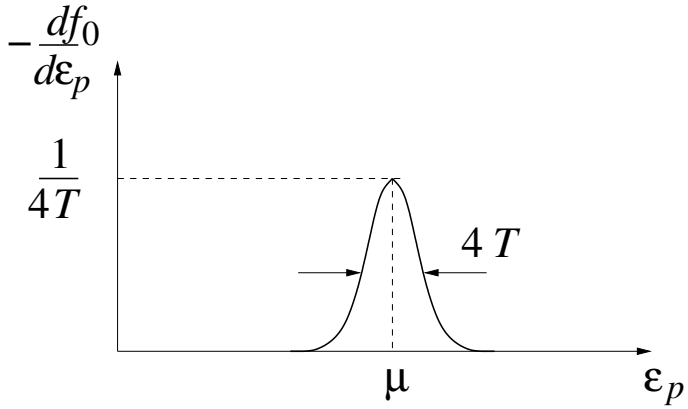

Fig. 4.4. The Fermi function energy derivative

sample. The proportionality coefficient, which we denoted above by the letter g, is the conductance quantum G_0.

Two remarks should be made in connection with the calculations given. First, from equation (4.1) it follows that even in the absence of any scattering, $\mathcal{T} = 1$, the conductance is finite: $G = G_0$. Thus, a one-dimensional ballistic channel connecting two reservoirs will itself create a resistance to the flow of current. This resistance is equal to $R_0 \equiv 1/G_0 = h/2e^2 \approx 12,9 \times 10^3\,\Omega$.

Secondly, we note that the conductance is defined as the ratio of the current I flowing through the sample to the potential difference V of the distant reservoirs, Fig. 4.5 a. This differs from the definition adopted in macroscopic physics, when conductance is defined as the ratio of current to the potential difference $\Delta\varphi$ between one and the other edge of the sample, Fig. 4.5 b.

Strictly speaking, the latter definition of conductance can also be used in mesoscopics, but a completely different answer will be obtained for the conductivity value, which in this case will be denoted by $G_{\mathcal{T}}$. Therefore, in order to compare the results of calculations with the results of measurements, it is necessary to know how the measurement is carried out.

To determine $G_{\mathcal{T}}$, it is necessary to calculate the change in potential, $\Delta\varphi$, in the immediate vicinity of the scatterer.

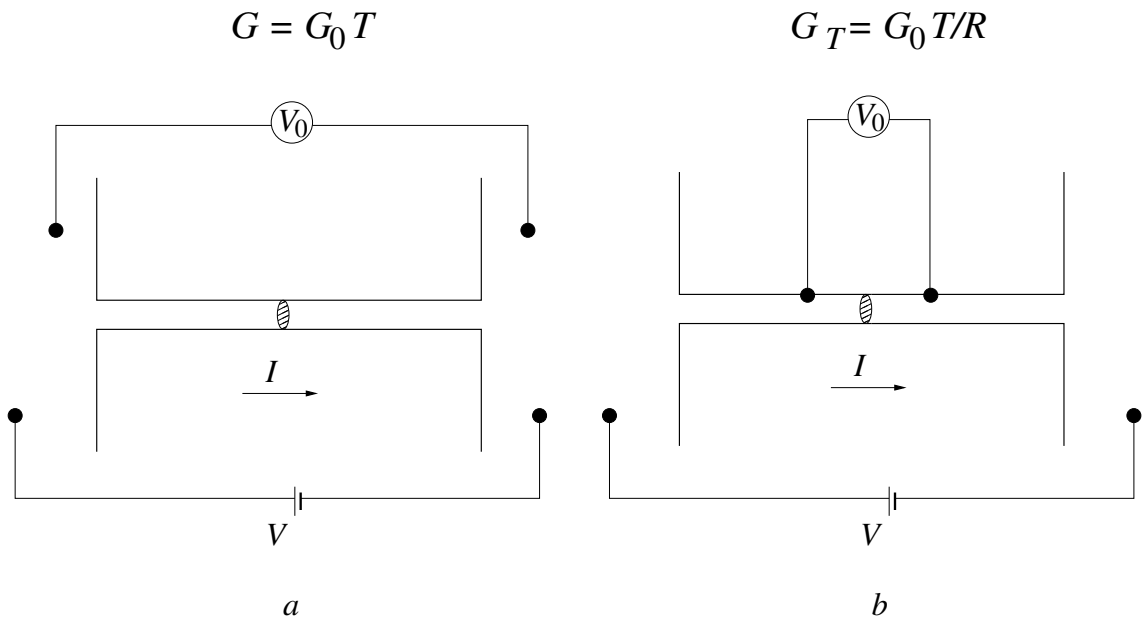

Fig. 4.5. The conductance measurement scheme $G = I/V_0$, where I is the current flowing through the sample; V_0 is the voltage measured by the voltmeter. The voltmeter, marked with a circle, can be connected far from the diffuser (a), in which case it measures the potential difference between the remote reservoirs $V_0 = V$, or in the immediate vicinity of the scatterer (b), in which case the voltmeter measures the potential change across the diffuser $V_0 = \Delta\varphi$

4.4. Electric potential distribution

As before, we assume that a voltage V is applied between the reservoirs. We determine the potentials immediately to the left $\varphi_{\mathcal{L}}$ and immediately to the right $\varphi_{\mathcal{R}}$ of the scatterer, assuming that the condition of electroneutrality is fulfilled. To do this, we calculate the density $n(V)$ of electrons in the channel when the voltage V is applied, and we require that this quantity equals the density $n(0)$ of electrons in the absence of the voltage $V = 0$:

$$n(V = 0) = n_{\mathcal{L}}(V) = n_{\mathcal{R}}(V)\,. \tag{4.22}$$

The electron density in a one-dimensional conductor is expressed in terms of the distribution function as follows:

$$n_i = \frac{2}{h} \int_{-\infty}^{\infty} dp\, f_i(p)\,, \quad i = \mathcal{L}, R\,. \tag{4.23}$$

The distribution function $f_{\mathcal{R}}$ is given in Eq. (4.12). By analogy, the distribution function on the left from the scatterer, $f_{\mathcal{L}}$, is defined as follows,

$$f_{\mathcal{L}}(\epsilon_p) = \begin{cases} f_0(\epsilon_p + e[\varphi_{\mathcal{L}} - \varphi_1])\,, & p > 0\,, \\ R f_0(\epsilon_p + e[\varphi_{\mathcal{L}} - \varphi_1]) + \mathcal{T} f_0(\epsilon_p + e[\varphi_{\mathcal{L}} - \varphi_2])\,, & p < 0\,, \end{cases} \tag{4.24}$$

where $\varphi_{\mathcal{L}}$ is a potential just on the left from the scatterer. Note that at $V = 0$ we have,

$$f_{\mathcal{R}} = f_{\mathcal{L}} = f_0\,.$$

Using (4.12) and (4.24) in (4.23)and then in (4.22) and expanding in terms of a small potential difference, we get,

$$\begin{gathered} \varphi_{\mathcal{R}} = -R\frac{V}{2}\,, \qquad \varphi_{\mathcal{L}} = R\frac{V}{2}\,, \\ \Delta\varphi = \varphi_{\mathcal{L}} - \varphi_{\mathcal{R}} = R\,V\,. \end{gathered} \tag{4.25}$$

Therefore, the conductance $G_{\mathcal{T}} = I/\Delta\varphi$ is:

$$G_{\mathcal{T}} = G_0 \frac{\mathcal{T}}{R}\,. \tag{4.26}$$

With decreasing the reflection coefficient $R \to 0$, the conductance defined above diverges,

$$G_{\mathcal{T}} \to \infty\,,$$

This is due to the fact that without back scattering the electrostatic potential is constant along the channel, and, therefore,

$$\Delta\varphi = 0\,.$$

It should be noted that in the original version, Landauer's formula had the form of Eq. (4.26). However, after numerous discussions, it became clear [1] that it is equation (4.1) that corresponds to the usual situation in an experiment, when the potential difference between the reservoirs is measured, and not the voltage on the sample.

Self-test questions

1. Write down Landauer's formula for electrical conductance and explain its structure.
2. What is a conductance quantum? What is its value?
3. Characterize the electron distribution function in a one-dimensional ballistic channel with a scatterer.
4. Derive an equation for the current in a one-dimensional ballistic channel with a scatterer.
5. Consider the distribution of electric potential near the scatterer and explain the difference between the conductance of an impurity in a ballistic channel and the conductance of a ballistic channel with an impurity.

5. Aharonov-Bohm effect

The preservation of phase coherence during electron propagation in mesoscopic samples at low temperatures determines the sensitivity of the transport properties of such objects to the phase of the electron wave function. This, on the one hand, provides an opportunity to study fundamental problems of quantum physics using well-developed methods for studying the transport properties of solids, and on the other hand, provides an additional opportunity to control the properties of samples, which can be used in the creation of new-generation electronic devices.

Next, we will consider one of the possibilities of influencing the phase of the electron wave function, associated with the Aharonov-Bohm effect [10].

5.1. The nature of the Aharonov-Bohm effect

In 1959, Aharonov and Bohm [10] showed that in quantum mechanics, the electromagnetic potentials, vector $\mathbf{A}$ and scalar φ, acquire a direct physical meaning and can be measured experimentally.

In this regard, it should be said that in classical physics, only the electric and magnetic fields are significant, which determine the force acting on an electric charge, Fig. 5.1. The electric field strength $\mathbf{E}$ and the magnetic field induction $\mathbf{B}$ are expressed in terms of the derivatives of the electromagnetic potentials as follows:

$$\begin{aligned} \mathbf{B} &= \mathrm{rot}\mathbf{A}\,, \\ \mathbf{E} &= -\mathrm{grad}\varphi - \frac{\partial \mathbf{A}}{\partial t}\,. \end{aligned} \tag{5.1}$$

The introduction of the vector $\mathbf{A}$ and scalar φ potentials can be considered

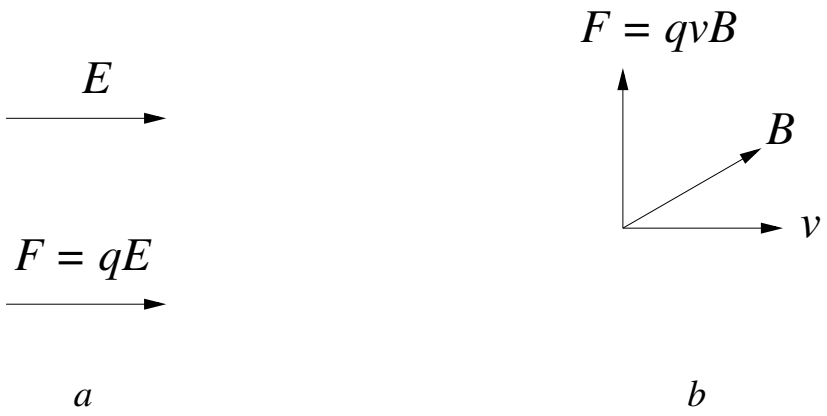

Fig. 5.1. The electric field strength E and magnetic field induction B determine the forces F acting on a charge q moving with velocity v: electric - $F = qE$(a) and magnetic - $F = qvB$ (b). The direction of the forces is shown for $q > 0$

as a convenient parameterisation, since the equations (5.1) automatically satisfy Maxwell's equations for the electromagnetic field in vacuum:

$$\begin{aligned} \mathrm{rot}\mathbf{E} &= -\frac{\partial \mathbf{B}}{\partial t}\,, \\ \mathrm{div}\mathbf{B} &= 0\,. \end{aligned} \tag{5.2}$$

In addition, the above equations (5.1) do not uniquely define vector and scalar potentials. If we make the following substitutions:

$$\begin{aligned} \mathbf{A} &\rightarrow \mathbf{A} + \mathrm{grad}\lambda\,, \\ \varphi &\rightarrow \varphi - \frac{\partial \lambda}{\partial t}\,, \end{aligned} \tag{5.3}$$

where λ is an arbitrary function of coordinates and time that is differentiable,

then neither the electric field strength nor the magnetic field induction will change, therefore electromagnetic potentials are not uniquely defined and, from the point of view of classical physics, should be considered only as mathematical objects that have no relation to the physical world. Within the framework of classical physics, only forces that depend on $\mathbf{E}$ and $\mathbf{B}$ can be measured.

In quantum theory, the situation is different. Aharonov and Bohm showed that the phase of the wave function of a particle directly depends on the electromagnetic potentials, and it is possible to set up an experiment where such a dependence will be observed.

The Aharonov–Bohm (AB) effect is that electromagnetic potentials directly affect the interference pattern formed by charged particles (electrons) moving in the region of space where vector and/or scalar potentials are present, but the electric and/or magnetic field strengths are equal to zero.

5.2. Aharonov-Bohm effect in vacuum

Let us explain the essence of the AB effect using the example of a free electron moving in a vector potential field. In the absence of electromagnetic fields $\mathbf{A} = 0$, $\varphi = 0$, the wave function ψ of a free electron is a plane wave (to simplify the formulas, we consider only the coordinate part of the wave function):

$$\psi_p(\mathbf{r}) = \exp\left(\frac{i}{\hbar}\,\mathbf{p}\,\mathbf{r}\right). \tag{5.4}$$

When there is an electromagnetic field in space, described by the vector potential $\mathbf{A}(\mathbf{r})$, the wave function of a free electron takes the form

$$\psi_p(\mathbf{r}, \mathbf{A}) = \exp\left(\frac{i}{\hbar}\int \big\{\mathbf{p} - i\mathbf{A}(\mathbf{r})\big\} d\mathbf{r}\right), \tag{5.5}$$

where integration is carried out along the trajectory of the particle. If neither electric nor magnetic forces act on the electron, then its trajectory remains the same as in the absence of a vector potential. However, the phase of the wave

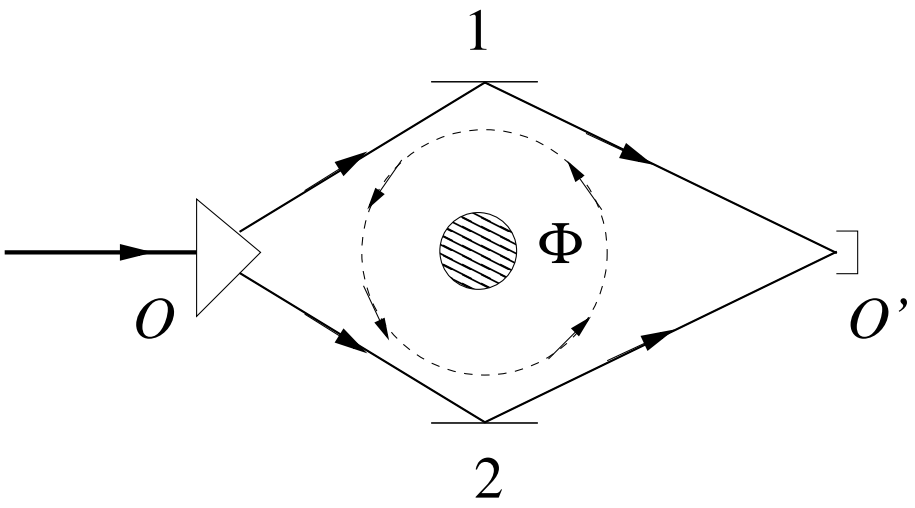

Fig. 5.2. Scheme of the Aharonov–Bohm electron interferometer. The electron beam is split into two beams at point O. Mirrors 1 and 2 direct the beams into detector O', where they interfere. The arrows show the direction of electron motion. A solenoid (shown by hatching) creates a magnetic flux Φ that penetrates the plane of the interferometer. The solenoid must be long enough so that the magnetic field is negligible along the electron path. The direction of the vector potential $\mathbf{A}$ is shown by the dotted circle with arrows.

function changes, which was recorded in the experiment on the interference of electron beams [11].

The scheme of the experiment on the interference of electron beams in a vacuum is presented in Fig. 5.2. In such an experiment, the electron beam is split into two beams, each of which travels the path $O'1O$, which has a length L_1, or $O'2O$, which has a length L_2, respectively. Then these beams should converge at one point and interfere. A long, thin solenoid with magnetic flux Φ creates a vector potential whose magnitude A outside the solenoid depends only on the distance R from the solenoid axis:

$$A = \frac{\Phi}{2\pi R}\,. \tag{5.6}$$

The vector potential is directed tangentially to a circle of radius R. The magnetic field induction corresponding to the potential (5.6) is equal to zero:

$$\mathbf{B} = \mathrm{rot}\mathbf{A} = 0\,. \tag{5.7}$$

The interference pattern, i.e. the intensity $J_{O'}$ of the electron beam at the receiver point O' registered by the detector, depends on the phase difference $\Delta\varphi = \varphi_1 - \varphi_2$, where φ_i, $i = 1, 2$, is the phase that the electron acquires when moving along a trajectory of length L_i. Let us determine this dependence. For this, we will assume that the value $J_{O'}$ is proportional to the probability $W(O', O)$ of the transition from the source O to the detector O'. This probability, in turn, is:

$$W(O', O) = |\mathcal{A}(O', O)|^2\,, \tag{5.8}$$

where $\mathcal{A}(O', O)$ is the transition amplitude. According to the basic principles of quantum mechanics, the total transition amplitude between some two points is the sum of the partial transition amplitudes corresponding to different possible transition paths between these points. In this case, there are only two such amplitudes: $\mathcal{A}_1$, corresponding to the path $O'1O$, and $\mathcal{A}_2$, corresponding to the path $O'2O$, so we have:

$$\mathcal{A}(O', O) = \mathcal{A}_1 + \mathcal{A}_2\,. \tag{5.9}$$

The amplitude of the transition between points with coordinates $\mathbf{r}$ and $\mathbf{r}'$ relates the values of the wave function at these points,

$$\psi(\mathbf{r}') = \mathcal{A}(\mathbf{r}', \mathbf{r})\,\psi(\mathbf{r})\,. \tag{5.10}$$

Substituting the equation (5.10) into (5.5), we obtain an equation for the transition amplitude in the following form:

$$\mathcal{A}(\mathbf{r}', \mathbf{r}) = \exp\left(\frac{i}{\hbar}\int\limits_{\mathbf{r}}^{\mathbf{r}'} \left\{\mathbf{p} - e\mathbf{A}(\mathbf{r}'')\right\} d\mathbf{r}''\right), \tag{5.11}$$

where integration is performed along the trajectory of the particle motion. Taking into account the obtained equation, we present the amplitudes $\mathcal{A}_1$ and $\mathcal{A}_2$ introduced above in the form $\mathcal{A}_i = e^{i\varphi_i}$, $i = 1, 2$, where the corresponding phases are:

$$\begin{aligned} \varphi_1 &= \frac{1}{\hbar} \int\limits_{O'1O} d\mathbf{r}(\mathbf{p} - e\mathbf{A}) \,, \\ \varphi_2 &= \frac{1}{\hbar} \int\limits_{O'2O} d\mathbf{r}(\mathbf{p} - e\mathbf{A}) \,. \end{aligned} \tag{5.12}$$

Substituting the above equations into (5.9) and then into (5.8), we calculate the probability of finding a particle at the registration site:

$$W(\mathbf{r}) = |\mathcal{A}_1 + \mathcal{A}_2|^2 = 2\big\{1 + \cos(\Delta\varphi)\big\} \,, \tag{5.13}$$

$$\begin{aligned} \Delta\varphi &= \frac{1}{\hbar} \int\limits_{O'1O} d\mathbf{r}(\mathbf{p} - e\mathbf{A}) - \frac{1}{\hbar} \int\limits_{O'2O} d\mathbf{r}(\mathbf{p} - e\mathbf{A}) \\ &= \frac{p}{\hbar}(L_1 - L_2) - \frac{e}{\hbar} \oint\limits_{O'1O2O'} d\mathbf{r}\mathbf{A} \,. \end{aligned} \tag{5.14}$$

Here we have taken into account that the momentum p remains constant in magnitude, since, by assumption, there are no forces acting on the electron. We transform the integral over the closed loop, $\oint d\mathbf{r}\mathbf{A}$ into the integral over the area S that this loop covers, and we obtain:

$$\oint d\mathbf{r}\mathbf{A} = \iint\limits_S d\mathbf{S}\,\mathrm{rot}\mathbf{A} \,. \tag{5.15}$$

According to equation (5.1), the vector potential rotor determines the magnetic

field induction **B**. The double integral in equation (5.15) is the magnetic flux Φ permeating the closed loop $O'1O2O'$:

$$\Phi = \iint\limits_S d\mathbf{S}\,\mathbf{B}\,. \tag{5.16}$$

Note that in the case of a uniform magnetic field, the magnitude of the magnetic flux is equal to $\Phi = B, S$. If the magnetic flux is created by a thin solenoid, as in this experiment, then $\Phi = B, S_0$, where $S_0 \ll S$ is the cross-sectional area of the solenoid.

Substituting the equations (5.14)-(5.16) into (5.13), we obtain:

$$W(O', O) = 2\left\{1 + \cos\left(\frac{p}{\hbar}[L_1 - L_2] - 2\pi\frac{\Phi}{\Phi_0}\right)\right\}\,. \tag{5.17}$$

Thus, the intensity $J_{O'} \sim W(O', O)$ of the registered electron beam is periodic in the magnetic flux with a period equal to the quantum of the magnetic flux.

Let us analyse the obtained equation. At first glance, there is nothing unusual. Everything is expressed in terms of the magnetic flux, which is the product of the magnetic induction and the area. The magnetic induction creates a force acting on the moving electron, which, it would seem, also changes the interference pattern. However, the unusual thing here is that the effect is also present in the case when the electrons move in a space free from force fields: on the trajectory of motion $\mathbf{B} = 0$ and $\mathbf{E} = 0$, and the magnetic flux exists in a small region covered by the trajectories $O'1O$ and $O'2O$, Fig. 5.2.

It should be noted that the electric and magnetic forces also affect the interference pattern. The forces change the trajectory of motion, which leads to a change in the so-called dynamical contribution to the phase, which is determined by the integral $\hbar^{-1}\int d\mathbf{r}\,\mathbf{p}$ in the equation (5.14).

5.3. Aharonov-Bohm effect in solids

Perhaps the first observation of the Aharonov–Bohm effect in a solid was the observation of magnetic flux quantization in superconducting cylinders by

Little and Parks in 1962 [12]. Such quantization was predicted by F. London in 1950 [13], that is, even before the work of Aharonov and Bohm in 1959.

Another manifestation of the AB effect is associated with the so-called weak localisation effect, namely, with the manifestation of interference phenomena in the conductivity of normal metal samples at low temperatures. In the work of Altshuler, Aronov, and Spivak in 1981 [14], the effect of oscillation in the magnetic field of the resistance of a hollow cylinder of normal metal at low temperatures was predicted. In the same year, this effect was experimentally discovered in the work of D. Yu. Sharvin and Yu. V. Sharvin [15].

Both of these effects, for completely different reasons, are periodic in magnetic fluxes with a period equal to the so-called superconducting quantum of magnetic flux Φ_{0s}:

$$\Phi_{0s} = \frac{h}{2e}\,. \tag{5.18}$$

In the case of a superconductor, this is due to the fact that the current carriers are pairs of electrons (Cooper pairs) with a charge $q = 2e$, which leads to a doubling of the contribution proportional to the vector potential to the phase of the wave function in the equation (5.12). This, in turn, leads to a doubling of the period of oscillations along the magnetic flux in the equation (5.17). In the case of weak localization, the doubling of the period is due to the fact that this effect is due to interference on the closed self-intersecting trajectories that the electron passes through, as shown in Fig. 5.3. In this case, the phase that the electron acquires when moving in the field of the vector potential is taken into account twice.

Oscillations with a period in the magnetic field equal to $\Phi_0 = h/e$ are observed only for mesoscopic samples. This history begins long before the work of Aharonov and Bohm. Thus, Hund in 1938 [16] and Dingle in 1952 [17] predicted that the energy spectrum and thermodynamic equilibrium properties, for example, the magnetisation of small electron systems, should oscillate as a function of the magnetic flux with a period of Φ_0.

However, the mesoscopic stage in the physics of the Aharonov–Bohm effect in solids actually began in the 1980s. Thus, in the work of Büttiker, Imry, and Azbel in 1984 [18] it was predicted that the resistance of a one-dimensional

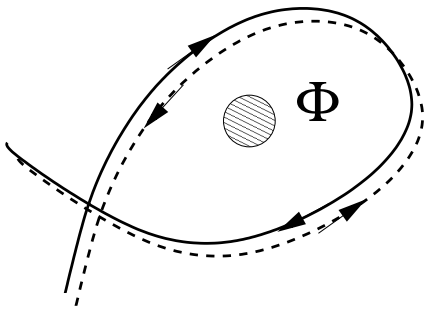

Fig. 5.3. Two self-intersecting electron trajectories, solid and dotted lines, determine the addition to the electrical conductivity of a macroscopic conductor due to the effect of weak localisation. The direction of electron motion is shown by arrows. An external magnetic field creates a magnetic flux Φ that penetrates the trajectory of motion.

mesoscopic ring with two contacts attached to it at low temperatures should oscillate with a period of Φ_0 when the magnetic flux passing through such a ring changes. This effect has been repeatedly observed experimentally since 1985 [19], [20].

5.3.1. Peculiarities of the observation of the Aharonov-Bohm effect in solids

The influence of the Aharonov–Bohm effect on the motion of electrons in a solid differs from the analogous influence on the motion of electrons in a vacuum. First, this difference is due to the fact that in a solid the source of the magnetic flux is always a magnetic field, which is also present on the trajectory of the electrons. Second, the difference is due to the fact that in a solid the electrons are not detected immediately after the interference, but continue their motion.

To explain the latter difference, let us consider two schemes. The first corresponds to an experiment on the interference of electron beams in a vacuum, Fig. 5.2. The second corresponds to the measurement of the electrical conductivity of a mesoscopic ring, Fig. 6.1. In both cases, the presence of a magnetic flux leads to a change in the partial amplitudes of the electron transition be-

tween the initial and final points. In the first case, there are only two such amplitudes, which determine the total amplitude of the transition (5.9). This is due to the fact that after interference at the final point O', the electrons are absorbed by the detector. In the second case, the electrons are not absorbed at the end point R, but can continue to move along the ring in the forward or reverse direction, therefore the total amplitude of the transition $\mathcal{A}(R, L)$ equals the sum of an infinite sequence of partial amplitudes:

$$\mathcal{A}(R, L) = \mathcal{A}_{R1L} + \mathcal{A}_{R1L2R1L} + ... + \mathcal{A}_{R2L} + \mathcal{A}_{R2L1R2L} + ... \tag{5.19}$$

The summation of an infinite sequence of amplitudes is equivalent to solving the Schrödinger equation with boundary conditions that take into account the geometry of the sample.

Self-test questions

1. What is the Aharonov–Bohm effect?
2. Under what conditions is the Aharonov–Bohm effect observed?
3. Explain the principle of operation of the Aharonov–Bohm interferometer.
4. What is the peculiarity of the manifestation of the Aharonov–Bohm effect in a solid?
5. What is the periodicity of the electrical conductivity in a magnetic flux due to the Aharonov–Bohm effect?

6. Ballistic channel conductance

Let us calculate the conductance of a one-dimensional ballistic ring connected by one-dimensional conductors to two reservoirs and penetrated by a magnetic flux Φ, Fig. 6.1.

According to the Landauer formula (4.1), the conductance G of the sample is proportional to the quantum mechanical probability of transfer $\mathcal{T}$ for electrons with Fermi energy $E = \mu$ through the sample from one reservoir to another.

In order to calculate the probability of transfer $\mathcal{T}$, we consider the problem of the transfer of an electron wave with unit amplitude moving along the left conductor through the ring, Fig. 6.1.

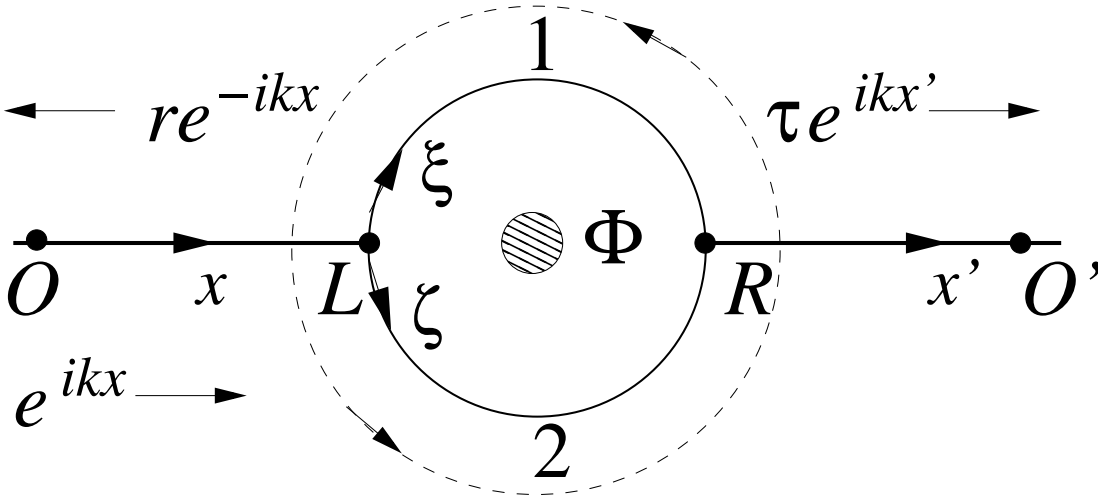

Fig. 6.1. The electron wave e^{ikx} propagation from the left reservoir through a ring permeated with magnetic flux Φ to the right reservoir. re re^{-ikx} is the amplitude of the reflected wave; $\tau e^{ikx'}$ is the amplitude of the transmitted wave. The probability of transmission through the ring is equal to $\mathcal{T} = |\tau|^2$. The direction of the vector potential is shown by a dotted circle with an arrow. The numbers 1 and 2 number the branches of the ring. The directions of the coordinate axes x, ξ, ζ, x' are shown by arrows. The origin of the coordinate axes x, ξ , ζ is located at point L, and the coordinate axis x' begins at point R.

6.1. General solution to the Schrödinger equation

Let us write the Schrödinger equation for the electron wave function ψ in the presence of a magnetic field (we take into account that the electron charge is negative: $e = -|e|$):

$$\frac{1}{2m_e}\big(-i\hbar\nabla + |e|\mathbf{A}\big)^2\psi = E\psi\,, \tag{6.1}$$

where $\mathbf{A}$ is the vector potential corresponding to the magnetic flux Φ created by the solenoid transmission through the ring. We choose the vector potential to be axially symmetric with the axis of symmetry passing through the centre of the ring perpendicular to the plane of the ring. The direction of the vector potential is shown by the dashed circle with arrows in Fig. 6.1. In such a calibration, the magnitude of the vector potential depends only on the radius of the circle R:

$$A = \frac{\Phi}{2\pi R}\,. \tag{6.2}$$

Let us consider how the vector potential affects the electron wave function in different sections of our sample. Let us select four one-dimensional sections OL, $L1R$, $L2R$ ¶ RO'. In each of them we introduce our coordinate axes x, ξ, ζ and x', respectively. The positive direction of the axes is shown by the arrows in Fig. 6.1. Let us denote the wave function for the electron in each section by ψ_L, ψ_1, ψ_2 and ψ_R, respectively. In each of the sections the wave function depends only on one coordinate.

On the sections OL and RO', the vector potential is directed perpendicular to the coordinate axes, so it falls out of the corresponding Schrödinger equation and does not affect the motion of electrons. The Schrödinger equation on the sections OL and RO' has the following form:

$$-\frac{\hbar^2}{2m_e}\frac{d^2\psi_\alpha}{dx^2} = E\psi_\alpha\,, \quad \alpha = L\,, R\,. \tag{6.3}$$

On the sections of the ring $L1R$ and $L2R$, the vector potential is di-

rected along the coordinate axes (in the negative and positive directions of the corresponding coordinate axes ξ and ζ), and therefore is preserved in the corresponding one-dimensional Schrödinger equation:

$$\begin{aligned} L1R: -\frac{\hbar^2}{2m_e}\left(\frac{d}{d\xi} - i\,\frac{2\pi}{L}\frac{\Phi}{\Phi_0}\right)^2 \psi_1 &= E\psi_1\,, \\ L2R: -\frac{\hbar^2}{2m_e}\left(\frac{d}{d\zeta} + i\,\frac{2\pi}{L}\frac{\Phi}{\Phi_0}\right)^2 \psi_2 &= E\psi_2\,. \end{aligned} \tag{6.4}$$

Here we have introduced the length of the ring $L = 2\pi R$.

Let us exclude the vector potential from the given equations. To do this, let us represent the wave function in the form

$$\begin{aligned} L1R: \psi_1 &= e^{i\xi\frac{2\pi}{L}\frac{\Phi}{\Phi_0}}\,\psi(\xi)\,, \\ L2R: \psi_2 &= e^{-i\zeta\frac{2\pi}{L}\frac{\Phi}{\Phi_0}}\,\psi(\zeta)\,. \end{aligned} \tag{6.5}$$

Next, we will perform calculations only for the $L1R$ branch. For the second branch, the calculations are carried out in a similar way.

Substitute (6.5) into equation (6.4) and obtain:

$$-\frac{\hbar^2}{2m_e}\left(\frac{d}{d\xi} - i\frac{2\pi}{L}\frac{\Phi}{\Phi_0}\right)^2 e^{i\xi\frac{2\pi}{L}\frac{\Phi}{\Phi_0}}\psi(\xi) = Ee^{i\xi\frac{2\pi}{L}\frac{\Phi}{\Phi_0}}\psi(\xi)\,.$$

Next, we square it:

$$-\frac{\hbar^2}{2m_e}\left(\frac{d^2}{d\xi^2} - 2i\frac{2\pi}{L}\frac{\Phi}{\Phi_0}\frac{d}{d\xi} - \left[\frac{2\pi}{L}\frac{\Phi}{\Phi_0}\right]^2\right) e^{i\xi\frac{2\pi}{L}\frac{\Phi}{\Phi_0}}\psi(\xi) = Ee^{i\xi\frac{2\pi}{L}\frac{\Phi}{\Phi_0}}\psi(\xi)$$

and we perform differentiation with respect to ξ:

$$-\frac{\hbar^2}{2m_e}\left(e^{i\xi\frac{2\pi}{L}\frac{\Phi}{\Phi_0}}\frac{d^2}{d\xi^2}\psi(\xi) + 2i\,\frac{2\pi}{L}\,\frac{\Phi}{\Phi_0}\,e^{i\xi\frac{2\pi}{L}\frac{\Phi}{\Phi_0}}\frac{d}{d\xi}\psi(\xi) - \right.$$
$$-\left[\frac{2\pi}{L}\,\frac{\Phi}{\Phi_0}\right]^2 e^{i\xi\frac{2\pi}{L}\frac{\Phi}{\Phi_0}}\psi(\xi) - 2i\,\frac{2\pi}{L}\,\frac{\Phi}{\Phi_0}\,e^{i\xi\frac{2\pi}{L}\frac{\Phi}{\Phi_0}}\frac{d}{d\xi}\psi(\xi) +$$
$$\left. +2\left[\frac{2\pi}{L}\,\frac{\Phi}{\Phi_0}\right]^2 e^{i\xi\frac{2\pi}{L}\frac{\Phi}{\Phi_0}}\psi(\xi) - \left[\frac{2\pi}{L}\,\frac{\Phi}{\Phi_0}\right]^2 e^{i\xi\frac{2\pi}{L}\frac{\Phi}{\Phi_0}}\psi(\xi)\right) = E\,e^{i\xi\frac{2\pi}{L}\frac{\Phi}{\Phi_0}}\psi(\xi)\,.$$

It can be seen that all terms in parentheses, except the first one, are cancelled: The second term is cancelled by the fourth one, and both the third and fifth terms are cancelled by the sixth term. Next, we divide the left and right sides of the equality by the nonzero factor $e^{i\xi\frac{2\pi}{L}\frac{\Phi}{\Phi_0}}$ and obtain an equation that is satisfied by the function $\psi(\xi)$ we introduced:

$$-\frac{\hbar^2}{2m_e}\frac{d^2\psi(\xi)}{d\xi^2} = E\psi(\xi)\,.$$

This equation is exactly the same as for straight sections, see (6.3). Note that the complete wave function for electrons moving along curvilinear sections is given by the equation (6.5), which also includes a phase factor depending on the magnetic flux.

Consider the solution of equation (6.3). This equation has two fundamental solutions $\psi^{(\pm)} = e^{\pm ikx}$, which are plane waves traveling in the positive and negative directions of the x-axis. $k = \sqrt{2m_eE}/\hbar$ is the modulus of the electron wave vector, depending on its energy $E > 0$. The partial solution of this equation is written as a sum of fundamental solutions with undetermined coefficients, which must be determined based on the boundary conditions.

Thus, we can write the solution of the Schrödinger equation in each of the selected regions in the following form:

$$\begin{aligned}
\psi_L &= e^{ikx} + re^{-ikx}\,, \\
\psi_1 &= \left(A_1 e^{ik\xi} + B_1 e^{-ik\xi}\right) e^{i2\pi\frac{\Phi}{\Phi_0}\frac{\xi}{L}}\,, \\
\psi_2 &= \left(A_2 e^{ik\zeta} + B_2 e^{-ik\zeta}\right) e^{-i2\pi\frac{\Phi}{\Phi_0}\frac{\zeta}{L}}\,, \\
\psi_R &= \tau e^{ikx'}\,,
\end{aligned} \tag{6.6}$$

where e^{ikx} is the incident wave, i.e. a plane wave corresponding to an electron moving from the left reservoir; re^{-ikx} is the reflected wave, i.e. a plane wave moving in the direction from the ring to the left reservoir; $A_1 e^{ik\xi} e^{i2\pi\frac{\Phi}{\Phi_0}\frac{\xi}{L}}$ and $A_2 e^{ik\zeta} e^{-i2\pi\frac{\Phi}{\Phi_0}\frac{\zeta}{L}}$ are the waves propagating from point L to point R along the corresponding arms of the ring; $B_1 e^{-ik\xi} e^{i2\pi\frac{\Phi}{\Phi_0}\frac{\xi}{L}}$ and $B_2 e^{-ik\zeta} e^{-i2\pi\frac{\Phi}{\Phi_0}\frac{\zeta}{L}}$ are the waves propagating from point R to point L along the corresponding arms of the ring; $\tau e^{ikx'}$ is the transmitted wave, i.e., a plane wave moving in the direction from the ring to the right reservoir. Note that in this problem there is no wave moving from the right reservoir to the ring.

The quantity r is called the reflection amplitude. The square of this quantity determines the probability of reflection:

$$\mathcal{R} = |r|^2\,. \tag{6.7}$$

The quantity τ is called the transmission amplitude, and its square

$$\mathcal{T} = |\tau|^2 \tag{6.8}$$

is called the probability of transmission.

6.2. Boundary conditions to the Schrödinger equation

The wave function (6.6) contains six unknown quantities: r, A_1, B_1, A_2, B_2 and τ. In order to determine them, it is necessary to use boundary conditions for equations (6.3) and (6.4). These conditions are the wave matching conditions at points L and R. At these points, the wave function must be continuous and the current must be conserved. Thus, to determine the six unknowns, we have six boundary conditions:

$$\begin{aligned}
&\text{(i)} && \psi_L(L) = \psi_1(L)\,, \\
&\text{(ii)} && \psi_L(L) = \psi_2(L)\,, \\
&\text{(iii)} && \psi_1(R) = \psi_R(R)\,, \\
&\text{(iv)} && \psi_2(R) = \psi_R(R)\,, \\
&\text{(v)} && (I_L - I_1 - I_2)\Big|_L = 0\,, \\
&\text{(vi)} && (I_1 + I_2 - I_R)\Big|_R = 0\,.
\end{aligned} \tag{6.9}$$

Here I_ii is the projection of the current in the branch $i = L, 1, 2, R$ onto the positive direction of the corresponding coordinate axis. In this case, the current entering the node, L or R, is taken into account with a plus sign, and the current leaving the node is taken into account with a minus sign, Fig. 6.2. A node in which three conductors converge is usually called a Y-contact.

The first four equations in (6.9) directly determine the relationship between the desired coefficients. The fifth and sixth equations must be transformed. To do this, we write the quantum mechanical equation for the current (in the branches $L1R$ and $L2R$, we take into account the presence of a longitudinal vector potential, see, for example, [7]):

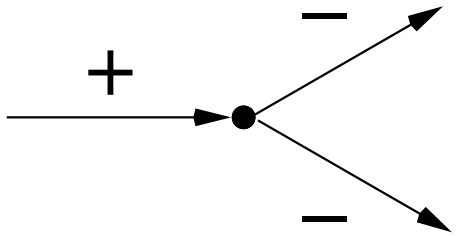

Fig. 6.2. A diagram illustrating the sign rule for currents in a Y-junction that we use. The current entering the node has a "+" sign, and the current leaving the node has a "-" sign. In electrical circuit theory, this rule is known as Kirchhoff's rule.

$$
\begin{aligned}
I_L &= -\frac{e\hbar}{m_e}\,\mathrm{Im}\left[\psi_L\,\frac{d\psi_L^*}{dx}\right]\,, \\
I_1 &= -\frac{e\hbar}{m_e}\,\mathrm{Im}\left[\psi_1\,\frac{d\psi_1^*}{d\xi}\right] + \frac{e^2}{m_e}\,A\,\psi_1\,\psi_1^*\,, \\
I_2 &= -\frac{e\hbar}{m_e}\,\mathrm{Im}\left[\psi_2\,\frac{d\psi_2^*}{d\zeta}\right] - \frac{e^2}{m_e}\,A\,\psi_2\,\psi_2^*\,, \\
I_R &= -\frac{e\hbar}{m_e}\,\mathrm{Im}\left[\psi_R\,\frac{d\psi_R^*}{dx'}\right]\,.
\end{aligned}
\tag{6.10}
$$

Substitute these equations into equation (v) of the system of equations (6.9) and obtain (omitting the common numerical factor $e\hbar/m_e$):

$$
\begin{aligned}
\text{(v)}\quad &\left(-\frac{e\hbar}{m_e}\,\mathrm{Im}\left[\psi_L\,\frac{d\psi_L^*}{dx}\right]\right) - \left(-\frac{e\hbar}{m_e}\,\mathrm{Im}\left[\psi_1\,\frac{d\psi_1^*}{d\xi}\right] - \frac{e^2}{m_e}\,A\,\psi_1\,\psi_1^*\right) - \\
&- \left(-\frac{e\hbar}{m_e}\,\mathrm{Im}\left[\psi_2\,\frac{d\psi_2^*}{d\zeta}\right] + \frac{e^2}{m_e}\,A\,\psi_2\,\psi_2^*\right) = 0\,.
\end{aligned}
$$

Here, all quantities are calculated at the point L. We note that, according to

equations (i) and (ii) of (6.9), the wave function is continuous at this point. Denoting this value by $\psi(L)$, we can rewrite the above equation in the form

$$\text{(v)} \quad -\frac{e\hbar}{m_e}\,\mathrm{Im}\left[\psi(L)\,\Pi^*\right] + \frac{e^2}{m_e}\,A\left(\psi_1\,\psi_1^* - \psi_2\,\psi_2^*\right) = 0\,,$$

$$\Pi = \frac{d\psi_L}{dx} - \frac{d\psi_1}{d\xi} - \frac{d\psi_2}{d\zeta}\,.$$

The multiplier at the vector potential A vanishes due to the continuity of the wave function. Thus, the condition for the conservation of current at the node takes the form

$$\mathrm{Im}\left[\psi\Pi^*\right] = 0\,. \tag{6.11}$$

The general solution for this equation is

$$\Pi = \alpha\psi\,, \tag{6.12}$$

where α is a real constant. The physical meaning of the parameter α is that it characterizes the transparency of the potential barrier, possibly present in a given node. If $\alpha = 0$, then the barrier is absent, and if $\alpha \to \infty$, then the node has a barrier that is opaque to electrons - electrons are completely reflected from the node.

Below we will consider a simple case: $\alpha = 0$. In this case, the current conservation condition takes the form

$$\Pi \equiv \sum_i \frac{d\psi_i}{dx_i} = 0\,. \tag{6.13}$$

It should be taken into account that the derivatives are included in the sum with a plus or minus sign according to the sign rule that we used earlier for currents, Fig. 6.2.

The boundary condition (6.13) is called the Griffis boundary condition [21]. He was probably the first to use this condition in problems of a similar kind. Sometimes this condition is called the Dirichlet condition according to the generally accepted terminology for boundary value problems in mathematical physics.

Writing the equation (6.13) at the points L and R, we transform the equations (v) and (vi) in (6.9) to the following form:

$$\begin{aligned} &\text{(v)} \quad \left(\frac{d\psi_L}{dx} - \frac{d\psi_1}{d\xi} - \frac{d\psi_2}{d\zeta}\right)\Big|_L = 0\,, \\ &\text{(vi)} \quad \left(\frac{d\psi_1}{d\xi} + \frac{d\psi_2}{d\zeta} - \frac{d\psi_R}{dx'}\right)\Big|_R = 0\,. \end{aligned} \tag{6.14}$$

Substituting (6.6) into (6.9), taking into account equation (6.14) and taking into account the values of the corresponding coordinates at the intersection points:

$$L: \quad x = 0\,, \quad \xi = 0\,, \quad \zeta = 0\,,$$

$$R: \quad \xi = \frac{L}{2}\,, \quad \zeta = \frac{L}{2}\,, \quad x' = 0\,,$$

we obtain the desired relations for determining the unknown coefficients (to simplify the calculations, we consider a symmetrical connection of the contacts to the ring, when the length of the upper and lower arms is the same and equals $L/2$):

$$
\begin{aligned}
&\text{(i)} && 1 + r = A_1 + B_1 \,, \\
&\text{(ii)} && 1 + r = A_2 + B_2 \,, \\
&\text{(iii)} && \left(A_1 \, e^{ik\frac{L}{2}} + B_1 \, e^{-ik\frac{L}{2}} \right) e^{i\pi\frac{\Phi}{\Phi_0}} = \tau \,, \\
&\text{(iv)} && \left(A_2 \, e^{ik\frac{L}{2}} + B_2 \, e^{-ik\frac{L}{2}} \right) e^{-i\pi\frac{\Phi}{\Phi_0}} = \tau \,, \\
&\text{(v)} && 1 - r - (A_1 - B_1) - (A_2 - B_2) = 0 \,, \\
&\text{(vi)} && \left(A_1 \, e^{ik\frac{L}{2}} - B_1 \, e^{-ik\frac{L}{2}} \right) e^{i\pi\frac{\Phi}{\Phi_0}} + \\
& && + \left(A_2 \, e^{ik\frac{L}{2}} - B_2 \, e^{-ik\frac{L}{2}} \right) e^{-i\pi\frac{\Phi}{\Phi_0}} - \tau = 0 \,.
\end{aligned}
\tag{6.15}
$$

Of all the coefficients, we are interested only in τ, the square of which, according to equations (6.8) and (4.1), determines the conductance of a given structure.

6.3. Calculation of conductance

To determine the coefficient τ, we exclude all coefficients corresponding to the internal branches of the system, i.e., we exclude the coefficients A_1, B_1, A_2 and B_2. As a result, we obtain two equations containing only r and τ.

To do this, we do the following. From equations (i) and (ii) in (6.15) we obtain:

$$
\begin{aligned}
B_1 &= 1 + r - A_1 \,, \\
B_2 &= 1 + r - A_2 \,.
\end{aligned}
\tag{6.16}
$$

Let us substitute the obtained equations into equations (iii) - (v). In the sixth equation, it is more convenient to substitute not B_1 and B_2, but the equation obtained from equations (iii) and (iv), respectively:

$$\begin{aligned} B_1\, e^{-ik\frac{L}{2}}\, e^{i\pi\frac{\Phi}{\Phi_0}} &= \tau - A_1\, e^{ik\frac{L}{2}}\, e^{i\pi\frac{\Phi}{\Phi_0}}\,, \\ B_2\, e^{-ik\frac{L}{2}}\, e^{-i\pi\frac{\Phi}{\Phi_0}} &= \tau - A_2\, e^{ik\frac{L}{2}}\, e^{-i\pi\frac{\Phi}{\Phi_0}}\,. \end{aligned}$$

After substitution we have:

$$\begin{aligned} &\text{(iii)} \quad A_1\left(e^{ik\frac{L}{2}} - e^{-ik\frac{L}{2}}\right) + (1+r)\, e^{-ik\frac{L}{2}} = \tau\, e^{-i\pi\frac{\Phi}{\Phi_0}}\,, \\ &\text{(iv)} \quad A_2\left(e^{ik\frac{L}{2}} - e^{-ik\frac{L}{2}}\right) + (1+r)\, e^{-ik\frac{L}{2}} = \tau\, e^{i\pi\frac{\Phi}{\Phi_0}}\,, \\ &\text{(v)} \qquad A_1 + A_2 = \frac{3}{2} + \frac{1}{2}\, r\,, \\ &\text{(vi)} \qquad A_1\, e^{i\pi\frac{\Phi}{\Phi_0}} + A_2\, e^{-i\pi\frac{\Phi}{\Phi_0}} = \frac{3}{2}\,\tau\, e^{-ik\frac{L}{2}}\,. \end{aligned} \tag{6.17}$$

From equation (v) we obtain $A_2 = \frac{3}{2} + \frac{1}{2}r - A_1$ and substitute this into the remaining equations:

$$\begin{aligned} &\text{(iii)} \qquad A_1\left(e^{ik\frac{L}{2}} - e^{-ik\frac{L}{2}}\right) = \tau\, e^{-i\pi\frac{\Phi}{\Phi_0}} - (1+r)\, e^{-ik\frac{L}{2}}\,, \\ &\text{(iv)} \quad A_1\left(e^{ik\frac{L}{2}} - e^{-ik\frac{L}{2}}\right) = \frac{3}{2}\, e^{ik\frac{L}{2}} - \frac{1}{2}\, e^{-ik\frac{L}{2}} + \frac{r}{2}\left(e^{ik\frac{L}{2}} + e^{-ik\frac{L}{2}}\right) - \tau\, e^{i\pi\frac{\Phi}{\Phi_0}}\,, \\ &\text{(vi)} \qquad A_1\left(e^{i\pi\frac{\Phi}{\Phi_0}} - e^{-i\pi\frac{\Phi}{\Phi_0}}\right) = \frac{3}{2}\,\tau\, e^{-ik\frac{L}{2}} - \left(\frac{3}{2} + \frac{r}{2}\right) e^{-i\pi\frac{\Phi}{\Phi_0}}\,. \end{aligned} \tag{6.18}$$

Next, we substitute equation (iii) into (iv) and obtain (after multiplying all terms by $e^{ik\frac{L}{2}}$):

$$\text{(iv)}\quad \tau\, e^{i\pi\frac{\Phi}{\Phi_0}}\, e^{ik\frac{L}{2}}\left(e^{-i2\pi\frac{\Phi}{\Phi_0}}+1\right)-r\left(\frac{1}{2}\,e^{ikL}+\frac{3}{2}\right)=\frac{3}{2}\,e^{ikL}+\frac{1}{2}\,. \tag{6.19}$$

Then we multiply equation (vi) $\left(e^{ik\frac{L}{2}}-e^{-ik\frac{L}{2}}\right)$, and equation (iii) by $\left(e^{i\pi\frac{\Phi}{\Phi_0}}-e^{-i\pi\frac{\Phi}{\Phi_0}}\right)$ and subtract equation (iii) from equation (vi). As a result, after multiplying by $e^{i\pi\frac{\Phi}{\Phi_0}}e^{ik\frac{L}{2}}$, we obtain the following equation:

$$\begin{aligned}\text{(vi)}\quad \tau\, e^{i\pi\frac{\Phi}{\Phi_0}}\, e^{ik\frac{L}{2}}\left(\frac{1}{2}-\frac{3}{2}\,e^{-ikL}+e^{-i2\pi\frac{\Phi}{\Phi_0}}\right)+r\left(e^{i2\pi\frac{\Phi}{\Phi_0}}-\frac{1}{2}\left\{1+e^{ikL}\right\}\right)=\\ =\frac{3}{2}\,e^{ikL}-e^{i2\pi\frac{\Phi}{\Phi_0}}-\frac{1}{2}\,.\end{aligned} \tag{6.20}$$

Equations (6.19) and (6.20) contain the characteristics of the system as a whole: the reflection coefficient r and the transmission coefficient τ.

The system of inhomogeneous linear equations (6.19) and (6.20) is solved by the method of determinants. To shorten the notation, we introduce the value $\tau' = \tau e^{i\pi\frac{\Phi}{\Phi_0}}e^{ik\frac{L}{2}}$ and we write:

$$\tau' = \frac{\Delta_{\tau'}}{\Delta}\,, \tag{6.21}$$

where the determinants of Δ and $\Delta_{\tau'}$ are:

$$\begin{aligned}
\Delta &= \begin{vmatrix} e^{-i2\pi\frac{\Phi}{\Phi_0}}+1 & -\dfrac{e^{ikL}+3}{2} \\ \dfrac{1-3\,e^{-ikL}+2\,e^{-i2\pi\frac{\Phi}{\Phi_0}}}{2} & \dfrac{2\,e^{i2\pi\frac{\Phi}{\Phi_0}}-1-e^{ikL}}{2} \end{vmatrix}, \\
\Delta_{\tau'} &= \begin{vmatrix} \dfrac{3\,e^{ikL}+1}{2} & -\dfrac{e^{ikL}+3}{2} \\ \dfrac{3\,e^{ikL}-2\,e^{i2\pi\frac{\Phi}{\Phi_0}}-1}{2} & \dfrac{2\,e^{i2\pi\frac{\Phi}{\Phi_0}}-1-e^{ikL}}{2} \end{vmatrix}.
\end{aligned} \tag{6.22}$$

Let's calculate the determinant Δ:

$$\begin{aligned}
\Delta &= \frac{1}{2}\left\{e^{-i2\pi\frac{\Phi}{\Phi_0}}+1\right\}\left\{2\,e^{i2\pi\frac{\Phi}{\Phi_0}}-1-e^{ikL}\right\}- \\
&\quad -\frac{1}{4}\left\{-e^{ikL}-3\right\}\left\{1-3\,e^{-ikL}+2\,e^{-i2\pi\frac{\Phi}{\Phi_0}}\right\}= \\
&= \frac{1}{2}+e^{i2\pi\frac{\Phi}{\Phi_0}}+e^{-i2\pi\frac{\Phi}{\Phi_0}}-\frac{1}{4}\,e^{ikL}-\frac{9}{4}\,e^{-ikL}= \\
&= \frac{1}{2}\left\{1+4\cos\left(2\pi\,\frac{\Phi}{\Phi_0}\right)-\cos(kL)-4\,e^{-ikL}\right\}= \\
&= \frac{1}{2}\left\{1+4\cos\left(2\pi\,\frac{\Phi}{\Phi_0}\right)-5\cos(kL)\right\}+i2\sin(kL)\,.
\end{aligned}$$

Multiplying by a complex conjugate number, we get:

$$|\Delta|^2=\frac{1}{4}\left\{1+4\cos\left(2\pi\frac{\Phi}{\Phi_0}\right)-5\cos(kL)\right\}^2+4\sin^2(kL)\,.$$

Next, we calculate $\Delta_{\tau'}$:

$$\begin{aligned}\Delta_{\tau'} &= \frac{1}{4}\left\{3\,e^{ikL}+1\right\}\left\{2\,e^{i2\pi\frac{\Phi}{\Phi_0}}-1-e^{ikL}\right\}- \\ &\quad -\frac{1}{4}\left\{-e^{ikL}-3\right\}\left\{3\,e^{ikL}-2\,e^{i2\pi\frac{\Phi}{\Phi_0}}-1\right\}= \\ &= -1+e^{ikL}\,e^{i2\pi\frac{\Phi}{\Phi_0}}+e^{ikL}-e^{i2\pi\frac{\Phi}{\Phi_0}}=\left(e^{ikL}-1\right)\left(e^{i2\pi\frac{\Phi}{\Phi_0}}+1\right).\end{aligned}$$

The square of the modulus of this determinant is

$$|\Delta_{\tau'}|^2=\left|e^{ikL}-1\right|^2\left|e^{i2\pi\frac{\Phi}{\Phi_0}}+1\right|^2=4\left\{1-\cos(kL)\right\}\left\{1+\cos\left(2\pi\frac{\Phi}{\Phi_0}\right)\right\}.$$

Therefore, we obtain the amplitude of the transfer:

$$\tau=\frac{e^{-i\pi\frac{\Phi}{\Phi_0}}\,e^{-ik\frac{L}{2}}\left(e^{ikL}-1\right)\left(e^{i2\pi\frac{\Phi}{\Phi_0}}+1\right)}{\frac{1}{2}\left\{1+4\cos\left(2\pi\frac{\Phi}{\Phi_0}\right)-5\cos(kL)\right\}+i2\sin(kL)}\,. \tag{6.23}$$

Calculating the probability of transfer $\mathcal{T}=|\tau|^2$, we obtain for the conductivity $G=\frac{2e^2}{h}\mathcal{T}(\mu)$ the following:

$$G=\frac{2e^2}{h}\,\frac{\left\{1-\cos(k_FL)\right\}\left\{1+\cos\left(2\pi\frac{\Phi}{\Phi_0}\right)\right\}}{\frac{1}{16}\left\{1+4\cos\left(2\pi\frac{\Phi}{\Phi_0}\right)-5\cos\left(k_FL\right)\right\}^2+\sin^2\left(k_FL\right)}\,, \tag{6.24}$$

where k_F is the wave number for an electron with Fermi energy $E=\mu$.

6.4. Properties of conductance

The conductance of a one-dimensional ring G depends on the magnetic flux Φ, the ring size L and on the wave number k_F. In this case, the effects of the kinematic phase $k_F L$ and the magnetic phase $2\pi\Phi/\Phi_0$ are independent of each other, which differs from the case of electron beams in vacuum, (5.17), when the specified phases are added.

6.4.1. Current reversal symmetry

It should be noted that if we were to consider the electron movement from the right reservoir to the left, we would obtain the same equation for the probability of transfer and, accordingly, for the conductance. This is a manifestation of the general rule that the conductance of a mesoscopic sample with two contacts does not depend on whether the current flows from left to right (conductance - G_{21}) or from right to left (conductance = G_{12}):

$$G_{12} = G_{21}\,. \tag{6.25}$$

This equality is due to the fact that the quantum-mechanical probability of transmission in the stationary case does not depend on the direction of motion. Such symmetry for the conductance of a mesoscopic sample is indeed observed in the experiment [22].

6.4.2. Magnetic flux dependence of conductance

Fig. 6.3 shows the dependence of the conductance G on the magnetic flux Φ, Eq.(6.24), calculated for the several values of the product $k_F L$. The following conclusions can be drawn from the figure mentioned above.

1. The dependence $G(\Phi)$ is periodic on the magnetic flux with a period equal to the magnetic flux quantum $\Phi_0 = h/e$. The latter value is twice as large as the so-called superconducting magnetic flux quantum $\Phi_0^{(s)} = h/(2e)$ which is characteristic of the phenomena observed in superconductors.

2. At the following values of the magnetic flux

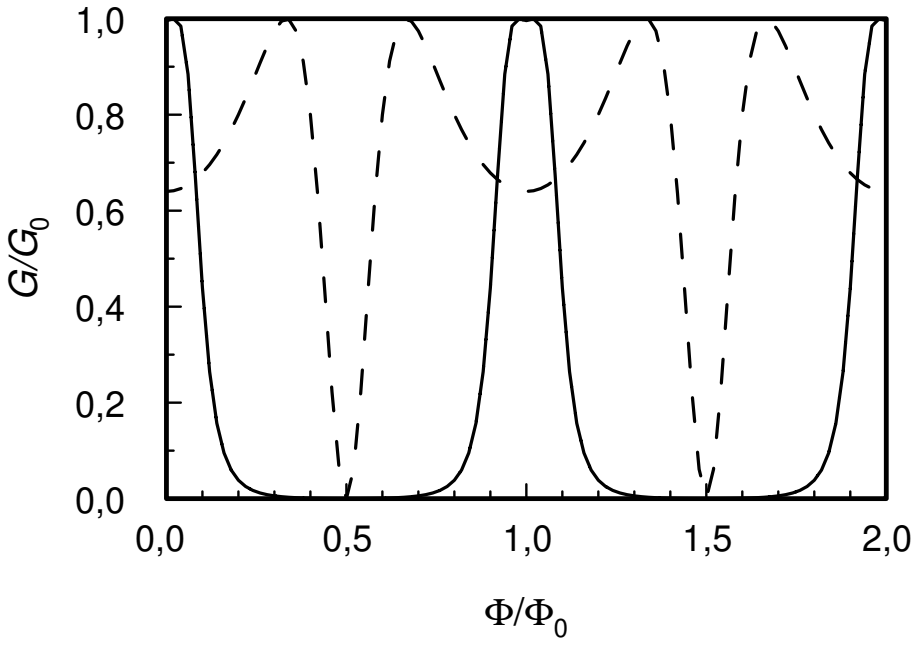

Fig. 6.3. Dependence of the conductance G of the ring on the trapped magnetic flux Φ for the values of the product $k_F L = 63$ (solid curve); 66 (dashed curve). $G_0 = 2e^2/h$ is the conductance quantum; $\Phi_0 = h/e$ is the magnetic flux quantum

$$\Phi = \frac{1}{2}\,\Phi_0 + n\,\Phi_0, \qquad n = 1, 2, \ldots \tag{6.26}$$

the conductance value turns to zero $G = 0$. This behavior is significantly different from the case of massive metals, for which the corrections to the conductivity due to the Aharonov–Bohm effect are small and amount to fractions of a percent.

3. The conductance is an even function of the magnetic flux:

$$G(\Phi) = G(-\Phi)\,. \tag{6.27}$$

The latter property can be explained based on the principle of symmetry of kinetic coefficients, Onsager's principle, according to which, with a change in

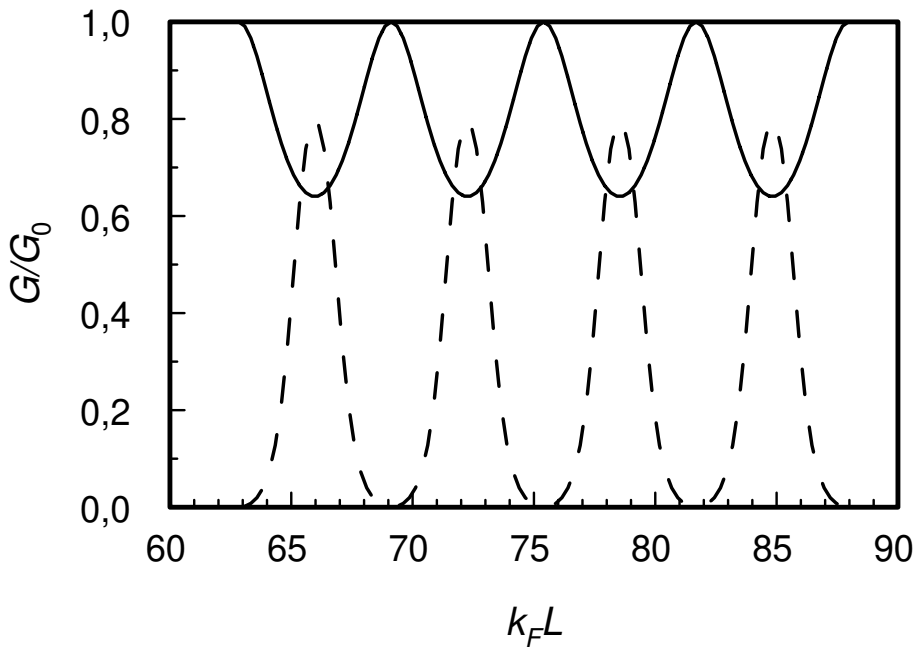

Fig. 6.4. Dependence of the conductance G of the ring on the product $k_F L$ for the magnetic flux values $\Phi = 2\pi n \Phi_0$, where $n = 0, 1, 2, \ldots$ (solid curve); $(0, 4 + 2\pi n)\,\Phi_0$ (dashed curve)

the direction of the magnetic field and a simultaneous change in the direction of motion to the opposite, the conductance value should remain unchanged:

$$G_{12}(\Phi) = G_{21}(-\Phi)\,. \tag{6.28}$$

From equations (6.25) and (6.28) we obtain the required equality (6.27).

6.4.3. Fermi energy dependence of conductance

When the Fermi energy changes, the product $k_F L$ changes, which is included in the equation for conductance (6.24). The dependence of $G(k_F L)$ for the several values of the magnetic flux Φ is given in Fig. 6.4. From the indicated figure it follows that:

1. The oscillations have a large amplitude. In the general case, the value of conductance G changes from G_0 to zero.

2. The period of oscillations is small, that is, with a small change in the Fermi energy, the conductance changes significantly. Let us estimate the value of the period. Since the oscillating factor is $\cos(k_F L)$ or $\sin(k_F L)$, the period of oscillations along the wave vector is:

$$\Delta k_F = \frac{2\pi}{L}\,. \tag{6.29}$$

The wave number is expressed in terms of the wavelength λ_F as follows: $k_F = 2\pi/\lambda_F$. Thus, for a mesoscopic ring, i.e., for a ring with a size significantly exceeding the electron wavelength $L \gg \lambda_F$, we obtain that the oscillation period Δk_F is small compared to the value of the wave number k_F :

$$\Delta k_F \ll k_F\,. \tag{6.30}$$

In this case, the equation for the period Δ_F of energy oscillations can be calculated as follows:

$$\Delta_F \approx \frac{d\mu}{dk}\Delta k_F = \hbar v_F \Delta k_F\,, \tag{6.31}$$

where $v_F = \hbar k_F/m_e$ is the velocity of an electron with the Fermi energy. Substituting the equation (6.29), we obtain:

$$\Delta_F = \frac{h v_F}{L}\,. \tag{6.32}$$

The relative value of the oscillation period is sufficiently small:

$$\frac{\Delta_F}{\mu} \sim \frac{\lambda_F}{L} \ll 1\,. \tag{6.33}$$

Let us estimate the value of the period Δ_F for the characteristic parameters of a two-dimensional electron gas: $\mu \sim 100\,\mathrm{K}$, $\lambda_F \sim 100\,\text{Å}$. A. For a ring of a micron size, $L \sim 10^{-6}\,m$, we obtain:

$$\Delta_F \sim 1\,\mathrm{K}\,.$$

To observe these oscillations of the conductance, both the temperature and the voltage at which the current is measured must be significantly less than the specified value.

6.4.4. Temperature effect on conductance

The equation (6.24) determines the conductance of the ring at zero temperature of the reservoirs to which it is connected. If the reservoirs have a nonzero temperature $T > 0$, then the conductance is,

$$G = \int_0^\infty dE\, G(E) \left(-\frac{\partial f_0(E)}{\partial E} \right) , \tag{6.34}$$

where $G(E)$ is defined in (6.24), only μ should be replaced by E.

With increasing temperature, the amplitude of conductance oscillations as a function of the Fermi energy decreases even at $T \gg T^*$, where

$$k_B T^* = \frac{h v_F}{2\pi^2 L} , \tag{6.35}$$

the specified oscillations completely disappear. Such a suppression of mesoscopic oscillations is associated with averaging over the energy of electrons contributing to the current. Note that in fact $k_B T^* \approx \Delta_F/20 \ll \Delta_F$.

Despite the fact that the above-mentioned suppression of oscillations is quite common in mesoscopics, not all phenomena are sensitive to averaging over the energy of electrons. Thus, in the considered case, at high temperatures $T \gg T^*$, the dependence of the conductance on the magnetic flux is preserved.

Indeed, substituting the equation (6.24) into (6.34) and performing integration over energy, at $T \gg T^*$ we obtain:

$$G = \frac{2e^2}{h} \frac{\cos\left(2\pi \dfrac{\Phi}{\Phi_0}\right) + 1}{\cos\left(2\pi \dfrac{\Phi}{\Phi_0}\right) + \dfrac{3}{2}} . \tag{6.36}$$

This equation does not depend on the Fermi energy, but it retains the dependence on the magnetic flux with a period equal to Φ_0. The graph of the dependence $G(\Phi)$, (6.36), is shown in Fig. 6.5.

The preservation of the dependence of the conductance on Φ at temperatures higher than T^*, but still low enough to satisfy the condition $L \ll L_\varphi(T)$,

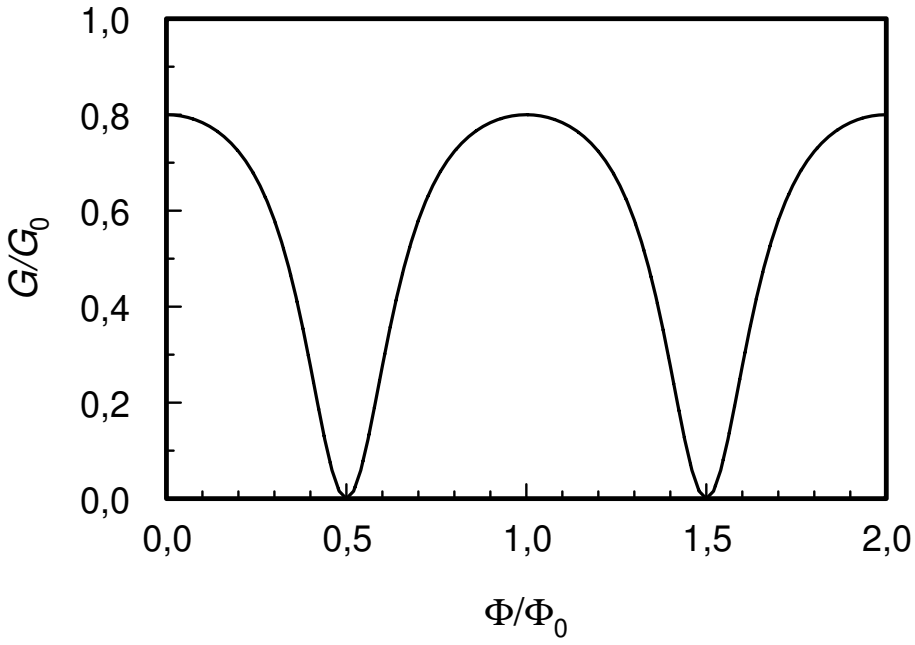

Fig. 6.5. Dependence of the conductance G of the ring on the trapped magnetic flux Φ at $T \gg T^*$

is due to the change in the phase of the wave function in the presence of a magnetic flux, which is the same for all electrons, so the energy averaging present in equation (6.34) does not eliminate the effect.

Self-test questions

1. Formulate a problem statement to determine the transmission coefficient through a one-dimensional ballistic ring with magnetic flux.
2. Derive the boundary condition for the wave function in a Y-contact.
3. Write an equation for the transmission coefficient through a ring with magnetic flux. What does the transmission coefficient depend on?
4. Why does the conductance of the ring depend on the Fermi energy?
5. Why does the conductance of the ring depend on the magnetic flux?

7. Spectrum quantization

Another aspect of quantum physics that manifests itself in mesoscopics is the quantization of the electron spectrum. An electron cannot leave the sample, so its wave function is zero at the sample surface. This leads to the fact that the electron energy levels are quantised, that is, the states in which the electron can be found can be numbered by integers. If the sample size is small enough, the difference between the allowed electron energy levels becomes large and significantly affects the properties of the sample.

The wave functions that describe the stationary states in which the electron can be found and the energies corresponding to these states depend on the shape and dimensions of the sample.

7.1. An electron in "a quantum box"

To illustrate the main features due to the quantization of the spectrum, we consider a simple case that admits an analytical solution, namely, consider a sample in the form of a parallelepiped with edge lengths L_x, L_y, L_z. Let us introduce the coordinate axes x, y, and z, as shown in Fig. 7.1. The region accessible to the electron is limited by the following boundaries:

$$0 \le x \le L_x\,, \quad 0 \le y \le L_y\,, \quad 0 \le z \le L_z\,. \tag{7.1}$$

Let the potential inside the "box" be zero. The Schrödinger equation in a rectangular coordinate system will take the form [7]

$$-\frac{\hbar^2}{2m_e}\left(\frac{\partial^2}{\partial x^2}+\frac{\partial^2}{\partial y^2}+\frac{\partial^2}{\partial z^2}\right)\psi(x,y,z) = E\psi(x,y,z)\,, \tag{7.2}$$

where $\psi(x,y,z)$ is the electron wave function; E is the electron energy.

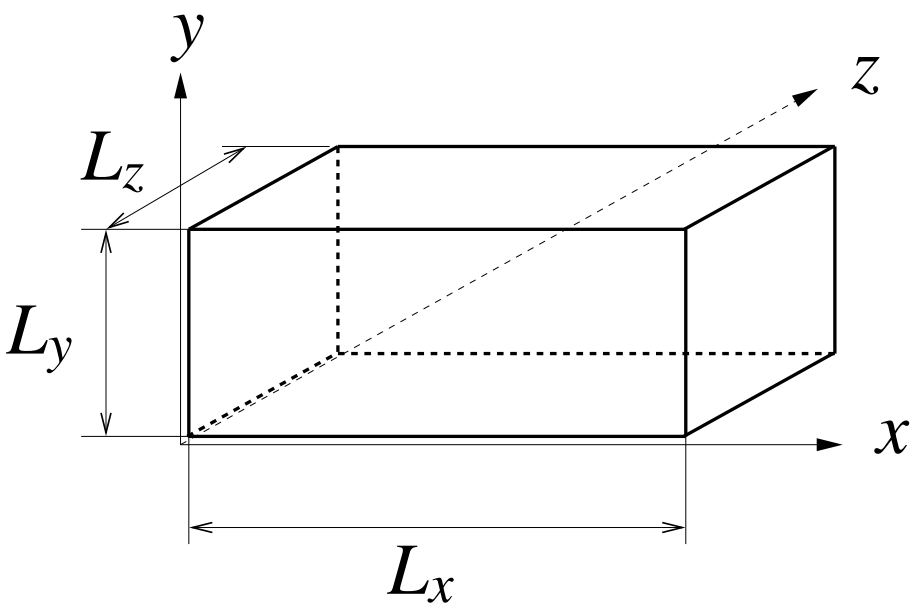

Fig. 7.1. Schematic representation of a "quantum box." An electron can move freely inside, but cannot go beyond the boundaries defined by the walls of the parallelepiped

The Schrödinger equation is a second-order differential equation. A general solution can be written for equation (7.2). We are interested in the partial solutions of this equation, which describe the states in which electrons in a given sample can be. In order to determine these partial solutions, we must formulate boundary conditions that the electron wave function satisfies.

The wave function ψ vanishes at the boundary of the "box". This requirement is a consequence of one of the principles of quantum mechanics, according to which ψ is a continuous function of coordinates and time. Therefore, the boundary conditions are as follows:

$$\begin{aligned} \psi(x=0,y,z) &= \psi(x=L_x,y,z)=0\,, \\ \psi(x,y=0,z) &= \psi(x,y=L_y,z)=0\,, \\ \psi(x,y,z=0) &= \psi(x,y,z=L_z)=0\,. \end{aligned} \tag{7.3}$$

In addition, the wave function must be normalised:

$$\int_0^{L_x} dx \int_0^{L_y} dy \int_0^{L_z} dz \, |\psi(x,y,z)|^2 = 1 \,. \tag{7.4}$$

This condition means that the electron is located only in the region bounded by the walls of the "box".

7.1.1. The wave function and spectrum

The solution of equation (7.2) can be represented as the product of three solutions of the one-dimensional Schrödinger equation:

$$\begin{aligned} \psi(x,y,z) &= \psi_x(x)\,\psi_y(y)\,\psi_z(z)\,, \\ E &= E_x + E_y + E_z\,, \end{aligned} \tag{7.5}$$

where each of the functions ψ_ξ, $\xi = x, y, z$, satisfies the following boundary value problem:

$$\begin{aligned} -\frac{\hbar^2}{2m_e}\frac{\partial^2 \psi_\xi}{\partial \xi^2} &= E_\xi \psi_\xi\,, \\ \psi_\xi(\xi = 0) = \psi_\xi(\xi = L_\xi) &= 0\,, \\ \int_0^{L_\xi} d\xi \, |\psi_\xi|^2 &= 1\,. \end{aligned} \tag{7.6}$$

The solution to this problem can be written in the following form:

$$\psi_\xi(\xi) = Ae^{ik_\xi\xi} + Be^{-ik_\xi\xi}\,, \qquad 0 \le \xi \le L_\xi\,, \tag{7.7}$$

where A, B are numerical factors. The boundary condition at the point $\xi = 0$, $\psi_\xi(0) = 0$ leads to the equality $B = -A$, from which it follows that

$$\psi_\xi(\xi) = A' \sin(k_\xi\xi)\,, \tag{7.8}$$

where $A' = 2iA$. In turn, the boundary condition at the point $\xi = L_\xi$: $\psi_\xi(L_\xi) = 0$ has the form $\sin(k_\xi L_\xi) = 0$. this condition determines the allowed values of the wave number k_ξ and the energy E_ξ corresponding to the electron wave function ψ_ξ:

$$\begin{aligned} k_\xi(n_\xi) &= \frac{\pi n_\xi}{L_\xi}\,, \quad n_\xi = 1, 2\ldots\,, \\ E_\xi(n_\xi) &= \frac{\hbar^2 k_\xi^2(n_\xi)}{2m_e} = \frac{h^2 n_\xi^2}{8m_e L_\xi^2}\,. \end{aligned} \tag{7.9}$$

The quantities k_ξ and E_ξ can be called the wave number and energy corresponding to the motion of the electron along the ξ axis.

According to (7.5) we obtain for the wave function and energy of the electron in a three-dimensional box:

$$\begin{aligned} \psi(x, y, z) &= \sqrt{\frac{2}{L_x}}\sin(k_x x)\sqrt{\frac{2}{L_y}}\sin(k_y y)\sqrt{\frac{2}{L_z}}\sin(k_z z)\,, \\ E(n_x, n_y, n_z) &= \frac{h^2}{8m_e}\left(\frac{n_x^2}{L_x^2} + \frac{n_y^2}{L_y^2} + \frac{n_z^2}{L_z^2}\right)\,. \end{aligned} \tag{7.10}$$

From the obtained equations it is clear that the permissible electron states in the sample can be numbered by a set of three integers n_x, n_y and n_z.

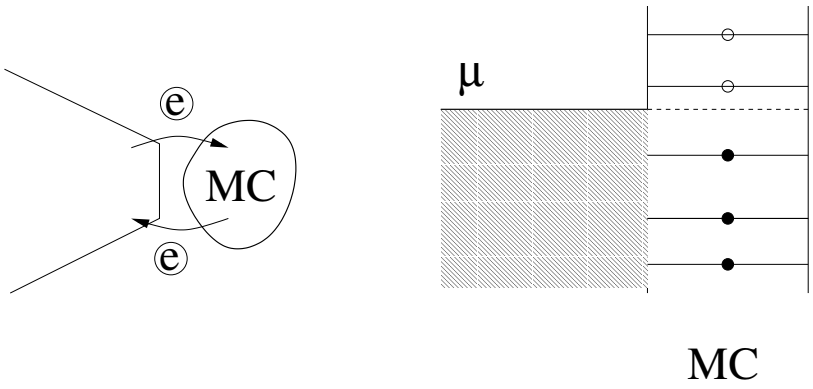

Fig. 7.2. Filling the quantum levels of a mesoscopic system (MS): black circles – filled levels; light circles – unfilled levels. The exchange of particles between the MS and the reservoir leads to the fact that all quantum levels of the MS, which have an energy less than the reservoir potential μ, are filled, and all levels with a higher energy are unfilled

7.1.2. Population of quantum levels

Let this sample be able to exchange particles with a reservoir of electrons, Fig. 7.2. Which quantum levels in the sample will be occupied and which will be free?

To answer this question, we note that in a state of thermodynamic equilibrium, a closed system, which in our case includes the electrons of the reservoir and the electrons of the mesoscopic sample, has a minimum energy:

$$\mathcal{E}_{tot} \equiv \mathcal{E}_{res} + \mathcal{E}_{MC} = \min\,, \tag{7.11}$$

where $\mathcal{E}_{tot}$ is the energy of the entire system; $\mathcal{E}_{res}$ is the energy of the reservoir; $\mathcal{E}_{MC}$ is the energy of the electrons in the sample.

The reservoir is a macroscopic system of electrons in an equilibrium state and is characterized by the value of the chemical potential μ, which in the three-dimensional case is related to the spatial density of particles n_e as follows:

$$\mu = (3\pi^2 n_e)^{\frac{2}{3}} \frac{\hbar^2}{2m_e}\,. \tag{7.12}$$

From a quantum mechanical point of view, the quantity μ is the Fermi energy, i.e. the maximum energy that electrons in a reservoir have at zero temperature. On the other hand, for a macroscopic system, the quantity μ also retains its thermodynamic meaning, namely: the chemical potential equals the change in the energy of the system when the number of particles in it changes by one.

Let us calculate by what amount $\delta\mathcal{E}_{tot}$ the energy of the system will change if one electron passes from the reservoir to the sample. The electron leaves the reservoir, so the energy of the reservoir will decrease by the amount μ, $\delta\mathcal{E}_{res} = -\mu$. In the sample, the electron will occupy an unoccupied level with the lowest energy. Let this be the level with the energy $E_{\min}^{(free)}$. Then the energy of the MS will increase by $E_{\min}^{(free)}$, $\delta\mathcal{E}_{MC} = E_{\min}^{(free)}$. In this case, the change in the energy of the entire system is, $\delta\mathcal{E}_{tot} = \delta\mathcal{E}_{res} + \delta\mathcal{E}_{MC}$,

$$\delta\mathcal{E}_{tot} = E_{\min}^{(free)} - \mu\,. \tag{7.13}$$

From here it is clear that the electron transitions from the reservoir to the sample will lead to a decrease in the energy of the system $\delta\mathcal{E}_{tot} < 0$ until all quantum levels with energy lower than the chemical potential μ of the reservoir are filled in the sample, Fig. 7.2.

Thus, if the electron energy levels in the sample are described by the equation (7.10), then at zero temperature all states satisfying the condition will be filled

$$E(n_x, n_y, n_z) = \frac{h^2}{8m_e}\left(\frac{n_x^2}{L_x^2} + \frac{n_y^2}{L_y^2} + \frac{n_z^2}{L_z^2}\right) \le \mu\,. \tag{7.14}$$

This condition determines the values of the natural numbers n_x, n_y and n_z that correspond to the filled states.

Let us estimate the value of $n_\xi^{(\max)}$, which corresponds to the occupied level with the maximum energy. To do this, we introduce the concept of the electron wavelength with the Fermi energy:

$$\lambda_F = \frac{h}{\sqrt{2m_e\mu}}\,. \tag{7.15}$$

For a 2D electron gas, $\mu_{2\mathrm{D}} = 10^{-2}\,\mathrm{eV}$, and instead of m_e, we need to use $m^* = 0,067\,m_e$ so for the Fermi wavelength we get: $\lambda_{F,2D} \approx 4,7 \times 10^{-8}\,\mathrm{m}$.

Using the value λ_F, we can estimate the number of filled states n(max) ξ , which correspond to the motion along the chosen direction $\xi = x, y, z$, as follows:

$$n_\xi^{\max} = \left[\frac{L_\xi}{\lambda_F/2}\right]\,, \tag{7.16}$$

where $[X]$ denotes the integer part of the number X. For a sample with size $L_\xi = = 10^{-6}\,\mathrm{m}$, created in a 2D electron gas, we obtain: $n_\xi^{\max} \approx 10^{-6}/(2 \times \times 10^{-8}) = 50$. In this case, the total number N of filled levels in the sample is, in order of magnitude, equal to: $N \sim n_x^{\max}\, n_y^{\max}\, n_z^{\max}$.

If the sample size in at least one measurement is less than half the Fermi wavelength

$$L_\xi < \frac{\lambda_F}{2}\,, \tag{7.17}$$

then no quantum state will be filled. No electrons will pass from the reservoir into such a sample, so at low voltage such a sample will not conduct current.

7.2. Effective dimension of a sample

Equation (7.16) allows us to classify samples in this way.

7.2.1. $0D$ - "an artificial atom or a quantum dot"

Let all three dimensions of the sample be compared with the electron wavelength λ_F, Fig. 7.3, $0D$:

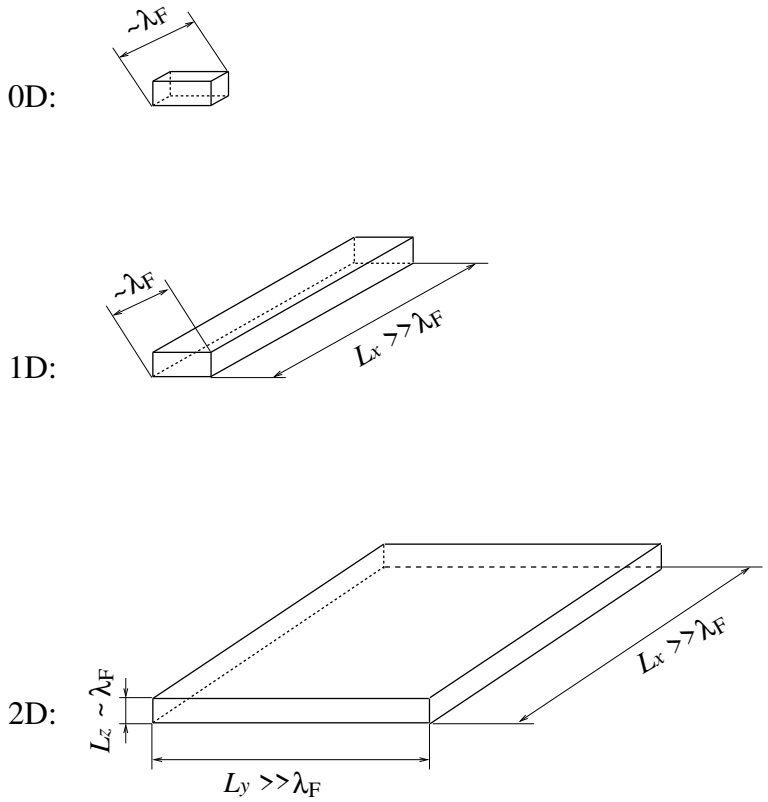

Fig. 7.3. Classification of mesoscopic conductors by dimensionality: $0D$ is a zero-dimensional conductor (a quantum dot); $1D$ is a (quasi)one-dimensional conductor; $2D$ is a (quasi)two-dimensional conductor. The wavelength λ_F of an electron with Fermi energy is a characteristic length that determines the effective dimensionality of the conductor

$$
\begin{aligned}
L_x \geq \frac{\lambda_F}{2} \;\; &\Rightarrow \;\; n_x^{(\max)} \geq 1\,, \\
L_y \geq \frac{\lambda_F}{2} \;\; &\Rightarrow \;\; n_y^{(\max)} \geq 1\,, \\
L_z \geq \frac{\lambda_F}{2} \;\; &\Rightarrow \;\; n_z^{(\max)} \geq 1\,,
\end{aligned}
\tag{7.18}
$$

then only a few states will be filled in the sample. The number of electrons N_e in the sample at zero temperature can be calculated by the formula,

$$N_e = 2 \sum_{n_x=1}^{n_x^{(\max)}} \sum_{n_y=1}^{n_y^{(\max)}} \sum_{n_z=1}^{n_z^{(\max)}} \theta\Big(\mu - E(n_x, n_y, n_z)\Big) \,. \tag{7.19}$$

Here, the coefficient 2 takes into account the presence of spin in the electron; $\theta(x)$ is the Heaviside step function,

$$\theta(x) = \begin{cases} 1\,, & x > 0\,, \\ \\ 0\,, & x < 0\,. \end{cases} \tag{7.20}$$

If $N_e \sim 1$, then in this case we say that the sample is an artificially created atom. Such objects are also called quantum dots, thereby emphasising that they do not have macroscopic dimensions in any measurement.

If each occupied level makes an additive contribution to any physical quantity X, then the value of this quantity is determined at zero temperature as follows:

$$X = 2 \sum_{n_x=1}^{n_x^{(\max)}} \sum_{n_y=1}^{n_y^{(\max)}} \sum_{n_z=1}^{n_z^{(\max)}} X(n_x, n_y, n_z)\, \theta\Big(\mu - E(n_x, n_y, n_z)\Big) \,. \tag{7.21}$$

A generalisation to the case of non-zero temperatures will be given below.

7.2.2. $1D$ - a wire

Let L_x be much greater than λ_F, Fig. 7.3, $1D$:

$$\begin{aligned} L_x &\gg \frac{\lambda_F}{2} \quad \Rightarrow \quad n_x^{(\max)} \gg 1\,, \\ L_y &\geq \frac{\lambda_F}{2} \quad \Rightarrow \quad n_y^{(\max)} \geq 1\,, \\ L_z &\geq \frac{\lambda_F}{2} \quad \Rightarrow \quad n_z^{(\max)} \geq 1\,. \end{aligned} \tag{7.22}$$

In this case, many levels corresponding to motion along the x-axis are occupied. The difference between the energies of neighbouring levels becomes extremely small $\Delta E_x \sim \mu/n_x^{(\max)} \to 0$, so the spectrum corresponding to motion along the x-axis can be considered continuous. In this case, we can rewrite the equation (7.10) for the electron energy in the following form:

$$E(p_x, n_y, n_z) = \frac{p_x^2}{2m_e} + \frac{h^2}{8m_e}\left(\frac{n_y^2}{L_y^2} + \frac{n_z^2}{L_z^2}\right) , \tag{7.23}$$

where we introduced the electron momentum $p_x = \hbar k_x$.

From equation (7.23) it follows that it is convenient to divide all energy levels into groups. To do this, we do the following. We fix some values of the natural numbers $n_y = n_y^{(0)}$ and $n_z = n_z^{(0)}$. The dependence $E(p_x, n_y^{(0)}, n_z^{(0)})$, in fact, is the spectrum of a one-dimensional particle, i.e. a particle that moves freely along the x-axis and has momentum p_x. The group of levels $E(p_x, n_y^{(0)}, n_z^{(0)})$ is called a one-dimensional sub-band. Such sub-bands are numbered by the numbers n_y and n_z.

Let us rewrite equation (7.23) in the following form:

$$E(p_x, n_y, n_z) = E(p_x) + E(n_y, n_z) , \tag{7.24}$$

where $E(p) = p^2/(2m_e)$ is the energy of the particle in the sub-band. The value $E(n_y, n_z)$, fixed for a given sub-band, is called the energy of the sub-band bottom.

How many sub-bands will have filled levels depends on the Fermi energy μ and the dimensions of the sample along the y and z axes. The numbers of sub-bands in which there will be at least one filled level are determined by the following condition, Fig. 7.4:

$$E(n_y, n_z) < \mu . \tag{7.25}$$

This inequality differs from condition (7.14) only in that we neglect the contribution of energy corresponding to the motion along the x-axis. From a formal

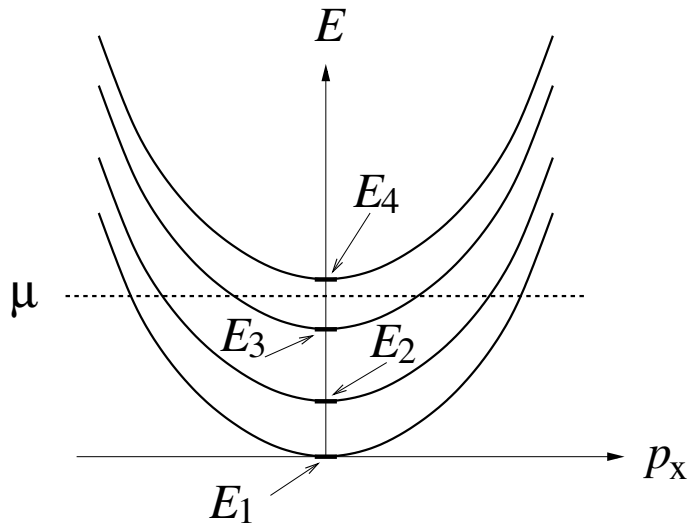

Fig. 7.4. Filling the sub-bands: E_1, E_2 and E_3 are conducting sub-bands; E_4 is a non-conducting sub-band. If the bottom of a one-dimensional sub-band has an energy lower than the Fermi energy μ, then such a sub-band contains filled energy levels and therefore contributes to the conductance.

(mathematical) point of view, this neglect is due to the fact that we assume $L_x \to \infty$. From a physical point of view, this corresponds to the fact that in the case of a continuous spectrum, the energy $E(p_x)$ can be arbitrarily small and therefore does not affect the inequality under consideration. As soon as the Fermi energy exceeds the bottom of the band, the levels corresponding to the motion along the x-axis will immediately begin to be filled.

If the filled levels are only in one sub-band $n_y = 1$, $n_z = 1$, then the sample is called one-dimensional. If several sub-bands have filled levels, then the sample is called quasi-one-dimensional.

The number of sub-bands containing filled states can be changed in various ways. For example, by changing the value of the electron potential μ of the reservoir. If the reservoir is a two-dimensional electron gas, then the electron density and, accordingly, the value of the potential are easily regulated by an external metal gate, to which a negative (about 1 V) potential is applied. Another way is to apply the potential difference $\Delta\varphi = \varphi_{MC} - \varphi$ between the sample (potential φ_{MC}) and the reservoir (potential φ). Then equation (7.25)

will take the form

$$E(n_y, n_z) + e\varphi_{MC} < \mu + e\varphi\,. \tag{7.26}$$

It can be seen that by changing the value of $\Delta\varphi$, the number of filled sub-bands $E(n_y, n_z) < \mu - e\Delta\varphi$ can be changed. In addition, the number of filled sub-bands can be changed by changing the dimensions of the sample L_y, L_z. This is convenient for conductive structures created in a two-dimensional electron gas. In this case, the boundaries of the sample are created using additional metal gates that have a negative potential. By changing the value of this potential, the geometric dimensions of the sample can be changed. We will analyze this case in more detail in the next section, where we will consider the features of the conductance of a one-dimensional ballistic bridge with a variable thickness.

The maximum energy to which the levels in a given sub-band are filled at zero temperature is called the chemical potential of the given sub-band $\mu(n_y, n_z)$. This quantity depends on the chemical potential of the reservoir μ and the sub-band number (below we assume $\Delta\varphi = 0$):

$$\mu(n_y, n_z) = \mu - E(n_y, n_z)\,. \tag{7.27}$$

Thus, in a quasi-one-dimensional sample, the chemical potentials corresponding to different one-dimensional sub-bands are different. In particular, this distinguishes a quasi-one-dimensional sample containing N sub-bands from a set of N one-dimensional samples.

Let us consider the rule of summation over energy levels in the quasi-one-dimensional case at zero temperature. In fact, the equation (7.21) remains valid. Let us show how to go from summation over discrete states, numbered by the number n_x, to integration over the "continuous" variable p_x. Strictly speaking, for finite dimension $L_x < \infty$ the quantity $p_x = \hbar k_x$ is discrete (see equation (7.9) for k_ξ –"... $\xi = x$). However, if L_x is large enough, then the difference

$$\delta p_x = p_x(n_x + 1) - p_x(n_x) = \frac{h}{2L_x} \to 0$$

is so small that when calculating physical quantities it can be replaced by its differential, $\delta p_x \to dp_x$. In this case, the summation over n_x is replaced by integration over p_x as follows (we use $1 = (2L_x/h)\delta p_x$)

$$\sum_{n_x} \equiv \frac{2L_x}{h} \sum_{n_x} \delta p_x = \frac{2L_x}{h} \int_0^{p_x^{(\max)}} dp_x = \frac{L_x}{h} \int_{-p_x^{(\max)}}^{p_x^{(\max)}} dp_x \,.$$

Here, positive and negative momentum values correspond to an electron moving in the positive and negative directions of the x-axis, respectively.

Thus, we obtain the rule for summation over the spectrum in the quasi-one-dimensional case (denoted by $p_x^{(\max)} = p_F(n_y, n_z)$):

$$X = \frac{L_x}{h} \sum_{n_y=1}^{n_y^{(\max)}} \sum_{n_z=1}^{n_z^{(\max)}} \int_{-p_F(n_y,n_z)}^{p_F(n_y,n_z)} dp_x \, X(p_x, n_y, n_z)\theta(\mu - E(p_x, n_y, n_z)) \,. \qquad (7.28)$$

As an example, let us use the equation (7.28) and calculate the number of electrons in the sample at $T = 0$. Considering that

$$\begin{aligned} p_F(n_y, n_z) &= \sqrt{2m_e\mu(n_y, n_z)} \,, \\ \mu(n_y, n_z) &= \mu - E(n_y, n_z) \,, \end{aligned}$$

we get (without taking into account the spin):

$$
\begin{aligned}
N_e &= L_x \frac{2\sqrt{2m_e\mu}}{h} \sum_{n_y=1}^{n_y^{(\max)}} \sum_{n_z=1}^{n_z^{(\max)}} \sqrt{A}\theta(A)\,, \\
A &= 1 - n_y^2 \left(\frac{\lambda_F/2}{L_y}\right)^2 - n_z^2 \left(\frac{\lambda_F/2}{L_z}\right)^2 .
\end{aligned}
\tag{7.29}
$$

Taking into account the electron spin and in the absence of an external magnetic field, the equation (7.29) should be multiplied by two

7.2.3. $2D$ - a plane

If the size of the sample in two directions, for example L_x and L_y, is much larger than the wavelength of an electron with the Fermi energy, λ_F, and in the third direction, L_z, the size of the sample is comparable to the Fermi wavelength,

$$
\begin{aligned}
L_x &\gg \frac{\lambda_F}{2}\,, \quad \Rightarrow \quad n_x^{(\max)} \gg 1\,, \\
L_y &\gg \frac{\lambda_F}{2}\,, \quad \Rightarrow \quad n_y^{(\max)} \gg 1\,, \\
L_z &\geq \frac{\lambda_F}{2}\,, \quad \Rightarrow \quad n_z^{(\max)} \geq 1\,,
\end{aligned}
\tag{7.30}
$$

then such a sample is called a quasi-two-dimensional sample, Fig. 7.5, $2D$.

The electron spectrum in a quasi-two-dimensional sample consists of a discrete part $E(n_z)$, corresponding to the quantization of the motion along the z-axis, and a continuous part, corresponding to the free motion in the plane, Fig. 7.5. Let us introduce the notation for the components of the two-dimensional momentum of the electron:

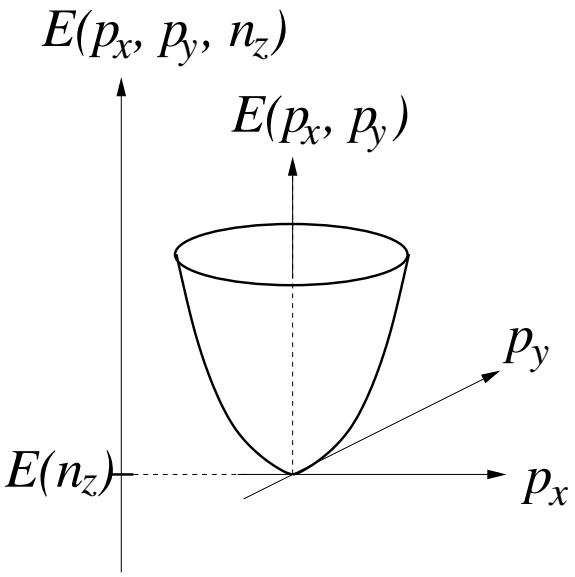

Fig. 7.5. Schematic representation of a two-dimensional energy sub-band $E(p_x, p_y)$. $E(n_z)$ is the energy of the bottom of the sub-band

$$p_x = \frac{hn_x}{2L_x}\,, \quad p_y = \frac{hn_y}{2L_y}\,.$$

Then we write the electron spectrum in the following form:

$$\begin{aligned} E(p_x, p_y, n_z) &= E(p_x, p_y) + E(n_z)\,, \\ E(p_x, p_y) &= \frac{p_x^2 + p_y^2}{2m_e}\,, \\ E(n_z) &= \frac{h^2}{8m_e L_z^2}\, n_z^2\,. \end{aligned} \tag{7.31}$$

The set of quantum energy levels corresponding to a fixed $n_z = n_z^{(0)}$ is called a two-dimensional sub-band. The quantity $E(n_z^{(0)})$ is called the bottom energy of the two-dimensional sub-band. Filled levels are only in those sub-bands for which the condition is fulfilled

$$E(n_z) < \mu\,. \tag{7.32}$$

If, at a given Fermi energy μ, only one $2D$ sub-band ($n_z^{(\max)} = 1$) is filled in the sample, then such a sample is called two-dimensional. If several sub-bands are filled, then the sample is called quasi-two-dimensional. The difference

$$\mu(n_z) = \mu - E(n_z) \tag{7.33}$$

is called the chemical potential of a given (n_z) sub-zone.

The summation over the spectrum in the quasi-two-dimensional case is written as follows:

$$X = \frac{L_x L_y}{h^2} \sum_{n_z=1}^{n_z^{(\max)}} \iint_{-p_F(n_z)}^{p_F(n_z)} dp_x dp_y\, X(p_x, p_y, n_z)\theta(\mu - E(p_x, p_y, n_z))\,. \tag{7.34}$$

For the number of electrons in the sample, we obtain (without taking into account the spin):

$$\begin{aligned} N_e &= L_x\, L_y\, \frac{2\pi m_e \mu}{h^2} \sum_{n_z=1}^{n_z^{(\max)}} \sqrt{A}\,\theta(A)\,, \\ A &= 1 - n_z^2 \left(\frac{\lambda_F/2}{L_z}\right)^2\,. \end{aligned} \tag{7.35}$$

7.2.4. 3D

Finally, let us consider the three-dimensional case, where the dimensions of the sample in three directions are much larger than the Fermi wavelength:

$$
\begin{aligned}
L_x &\gg \frac{\lambda_F}{2}\,, \;\; \Rightarrow \;\; n_x^{(\max)} \gg 1\,, \\
L_y &\gg \frac{\lambda_F}{2}\,, \;\; \Rightarrow \;\; n_y^{(\max)} \gg 1\,, \\
L_z &\gg \frac{\lambda_F}{2}\,, \;\; \Rightarrow \;\; n_z^{(\max)} \gg 1\,.
\end{aligned}
\tag{7.36}
$$

In this case, the spectrum no longer contains a discrete part and corresponds to the free motion of the electron in the volume. The components of the three-dimensional momentum of the electron are:

$$
p_x = \frac{hn_x}{2L_x}\,, \quad p_y = \frac{hn_y}{2L_y}\,, \quad p_z = \frac{hn_y}{2L_z}\,.
$$

The electron spectrum does not contain a discrete part:

$$
E(p_x, p_y, p_z) = \frac{p_x^2 + p_y^2 + p_z^2}{2m_e}\,. \tag{7.37}
$$

The electron chemical potential in the sample coincides with the electron reservoir chemical potential.

The summation over the spectrum is written as follows:

$$
X = \frac{L_x L_y L_z}{h^3} \iiint\limits_{-p_F}^{p_F} dp_x dp_y dp_z \, X(p_x, p_y, p_z)\theta\big(\mu - E(p_x, p_y, p_z)\big)\,. \tag{7.38}
$$

Number of electrons in the sample:

$$
N_e = L_x\, L_y\, L_z \frac{4\pi\,(2m_e\mu)^{\frac{3}{2}}}{3h^3}\,. \tag{7.39}
$$

The electron density $n_e = N_e/V$ (where $V = L_x L_y L_z$ is the volume of the sample) is related to the chemical potential μ by the same relation as for a macroscopic body (7.12) (the difference of two times is due to the electron spin, which was not taken into account in the equation (7.39)).

7.2.5. The temperature effect

If the temperature of the reservoir is nonzero $T \neq 0$, then the energy levels in the reservoir are filled according to the Fermi distribution function:

$$f_0(E) = \frac{1}{1 + e^{\frac{E-\mu}{k_B T}}} \,. \tag{7.40}$$

If a given sample exchanges energy and electrons with a reservoir, then in a state of thermodynamic equilibrium the distribution function for electrons in the sample is also a Fermi distribution function with the same temperature and chemical potential as in the reservoir,

$$f_{MC}(E) = f_0(E) \,.$$

In all formulas where we summed up contributions from individual quantum levels, it is necessary to take into account the probability of filling these levels, i.e., to introduce the distribution function $f_0(E)$ under the summation (or integration) sign.

For example, in the quasi-one-dimensional case, we must write:

$$X = \frac{L_x}{h} \sum_{n_y=1}^{\infty} \sum_{n_z=1}^{\infty} \int_{-\infty}^{\infty} dp_x \, f_0\big(E(p_x, n_y, n_z)\big) \, X(p_x, n_y, n_z) \,. \tag{7.41}$$

Note that for $T = 0$ we have,

$$f_0(E) = \theta(\mu - E) \,,$$

and the above equation transforms into the equation (7.28).

In the non-equilibrium case, instead of the Fermi distribution function f_0, it is necessary to use a non-equilibrium distribution function, which should be determined in each specific case separately.

Self-test questions

1. Formulate the problem statement: "electron in a quantum box".
2. Obtain the energy spectrum and eigen wave functions for an electron in a one-dimensional "quantum box".
3. Obtain the energy spectrum and eigen wave functions for an electron in a two-dimensional "quantum box".
4. Obtain the energy spectrum and eigen wave functions for an electron in a three-dimensional "quantum box".
5. Describe the level filling in a "quantum box" connected to a reservoir.
6. What is the effective size of a sample?
7. What is an energy sub-band?
8. How does temperature affect the level filling in a "quantum box"?

8. Ballistic conductor

Below we will consider one of the examples illustrating how the quantization of the spectrum affects the properties of mesoscopic samples. We will consider the conductance of a (quasi) one-dimensional ballistic bridge connecting two electron reservoirs between which a potential difference V is applied, Fig. 8.1. We will show that the conductance G changes in jumps when the width L_y of the bridge [23]. We will assume that the thickness L_z of the bridge, equal to the thickness of the two-dimensional electron layer, is fixed.

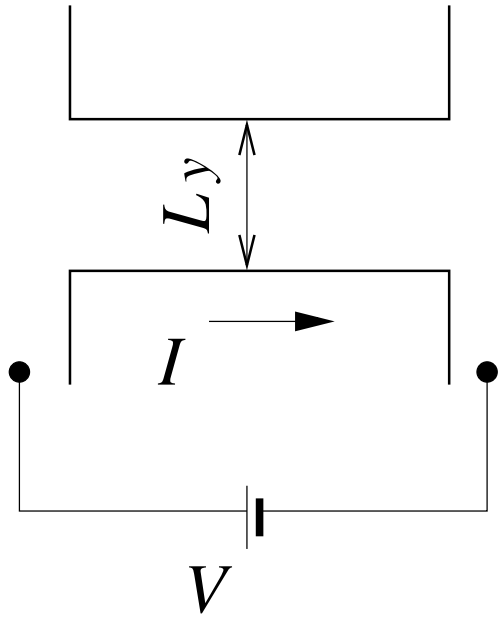

Fig. 8.1. Ballistic quasi-one-dimensional channel with width L_y. The conductance of such a channel is $G = (2e^2/h)\, N_y$, where $N_y = [L_y/\lambda_F]$ is the number of conducting one-dimensional sub-bands; $[X]$ is the integer part of X; λ_F is the wavelength of the electron with the Fermi energy

Conducting bridges, the width of which can be easily changed, are ob-

tained, in particular, in a two-dimensional electron layer formed at the boundary of the distribution between gallium arsenide (GaAs) and aluminium-doped gallium arsenide (AlGaAs), Fig. 8.2, top. The width L_y of the conducting channel is changed using control metal electrodes, depicted in the diagram by black rectangles located in the upper plane, Fig. 8.2, bottom. The two-dimensional electron gas is located in the lower plane.

If a negative potential of $V_g \sim -3V$ is applied to the metal electrodes (gates), then in the region of the geometric shadow of the gates (the projection is shown by thin dashed lines) in the two-dimensional electron gas, non-conducting regions are formed, between which a conducting channel is formed. In the figure, the non-conducting regions are limited by thick solid lines. The direction of current I is shown by an arrow. With an increase in the negative potential of the gates $-V_{g1} > -V_{g0}$, the shadow region increases (shown by thick dashed lines), which leads to a decrease in the width of the conducting channel $L_{y1} < L_{y0}$.

8.1. Conducting zones

When the width of the bridge changes, the number of one- dimensional sub-bands containing occupied levels also changes. Such sub-bands are called "conducting" because the electrons occupying the levels in these sub-bands participate in the current transfer through the bridge.

Let us define the number of conducting sub-bands N. Since the bridge thickness is fixed $L_z = L_{z0}$, we define the chemical potential of the two-dimensional layer as follows (we assume that only at $n_z = 1$ the sub-band is filled):

$$\mu_{2D} = \mu - \frac{h^2}{8m_e L_{z0}^2} \,. \tag{8.1}$$

The leading sub-zones will be those for which the condition is fulfilled

$$E(n_y) \equiv \frac{h^2 n_y^2}{8m_e Ly^2} < \mu_{2D} \,. \tag{8.2}$$

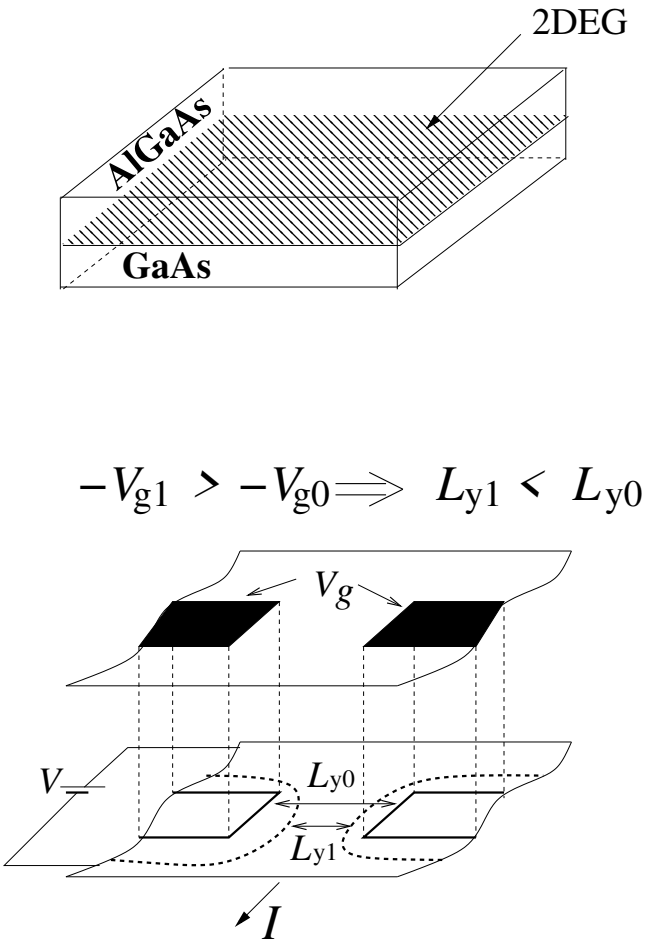

Fig. 8.2. Two-dimensional electron gas

Let us recall that the Fermi energy for electrons in a one-dimensional sub-band is:

$$\mu(n_y) = \mu_{2D} - E(n_y)\,. \tag{8.3}$$

Only those one-dimensional zones for which $\mu(n_y) > 0$ contain electrons and contribute to the current.

First, let us assume that the width of the bridge is so small that condition (8.2) is not satisfied for any subzone. This means that the energy of the trans-

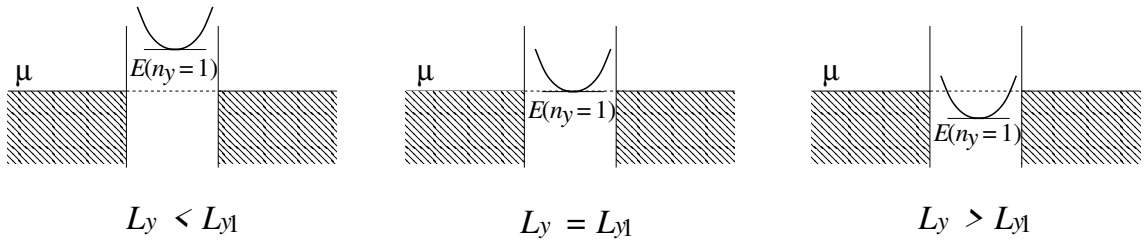

Fig. 8.3. The decrease in the bottom energy of a one-dimensional sub-band $E(n_y)$ with increasing channel width L_y. Starting from the critical value $L_y \geq L_{y1}$, when $E(n_y) \leq \mu$, this sub-band becomes conductive

verse motion $E(n_y)$ exceeds the chemical potential μ_{2D}, so the electrons in the reservoir do not have enough energy to enter the bridge, Fig.. 8.3. The energy of the transverse motion $E(n_y)$ plays the role of a kind of potential barrier.

As the width of the bridge L_y increases, the potential barrier $E(n_y)$ will decrease, since $E(n_y) \sim 1/L_y^2$. And at some value of L_{y1} the first subzone will start to fill. This will happen if the condition is fulfilled

$$E(n_y = 1) = \mu_{2D}\,, \tag{8.4}$$

$$L_{y1} = \frac{h}{2\sqrt{2m_e\mu_{2D}}} = \frac{\lambda_F}{2}\,, \tag{8.5}$$

$$\lambda_F = \frac{h}{\sqrt{2m_e\mu_{2D}}}\,.$$

Strictly speaking, at $L_y = L_{y1}$ the value of the chemical potential corresponding to this zone will be equal to zero, $\mu(n_y = 1) = 0$, so electrons will not yet start to fill this zone. However, already at $L_y > L_{y1}$ this zone will start to fill. Let us emphasize that when passing from the reservoir to the bridge, the full energy of the electron is conserved. In this case, part of the energy is spent on the transverse degree of freedom $E(n_y)$, and the remaining energy corresponds to the motion of the electron along the bridge.

With a further increase in the width of the bridge, the bottom of the second zone will fall below the chemical potential level and the second zone will start to fill. This will happen when the equality

$$\begin{aligned} E(n_y = 2) &= \mu_{2\mathrm{D}}\,, \\ L_{y2} &= \frac{2h}{2\sqrt{2m_e\mu_{2\mathrm{D}}}} = 2\,\frac{\lambda_F}{2}\,. \end{aligned} \tag{8.6}$$

And so on. The Nth sub-band will begin to fill when $L_y > L_{yN}$, where

$$L_{yN} = N\,\frac{\lambda_F}{2}\,. \tag{8.7}$$

From here it is easy to get the answer to the question: how many sub-bands will be conductive for a given bridge width L_y? The answer follows directly from equation (8.7): the number N_y of conductive sub-bands is:

$$N_y = \left[\frac{L_y}{\lambda_F/2}\right]\,. \tag{8.8}$$

Here $[X]$ is the integer part of the number. There are as many conduction sub-bands as the half Fermi wavelength fits into the width of the bridge. One Fermi half-wavelength corresponds to one conduction sub-band. The graph of the $N_y(L_y)$ dependence is an ascetic function, Fig. 8.4.

8.2. Quasi 1D conductor

conductance is defined as follows:

$$G = \lim_{V\to 0}\frac{I}{V}\,. \tag{8.9}$$

Here I is the current flowing through the bridge if a potential difference is applied to the contacts:

$$V = \varphi_{left} - \varphi_{right}\,, \tag{8.10}$$

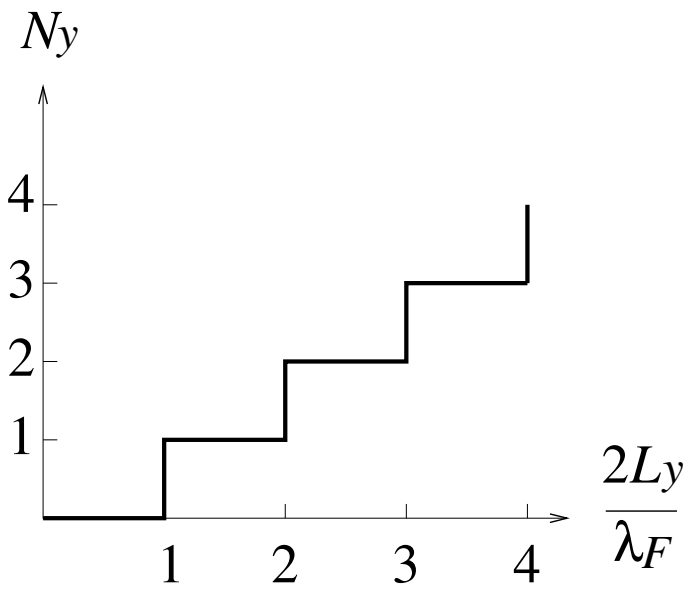

Fig. 8.4. The change in the number of conducting sub-bands N_y when the channel width L_y changes. The channel conductance $G \sim N_y$ as a function of L_y changes in steps

where $\varphi_{right(left)}$ is the potential of the right (left) reservoir.

Earlier we have already written the equation for the current in a one-dimensional conductor. In a quasi-one-dimensional conductor (when there are several conducting subzones), the difference will be that it is necessary to additionally sum over these subzones. From a physical point of view, this corresponds to the fact that the subzones simultaneously conduct current, that is, they are connected in parallel, so the currents flowing through such subzones must be added. From the formal point of view of summing the contributions of individual sub-bands, it follows that when calculating the current, it is necessary, first, to calculate the current carried by an electron in any quantum state, and, second, to sum over all states in which the electrons are. In this case, the filling of the states is taken into account by the distribution function.

Let us start with the first point. In quantum mechanics, in the absence of a magnetic field, the current density $\mathbf{j}$ carried by an electron in the state described

by the wave function $\psi(x, y, z)$ is determined by the following equation:

$$\mathbf{j}(x, y, z) = -\frac{e\hbar}{m_e}\mathrm{Im}\left[\psi(x, y, z)\vec{\nabla}\psi^*(x, y, z)\right] .$$

Here the vector operator $\vec{\nabla} = (\nabla_x, \nabla_y, \nabla_z)$ has the following projections onto the coordinate axes:

$$\nabla_x = \frac{\partial}{\partial x} , \quad \nabla_y = \frac{\partial}{\partial y} , \quad \nabla_z = \frac{\partial}{\partial z} .$$

The wave function $\psi(x, y, z)$ (7.5) is equal to the product of $\psi_x(x)$, $\psi_y(y)$ and $\psi_z(z)$. The wave functions $\psi_y(y)$ and $\psi_z(z)$ correspond to the motion across the bridge. If the side walls of the bridge are impermeable, then we have:

$$\psi_y(y) = \sqrt{\frac{2}{L_y}}\sin(k_y y) , \quad \psi_z(z) = \sqrt{\frac{2}{L_z}}\sin(k_z z) .$$

Along the x-axis, the bridge is connected to the reservoirs. We assume that the electron can pass freely (without reflection) from the bridge to the reservoir and back, therefore, to determine the coefficients A and B in the equation for the wave function (7.7):

$$\psi_x(x) = A\, e^{ik_x x} + B\, e^{-ik_x x}$$

We can use the fact that the states corresponding to different directions of the electron momentum $p_x = \hbar k_x > 0$ and $p_x = \hbar k_x < 0$ are not connected to each other. These states correspond to particles that came from different reservoir contacts. Thus, we can write

$$\psi_x(x, p_x) = \begin{cases} p_x > 0 , & Ae^{ik_x x} , \\ p_x < 0 , & Be^{-ik_x x} . \end{cases}$$

From the normalization condition

$$\int_0^{L_x} dx|\psi_x|^2 = 1$$

we find

$$A = B = \frac{1}{\sqrt{L_x}}\,.$$

Using the wave functions given above, we calculate:

$$\begin{aligned} j_x(y,z) &= \frac{ev_x}{L_x}\,|\psi_y(y)|^2\,|\psi_z(z)|^2\,, \\ j_y &= 0\,, \quad j_z = 0\,, \end{aligned}$$

where $v_x = p_x/m_e$ is the electron velocity in the bridge.

Next, we define the current $I(p_x, n_y, n_z)$, which flows through the entire cross-section of the bridge. Recall that we are considering a fixed quantum state characterized by the quantum numbers n_y, n_z and p_x. For the current, we obtain:

$$I(p_x, n_y, n_z) = \int_0^{L_y} dy \int_0^{L_z} dz\, j_x(y,z)\,.$$

Substituting the equation for the current density and for the wave functions, we find:

$$I(p_x, n_y, n_z) = \frac{ev_x}{L_x} \int_0^{L_y} dy |\psi(y)|^2 \int_0^{L_z} dz |\psi(z)|^2 =$$

$$= \frac{ev_x}{L_x} \int_0^{L_y} dy \frac{2}{L_y} \sin^2(k_y y) \int_0^{L_z} dz \, \frac{2}{L_z} \sin^2(k_z z) = \frac{ev_x}{L_x} \, .$$

Note that we would obtain the same equation for the current if we forgot about the transverse dimensions and considered the bridge to be one-dimensional. This justifies the use of the term "one-dimensional" in the characterization of the sub-bands.

Next, we consider the second point. To calculate the total current I flowing through the bridge, it is necessary to use the formula for summation over quantum states in the quasi-one-dimensional case, (7.41), in which instead of X we substitute the equation for the current $I(p_x, n_y, n_z)$, carried by one quantum state. Additionally, we take into account that an electron has a spin, so in each state we define there can be two electrons, for example, one electron with an "up" spin and the second electron with an "down" spin.

In the absence of a magnetic field, the direction of the axis, relative to which the direction "up" and "down" is determined, is not fixed. Note that such spin degeneracy is inherent in the Schrödinger equation (1.2), which does not contain spin-dependent quantities. Therefore, taking into account the electron spin (additional factor 2), the total current is:

$$I = \frac{2e}{h} \sum_{n_y=1}^{\infty} \int_{-\infty}^{\infty} dp_x \, v_x f\big(p_x, \mu(n_y)\big) \, . \tag{8.11}$$

We omitted the summation over n_z, since we assume that only one (two-dimensional) sub-band $n_z = 1$ is filled. Here v_x, p_x are the velocity and momentum of the longitudinal (along the x-axis) motion.

Since we are considering the case when a current flows through the sample and, therefore, the sample is in a nonequilibrium state, the distribution function

$f\left(p_x, \mu[n_y]\right)$ is not a Fermi distribution function. Let us define this distribution function. Its arguments indicate two important circumstances. First, the distribution function depends on the magnitude and direction of the momentum p_x. Second, the chemical potential for different sub-bands is different.

In the ballistic case, when there is no backscattering, each electron with positive momentum arrived from the left reservoir, and each electron with negative momentum from the right reservoir (we consider the direction from the left reservoir to the right reservoir to be positive, in Fig. 8.1 this direction is indicated by the arrow). Therefore, for the electron distribution function in the bridge we have:

$$\begin{aligned} f(p_x > 0) &= f_{left}(p_x)\,, \\ f(p_x < 0) &= f_{right}(p_x)\,. \end{aligned} \tag{8.12}$$

Підставимо рівняння (8.12) в рівняння (8.11) і перейдемо від інтегрування за імпульсом p_x до інтегрування за енергією E_x:

$$E_x = \frac{p_x^2}{2m_e} \quad \Rightarrow \quad dE_x = v_x\, dp_x\,.$$

As a result we get:

$$I = \frac{2e}{h} \sum_{n_y=1}^{\infty} \int_0^{\infty} dE_x \Big\{ f_{left}(p_x > 0, n_y) - f_{right}(p_x < 0, n_y) \Big\}\,. \tag{8.13}$$

From this equation it is clear that practically all the current carried to the right by electrons flying from the left reservoir is compensated by electrons flying in the opposite direction. In the equilibrium state, when the potentials of both contacts are the same, $\varphi_{right} = \varphi_{left} \Rightarrow f_{right} = f_{left}$, these so-called fluctuation currents are completely compensated by each other, and the current is absent, $I = 0$.

If the potentials of the contacts are different, $V \neq 0$, then the current $I \neq 0$ flows through the sample. Let us pay attention to the fact that, in fact, the current is carried by electrons that have an energy close to the Fermi energy (in the energy interval $\mu \pm eV/2$). Contributions to the current of electrons with energies significantly different from the Fermi energy are completely compensated and can be ignored when calculating the current.

To calculate $f_{right(left)}$, we take into account that the total energy of the electron is conserved during motion. Consider an electron that arrived from the left contact at some chosen point on the bridge, the point where we calculate the current. In the left reservoir, the electron energy was:

$$E = \frac{p^2}{2m_e} + e\varphi_{left}\,,$$

where p is the momentum of the electron in the left contact; φ_{left} is the potential of the left contact. In the bridge, the electron energy will be

$$E = \frac{p_x^2}{2m_e} + E(n_y) + e\varphi_0\,,$$

where φ_0 is the electrostatic potential at the selected point of the bridge. Equating these quantities, we obtain:

$$\frac{p^2}{2m_e} + e\varphi_{left} = \frac{p_x^2}{2m_e} + E(n_y) + e\varphi_0\,. \tag{8.14}$$

This equality relates the momentum p, which the electron had in the left contact, to the momentum p_x, which the electron has in the bridge in the one-dimensional sub-band n_y. Further, we consider that in the reservoir the distribution function is the Fermi distribution function, which depends on the kinetic energy of the electron $p^2/(2m_e)$ as follows:

$$f_0(p) = \frac{1}{1 + \exp\left(\dfrac{p^2/(2m_e) - \mu_{2\mathrm{D}}}{k_B T}\right)}\,. \tag{8.15}$$

The distribution function is the probability of filling a level. In the bridge, a level with $p_x > 0$ will be filled if the level with momentum $p = p(p_x)$ in the left reservoir is filled. The dependence $p(p_x)$ is determined by equation (8.14). Then from equation (8.15) we obtain the desired distribution function in the bridge for electrons flying from the left reservoir $p_x > 0$:

$$\begin{aligned} f_{left}(p_x > 0, n_y) &= \frac{1}{1 + \exp\left(\dfrac{E_x + e(\varphi_0 - \varphi_{left}) - \mu(n_y)}{k_B T}\right)}, \\ E_x &= \frac{p_x^2}{2m_e}, \\ \mu(n_y) &= \mu_{2\mathrm{D}} - E(n_y). \end{aligned} \tag{8.16}$$

We emphasize that we cannot directly use the function (8.15), since the equation (8.11) contains integration over p_x, not over p.

Similarly, we obtain the distribution function for electrons in the bridge, moving from the right reservoir to the left:

$$f_{right}(p_x < 0, n_y) = \frac{1}{1 + \exp\left(\dfrac{E_x + e(\varphi_0 - \varphi_{right}) - \mu(n_y)}{k_B T}\right)}. \tag{8.17}$$

Since to calculate the conductance G, (8.9), it is necessary to calculate the current I at a small voltage $V = \varphi_{left} - \varphi_{right} \to 0$, we can assume that the potential difference $\varphi_{right(left)} - \varphi_0$ is also small. Let us expand $f_{right(left)}$ in a Taylor series with a small potential difference:

$$f_{right(left)} = f(E_x, \mu(n_y)) + \frac{\partial f\big(E_x, \mu(n_y)\big)}{\partial E_x}\, e\left(\varphi_0 - \varphi_{right(left)}\right).$$

Substituting this expansion into equation (8.13), we obtain an equation for the current flowing through the bridge:

$$I = \frac{2e^2}{h} V \sum_{n_y=1}^{\infty} \int_0^{\infty} dE_x \left(-\frac{\partial f_0\big(E_x, \mu(n_y)\big)}{\partial E_x} \right) . \tag{8.18}$$

At low temperatures, $|\mu(n_y)| \gg k_B T$, the energy integral equals unity for conducting sub-bands $\mu(n_y) > 0$ and equals zero for nonconducting sub-bands $\mu(n_y) < 0$.

Equation (8.18) determines the dependence of the current on the voltage for a quasi-one-dimensional bridge with width L_y. This dependence is linear, therefore, in this case, Ohm's law is fulfilled and the conductance $G = I/V$ does not depend on the applied voltage V.

At zero temperature, $T = 0$, the dependence of the conductance G on the bridge width L_y is an ascetic function, which is completely analogous to the dependence of the number of conducting sub-bands on the bridge width (see Eq.(8.8) and Fig. 8.4):

$$G = G_0 N_y = G_0 \left[\frac{L_y}{\lambda_F/2} \right] . \tag{8.19}$$

Here $G_0 = 2e^2/h$ is the conductance quantum. From the obtained equation it is clear that the conductance of a ballistic (quasi-one-dimensional) channel can only take values that are multiples of G_0. The equation (8.19) has such a simple form because the current flowing in a one-dimensional channel, (8.13), does not depend on the energy characteristics of the electronic system. For example, the current does not depend on the Fermi energy, which is different for different conductive sub-bands. As a result, the contribution of different sub-bands to the total electrical conductance of the channel is the same and amounts to one conductance quantum G_0 from each sub-band. The equality of the contributions is due to the peculiarity of the density of states of electrons in the one-dimensional case, $dN/dE_x \sim 1/v_x$. As a result, the electron velocity v_x is reduced by the product $I(p_x)\, dN/dE_x$ and does not enter the final equation (8.18) for the current.

In 1988, the quantization of the conductanceconductance of a ballistic channel was discovered experimentally [24, 25], which became one of the most striking proofs that the quantization of electron motion significantly affects the properties of mesoscopic systems.

Note that as the temperature increases, when the temperature is compared with the distance between neighboring sub-bands, $k_B T \sim h^2/(8 m_e L y^2)$, the slopes in the $G(L_y)$ dependence are smoothed and the slope becomes linear.

Finally, let us consider how the obtained equation for conductance is related to the electrical conductivity of samples of macroscopic dimensions. To do this, we compare the conductances G_1 and G_2 of two bridges, a narrow and a wide one. In the latter case, we note that for large $N_y \gg 1$, we can replace the integer part of the number $[2L_y/\lambda_F]$ with the number $2L_y/\lambda_F$ itself. Such a replacement leads to a relative error of the result of the order of $1/N_y$, which decreases with increasing bridge width. For $L_y \gg \lambda_F$, the number of conducting sub-bands is equal to $N_y = [2L_y/\lambda_F] \approx 2L_y/\lambda_F$ with high accuracy. Therefore:

$$\begin{aligned} G_1 &= \frac{2e^2}{h}\,, \qquad\qquad \frac{\lambda_F}{2} < L_y < \lambda_F\,, \\ G_2 &= \frac{2e^2}{h}\,\frac{2L_y}{\lambda_F} = \frac{4e^2}{h^2}\,L_y\,p_F\,, \quad L_y \gg \lambda_F\,. \end{aligned} \tag{8.20}$$

We see that the conductance G_1 of a one-dimensional ballistic conductor is determined only by the world constants, such as the electron charge e and the Planck constant h. At the same time, the conductance G_2 of a wide bridge already depends on both the geometry, the width of the sample L_y, and the characteristics of the electronic spectrum, the momentum p_F of electrons with the Fermi energy.

Further, let us assume that the thickness L_z of the sample also increases. In this case, the number of conducting two-dimensional layers will also increase. For $L_z \gg \lambda_F$ we write:

$$N_z = \left[\frac{L_z}{\lambda_F/2}\right] \approx \frac{2L_z}{\lambda_F}\,.$$

The conductance in this case is:

$$G = G_0\, N_y\, N_z\,.$$

Thus, the electrical conductance of a large mesoscopic ballistic bridge is defined as follows:

$$\begin{aligned} G &= \frac{2e^2}{h}\,\frac{2L_y}{\lambda_F}\,\frac{2L_z}{\lambda_F} = \frac{8e^2}{h^3}\,S\,p_F^2\,, \qquad (8.21)\\ L_y, L_z &\gg \lambda_F\,, \end{aligned}$$

where $S = L_y L_z$ is the cross-sectional area of the bridge; $p_F = h/\lambda_F$ is the momentum of the electron with the Fermi energy.

Let us consider a macroscopic bridge with a length L_x and a cross-sectional area S. It is known that the resistance of such a sample

$$R = \rho\,\frac{L_x}{S}\,,$$

where the resistivity ρ depends on the electron mean free path li. According to the Drude–Lorentz formula [8] we have:

$$\rho = \frac{p_F}{ne^2 l_i}\,,$$

where n is the electron density, which in the three-dimensional case is determined by the following equation, see (7.12):

$$n = \frac{8\pi p_F^3}{3h^3}\,.$$

Therefore, the electrical conductivity $\Sigma = 1/R$ of the macroscopic sample is:

$$\Sigma = \frac{8e^2}{h^3} S p_F^2 \frac{l_i}{L_x} \frac{\pi}{3} .$$

In order to compare G and Σ, we take into account that when performing the quantum calculation we considered a ballistic bridge, i.e. a bridge through which the electron flies without colliding with impurities. This corresponds to the case when the path length l_i is greater than or equal to the bridge length. Substituting $l_i/L_x \sim 1$ into the above equation, we obtain:

$$\Sigma = \frac{8e^2}{h^3} S p_F^2 \frac{\pi}{3} . \tag{8.22}$$

Comparing the equations (8.21) and (8.22), we see that for the same sample, quantum and macroscopic calculations of electrical conductivity give practically coincident results $\Sigma/G = \pi/3 \approx 1,05$.

Self-test questions

1. What does the number of conducting sub-bands depend on?
2. How does the conductance of a quasi-one-dimensional ballistic bridge depend on its thickness?
3. Calculate the current carried by an electron in a certain quantum state.
4. Calculate the distribution function for electrons in the bridge belonging to a certain sub-band.
5. Calculate the current carried by electrons belonging to a certain sub-band.
6. Compare the conductivity of quantum and classical ballistic bridges.

9. Electrons on a 1D ring

Earlier, we considered how the quantization of the electron spectrum in mesoscopic samples affects the electrical conductance, a physical quantity that characterizes the phenomenon of current flowing through a sample under the action of an applied voltage. This phenomenon is inherent in both macroscopic and mesoscopic conductors. When the dimensions of the conductor are reduced, only the electrical conductance changes.

Now we will consider an example of a physical phenomenon of a fundamentally different nature, namely, a phenomenon that exists in mesoscopic samples, but completely disappears in samples with macroscopic dimensions. It is said that such phenomena disappear in the macroscopic limit, $L \to \infty$, where L is the size of the sample. This category of phenomena is characteristic only of samples with a discrete spectrum and is absent in macroscopic samples with a continuous spectrum.

In the phenomenon considered below, two effects play a significant role simultaneously. Namely, the Aharonov–Bohm effect and spectrum quantization. Together, these effects lead to the fact that at low temperatures in a normal, non-superconducting ring, which is permeated by a magnetic flux, Fig. 9.1, there is a permanent current, the magnitude of which varies periodically with the magnetic flux Φ :

$$I \sim \sin\left(2\pi\frac{\Phi}{\Phi_0}\right) . \tag{9.1}$$

Such a current is called a persistent current.

The existence of persistent currents in doubly connected non - superconducting samples (rings) was predicted by Kulik in 1970 [26] for ballistic rings, and by Büttiker, Imry, and Landauer in 1983 [27] for rings in which electrons are scattered by impurities. Persistent currents were first measured experimentally in the 1990s [28, 29, 30].

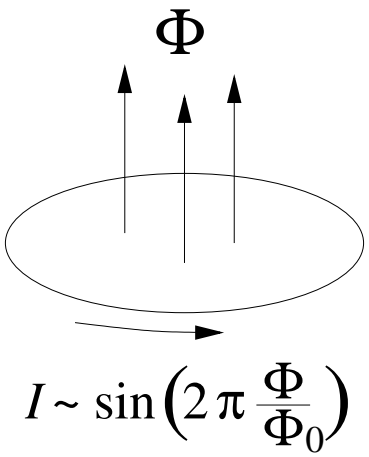

Fig. 9.1. At zero temperature, a thermodynamically-equilibrium, persistent current flows in a mesoscopic nonsuperconducting ring, penetrated by a constant in time magnetic flux Φ.

To calculate the current, it is necessary, first, to determine the spectrum of electrons in the ring, second, to calculate the current carried by an electron in a certain quantum state, and third, to sum the contributions to the current from all levels occupied by electrons, i.e., levels whose energy is less than the Fermi energy μ.

First, consider a one-dimensional ring without magnetic flux,

$$\Phi = 0\,,$$

and then we generalize the obtained results to the case when the ring is penetrated by a magnetic flux.

9.1. Ring without a magnetic field

9.1.1. Electron spectrum

To find the allowed states of electrons in the ring, it is necessary to solve the one-dimensional stationary Schrödinger equation for the electron wave function $\psi(x)$:

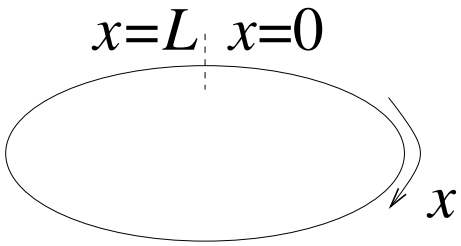

Fig. 9.2. A one-dimensional ring of length L. The arrow indicates the direction of the x-axis. The dotted line indicates the origin of the calculation.

$$-\frac{\hbar^2}{2m_e}\frac{d^2}{dx^2}\psi = E\,\psi\,. \tag{9.2}$$

The x-axis is directed along the ring, Fig. 9.2.

This equation should be supplemented with the appropriate boundary condition. When we considered a limited region of space with impermeable walls, the boundary conditions followed from the condition of non-penetration of the particle beyond the region boundary. In this case, the wave function of the electron at the region boundary turns to zero. For an electron in a ring, the situation is different, since the electron's motion along the x-axis is not limited by anything. However, after a complete revolution,

$$x \to x + L\,,$$

The electron returns to the same place, so the wave function, being a single-valued function, must be periodic in the coordinate x with a period equal to the ring length L:

$$\psi(x) = \psi(x + L)\,. \tag{9.3}$$

This equation will be the boundary condition in this case.

The wave function must be normalized, according to the fact that one quantum state can be occupied by only one electron. In the case of a ring, the normalization condition is:

$$\int_0^L dx\,|\psi(x)|^2 = 1\,. \tag{9.4}$$

According to quantum mechanics, the equation $|\psi(x)|^2\,dx$ determines the probability that a particle described by the wave function $\psi(z)$ is in the interval dx near a point with coordinate x. The integral along the perimeter of the ring determines the probability of finding a particle in the ring. Since a particle can only be in the ring, this probability must be equal to unity.

Normalized solution of the equation (9.2):

$$\psi_k(x) = \frac{1}{\sqrt{L}}\,e^{ikx}\,. \tag{9.5}$$

Note that the quantity k, which is in the exponent, is the projection of the wave vector onto the positive direction of the x-axis. Therefore, the quantity k can be both positive and negative. In the ballistic ring, there are no impurities and/or boundaries that could lead to a change in the direction of electron motion. Therefore, states with $k > 0$ and states with $k < 0$ are independent of each other and can be considered separately. The solution with a certain sign of the wave vector k corresponds to a fixed direction of electron motion.

The boundary condition (9.3) imposes the following restrictions on the allowed values of the wave vector $k = p/\hbar$:

$$\frac{1}{\sqrt{L}}\,e^{ikx} = \frac{1}{\sqrt{L}}\,e^{ik(x+L)} \quad \Rightarrow \quad e^{ikL} = 1\,.$$

From this we obtain that the wave vector k of an electron in the ring must satisfy the condition,

$$\cos(kL) = 1\,.$$

This equation has a discrete set of solutions:

$$k_n = \frac{2\pi}{L}\, n\,, \quad n = 0, \pm 1, \pm 2 \pm 3 \cdots\,. \tag{9.6}$$

Therefore, the wave vector of an electron in a ring can only take on fixed discrete values, $k = k_n$. In other words, only the values of k_n are allowed for the wave vector of an electron in a ring.

The allowed values of the energy $E_n = \hbar^2 k_n^2/(2m_e)$ are as follows:

$$E_n = \frac{h^2 n^2}{2m_e L^2}\,. \tag{9.7}$$

It should be noted that the energy of level n does not depend on the direction of motion, i.e., on the sign of n:

$$E_n = E_{-n}\,. \tag{9.8}$$

In such a case, the energy level is said to be (doubly) degenerate. This kinematic degeneracy is caused by the equivalence of clockwise and counterclockwise motion. If we take into account the spin of the electron, then the kinematic degeneracy must be supplemented by a twofold spin degeneracy. Thus, the energy levels of electrons in a ballistic ring are fourfold degenerate. We will not take into account the spin of the electron, so we will only talk about kinematic degeneracy.

Note that if the energy level corresponding to some n is occupied by an electron, then the energy level corresponding to the opposite direction of motion, i.e. $-n$, is also occupied. From here it can be understood that the total current in the ring will be zero. This happens because the current created by an electron moving clockwise will be exactly compensated by the current created by another electron, namely the one moving counterclockwise.

Such compensation is due to the fact that both states have the same energy. As a result, firstly, both states are occupied or free simultaneously and, secondly, if these states are occupied, then they make the same contribution to

the current in absolute value, since the current is proportional to the velocity, and the velocities are the same if the energies are the same. Let us confirm these qualitative considerations by formal calculations.

9.1.2. Current of a single quantum state

Let us consider the quantum mechanical equation for the current

$$I[\psi] = -\frac{e\hbar}{m_e} \operatorname{Im}\left[\psi \frac{d\psi^*}{dx}\right] \tag{9.9}$$

and we substitute here the wave function (9.5) with the wave vector (9.6). As a result, we obtain:

$$I_n = \frac{ehn}{m_e L^2} = \frac{ev_n}{L}\,, \tag{9.10}$$

where v_n is the velocity of an electron in the state with quantum number n. It is equal to:

$$v_n = \frac{p_n}{m_e} = \frac{\hbar k_n}{m_e} = \frac{hn}{m_e L}\,. \tag{9.11}$$

9.1.3. Total current

To determine the total current I flowing in the ring, we must sum over all occupied states:

$$I = \sum_{n=-\infty}^{\infty} I_n\, f_0(E_n) = \sum_{n=-\infty}^{\infty} \frac{eh}{m_e L^2}\, n\, f_0(E_n)\,. \tag{9.12}$$

The Fermi distribution function $f_0(E_n)$ shows the probability of filling a state with energy E_n. Let us take into account that $E_n = E_{-n}$, and rewrite the equation for the current in the following form:

$$I = \sum_{n=1}^{\infty} \frac{eh}{m_e L^2} f(E_n) \left\{ n + (-n) \right\} \equiv 0 \,. \tag{9.13}$$

Thus, the total current in a ring without magnetic flux is identically equal to zero.

Let us emphasize that the zero value of the total current is associated with the compensation of partial currents flowing in individual quantum states. This does not mean that there is no motion in the ring. There is motion, but due to the symmetry of the properties of the electronic system with respect to the inversion of the direction of motion, the current in a ring without magnetic flux is absent.

Based on this, we can assume that if such symmetry is broken, then a circulating current will appear in the ring. And this actually turns out to be the case.

9.2. Ring with a magnetic field

One simple way to break the rotational symmetry is to place the ring in a magnetic field perpendicular to the plane of the ring, Fig. 9.3.

We will be interested in the effect of the magnetic flux created by the magnetic field on the current in the ring. This effect is actually due to the Aaronov–Bohm effect, which arises due to the fact that the vector potential affects the phase of the electron wave function. Note that for a strictly one-dimensional ring, the effect of the magnetic field is reduced exclusively to the Aaronov–Bohm effect, if we do not take into account the electron spin and, accordingly, the Zeeman splitting. If the ring is quasi-one-dimensional, i.e. has a finite width $L_y \neq 0$, then the additional influence of the magnetic field on the kinematics of electrons in the ring is manifested in such fields B_c, when the cyclotron radius r_c (i.e., the radius of the classical electron orbit in a magnetic field) is compared with the width of the ring $r_c \sim L_y$.

Let us estimate the magnitude of the magnetic field B_{AB} , at which the Aaronov–Bohm effect is manifested, and the field B_c , at which the dynamic, force-like influence of the magnetic field begins to be felt.

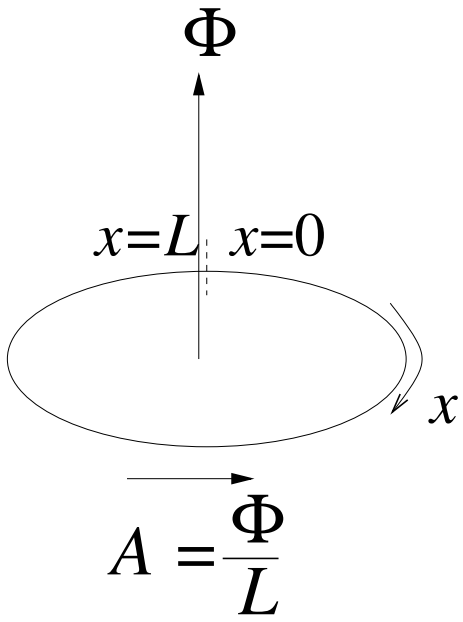

Fig. 9.3. The magnetic flux Φ directed perpendicular to the plane of the ring creates a vector potential $A = \Phi/L$ directed along the perimeter of the ring. The direction of the magnetic flux Φ and the vector potential A are shown in the figure by the corresponding arrows. The remaining notations are the same as in Fig. 9.2

As we have already discussed, the Aharonov–Bohm effect leads to the dependence of physical quantities on the magnetic flux with period $\Phi_0 = h/e$, therefore the characteristic field B_{AB} can be estimated as follows (we take the radius of the ring $R = 10^{-6}\,\mathrm{m}$):

$$BS \sim \Phi_0 \quad \Rightarrow \quad B_{AB} \sim \frac{4\pi h}{eL^2}\,,$$

$$B_{AB} \sim \frac{4\pi\, 6,62 \times 10^{-34}}{1,6 \times 10^{-19}\, 4\pi^2 \times 10^{-12}}\ \mathrm{J{\cdot}s/(C\,m^2)} \sim 10^{-3}\,\mathrm{T} = 10\,Gs\,.$$

Here the area of the ring is $S = L^2/(4\pi)$.

Let us estimate the value of B_c if the width of the ring is equal to $L_y =$

$0,1\,R$. For the electrons of a two-dimensional gas in the GaAs/ALGaAs heterostructure, the effective mass is $m^* = 0,067\,m_e$, the Fermi energy is $\mu_{2\mathrm{D}} \sim 10\,\mathrm{meV}$, therefore, the Fermi momentum is equal to ($p_F = h/\lambda_F$ $\lambda_F \sim 47 \times 10^{-9}\,\mathrm{m}$):

$$p_F = \sqrt{2m^*\mu_{2\mathrm{D}}} \sim$$

$$\sim \left(2 \times 0,067 \times 9,1 \times 10^{-31} \times 10 \times 10^{-3} \times 1,6 \times 10^{-19}\right)^{\frac{1}{2}} (\mathrm{kg} \cdot \mathrm{C} \cdot \mathrm{V})^{\frac{1}{2}} \sim$$

$$\sim 10^{-26}\ \mathrm{kg} \cdot \mathrm{m/s}\,.$$

The cyclotron radius for an electron with Fermi energy (it is particles with energies near the Fermi energy that make the main contribution to the persistent current) is:

$$r_c = \frac{m^* v_F}{eB} \sim L_y \quad \Rightarrow \quad B_c \sim \frac{p_F}{eL_y}\,,$$

$$B_c \sim \frac{10^{-26}}{1,6 \times 10^{-19} 0,1 \times 2\pi \times 10^{-6}}\ \mathrm{kg}\cdot\ \mathrm{m}/(\mathrm{s}\cdot\mathrm{C}\cdot\ \mathrm{m}) \sim 0,1\,\mathrm{T} = 1000\,\mathrm{Gs}.$$

We see that $B_c \gg B_{AB}$. And this equality holds the better, the narrower the ring, i.e. the smaller the ratio L_y/R.

So, in a not very strong magnetic field, only the Aaronov–Bohm effect is important. And we can assume that the ring is permeated by a magnetic flux, leaving aside the force action of the magnetic field that creates the magnetic flux.

9.2.1. Electron spectrum

Let the magnetic flux penetrating the ring be directed along the axis of the ring, Fig. 9.3. Then along the perimeter of the ring there exists a vector potential A such that:

$$\oint_L A dx = \Phi\,. \tag{9.14}$$

As positive, we will choose such a direction of the magnetic flux, in which the direction of the vector potential is opposite to the positive direction of the x-axis in the ring. The magnetic flux Φ corresponds to the vector potential

$$A = \frac{\Phi}{L}\,, \tag{9.15}$$

directed along the perimeter of the ring.

From quantum mechanics it is known [7] that in the presence of a vector potential, the momentum operator $\hat{p}_x$ for charged particles has the following form:

$$\hat{p}_x = -i\hbar\frac{d}{dx} - iA\,. \tag{9.16}$$

In this case, the stationary one-dimensional Schrödinger equation is:

$$\frac{\hat{p}_x^2}{2m_e}\,\psi \equiv -\frac{\hbar^2}{2m_e}\left(\frac{d}{dx} - 2\pi i\frac{\Phi}{\Phi_0}\,\frac{1}{L}\right)^2\psi = E\psi\,. \tag{9.17}$$

In the above equation, we have taken into account that the electron charge is negative and is equal to $-e < 0$.

The wave function ψ satisfies the periodicity condition (9.3), $\psi(x) = \psi(x+L)$, and the normalization condition (9.4), $\int_0^L dx\,|\psi(x)|^2 = 1$.

When solving equation (9.17), we will do the same as we already did when considering the electrical conductance of a ring with a magnetic flux. That is, we will eliminate the vector potential from the Schrödinger equation using a phase transformation for the wave function. In other words, we introduce a new function:

$$\varphi(x) = e^{-i2\pi\frac{\Phi}{\Phi_0}\frac{x}{L}}\,\psi(x)\,, \tag{9.18}$$

which satisfies the following boundary value problem:

$$-\frac{\hbar^2}{2m_e}\frac{d^2\varphi}{d^2x} = E\varphi\,, \tag{9.19}$$

$$\varphi(x+L) = e^{-i2\pi\frac{\Phi}{\Phi_0}}\varphi(x)\,, \tag{9.20}$$

$$\int_0^L dx|\varphi(x)|^2 = 1\,. \tag{9.21}$$

We see that the magnetic flux has "moved" from the Schrödinger equation to the boundary condition. This allows us to call the Aharonov–Bohm effect a topological effect, since it is caused by nontrivial boundary conditions that arise in the presence of a doubly connected, i.e., topologically nontrivial, geometry of the sample.

What is the difference and what is the similarity between the initial wave function ψ and the new function φ (9.18)? Let us emphasize once again that the real wave function is ψ. In particular, it satisfies the intuitively understandable condition of periodicity in the ring (9.3).

General properties for $\psi(x)$ and $\varphi(x)$.

1) The square of the modulus determines the probability density, therefore the normalization conditions, (9.4)and (9.21), are the same.

2) Both functions correspond to the same energy E, which follows from equations (9.17) and (9.19).

Differences between $\psi(x)$ and $\varphi(x)$.

1) These functions are solutions to different equations, see (9.17) and (9.19).

2) The functions $\psi(x)$ and $\varphi(x)$ satisfy different periodicity conditions in the ring. While the function $\psi(x)$ satisfies the normal periodicity condition, (9.3), the function $\varphi(x)$ satisfies the anomalous periodicity condition, (9.20), which depends on the magnitude of the magnetic flux Φ. Thus, if the magnetic flux equals an integer number of quanta, then the function $\varphi(x)$ satisfies the symmetric periodicity condition:

$$\Phi = n\,\Phi_0 \quad \Rightarrow \quad \varphi(x) = \varphi(x+L)\,.$$

If the magnetic flux is equal to a half-integer number of quanta, then the function $\varphi(x)$ satisfies the antisymmetric periodicity condition:

$$\Phi = \frac{\Phi_0}{2} + n\,\Phi_0 \quad \Rightarrow \quad \varphi(x) = -\varphi(x+L)\,.$$

In fact, we introduced the function $\varphi(x)$ for convenience, since the Schrödinger equation is simplified. However, this simplification requires the boundary conditions to be complicated.

Therefore, the normalized solution of equation (9.19), satisfying the periodicity condition (9.20), is as follows:

$$\begin{aligned} \varphi_n(x) &= \frac{1}{\sqrt{L}}\, e^{ik_n x}\, e^{-i2\pi \frac{\Phi}{\Phi_0}\frac{x}{L}}\,, \\ k_n &= \frac{2\pi}{L}\, n\,, \quad n = 0, \pm 1, \pm 2 \pm 3 \cdots\,, \\ E_n &= \frac{h^2}{2m_e L^2}\left(n - \frac{\Phi}{\Phi_0}\right)^2\,. \end{aligned} \tag{9.22}$$

We also present an equation for the initial wave function of an electron:

$$\psi_n(x) = \frac{1}{\sqrt{L}}\, e^{ik_n x}\,. \tag{9.23}$$

It should be noted that the quantity k_n is no longer the wave vector of the electron, but is simply a formal parameter. The wave vector (9.16), which determines the electron velocity, is the following:

$$K_n = \frac{p_n}{\hbar} = \frac{2\pi}{L}\left(n - \frac{\Phi}{\Phi_0}\right)\,.$$

The magnetic flux Φ is explicitly not included in the equation for the wave

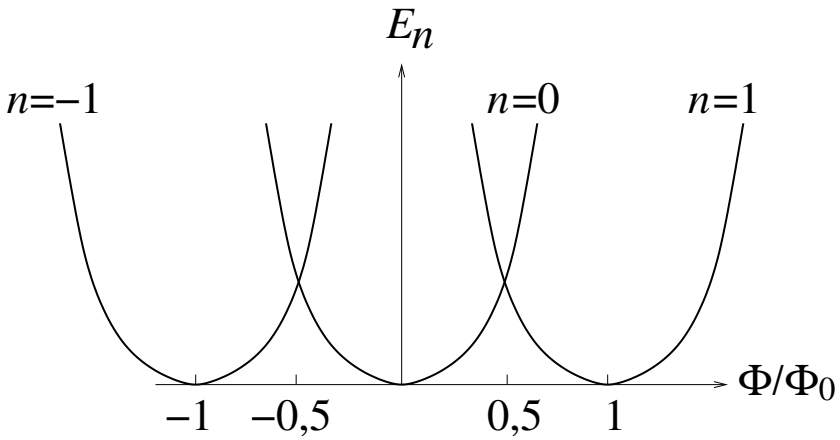

Fig. 9.4. Dependence of the energy E_n (for $n = -1, 0, +1$) of quantum levels in a one-dimensional ring on the magnitude of the magnetic flux Φ penetrating the plane of the ring. $\Phi_0 = h/e$ is the magnetic flux quantum

function $\psi_n(x)$. However, the energy E_n of the state to which the wave function $\psi_n(x)$ corresponds depends on the magnetic flux $E_n = E_n(\Phi)$.

From equation (9.22) it is clear that in the presence of a magnetic flux, the energy levels are non-degenerate - the symmetry with respect to the change in the direction of rotation is broken by the magnetic flux:

$$E_n(\Phi) \neq E_{-n}(\Phi)\,. \tag{9.24}$$

Thus, a doubly degenerate level in the presence of a magnetic flux splits into two non-degenerate levels, Fig. 9.4. In this case, the energy of the level corresponding to the clockwise motion, $n > 0$, decreases, while the energy of the level corresponding to the counterclockwise motion, $-n < 0$, increases:

$$E_{-n} - E_n = \frac{4h^2}{2m_e L^2}\, n\, \frac{\Phi}{\Phi_0}\,.$$

When the sign of the magnetic flux changes to the opposite, the level with positive n will have more energy.

Such splitting of levels in the presence of a magnetic flux leads to the appearance of a current in the ring. This is a thermodynamically-equilibrium current, undamped and non-dissipative, i.e., one that flows without the release of Joule heat.

The reason for the appearance of the current is that the quantum - mechanical currents, corresponding to the motion of electrons in opposite directions, do not compensate for each other. The equilibrium of the current is that no electromotive force is required to maintain the current.

9.2.2. Current of a single quantum state

Let us calculate the current carried by an electron in a quantum state with a wave function $\psi(x)$. In the presence of a vector potential $A = \Phi/L$, the equation for the current has the following form:

$$I[\psi] = -\frac{e\hbar}{m_e}\,\mathrm{Im}\left[\psi\,\frac{d\psi^*}{dx}\right] - \frac{e^2}{m_e}\,A\,|\psi|^2\,. \tag{9.25}$$

Let us substitute here the wave function ψ, expressed in terms of φ, (9.18), $\psi(x) = = e^{i2\pi\frac{\Phi}{\Phi_0}\frac{x}{L}}\varphi(x)$, and we obtain:

$$I[\varphi] = -\frac{e\hbar}{m_e}\,\mathrm{Im}\left[\varphi\,\frac{d\varphi^*}{dx}\right]\,. \tag{9.26}$$

Note that, just like the Schrödinger equation (9.19), the equation for the current, written in terms of the function $\varphi(x)$ does not explicitly contain the magnetic flux Φ.

Substituting the wave function $\varphi(x)$, (9.22), into equation (9.26), we find the current:

$$I_n = \frac{eh}{m_e L^2}\left(n - \frac{\Phi}{\Phi_0}\right)\,. \tag{9.27}$$

From the obtained equation it is clear that, unlike the ring without magnetic flux, in this case it is indeed

$$I_n \neq I_{-n}\,,$$

which leads to the appearance of a persistent current.

We calculated the current In using the equation for the wave function. However, comparing the equation for the current I_n, (9.27), with the equation for the energy E_n, (9.22), we see that the current can be calculated as the minus derivative of the energy level with respect to the magnetic flux:

$$I_n = -\frac{\partial E_n}{\partial \Phi}\,. \tag{9.28}$$

Or in other words, to calculate the current, it is sufficient to know the spectrum and not necessarily to calculate the wave functions.

We have obtained the relation (9.28) in the special case of non-interacting electrons in a ballistic ring. However, the equation (9.28) remains valid in the general case, when there are impurities in the ring, when the electrons interact among themselves and with other quasiparticles in the ring. The usefulness of the relation (9.28) is that, as a rule, calculating the spectrum, or rather its part, depending on the magnetic flux, turns out to be much simpler than calculating the wave function.

9.2.3. Total current

Direct calculations

To determine the total current I flowing in the ring, it is necessary to sum I_n over all occupied states:

$$\begin{aligned} I = \sum_{n=-\infty}^{\infty} I_n f_0(E_n) \;&=\; \sum_{n=-\infty}^{\infty} \left(-\frac{\partial E_n}{\partial \Phi}\right) f_0(E_n) = \\ &= \frac{eh}{m_e L^2} \sum_{n=-\infty}^{\infty} \left(n - \frac{\Phi}{\Phi_0}\right) f_0\big(E_n[\Phi]\big)\,. \end{aligned} \tag{9.29}$$

This equation is no longer exactly equal to zero, as in the case of a ring without magnetic flux. A little later we will transform the obtained equation so that the periodic dependence on the magnetic flux is obvious. Now we will show that the obtained current is actually the thermodynamic equilibrium response of the system to the magnetic flux.

Thermodynamic approach

To calculate the specified response, we recall from thermodynamics that a sample placed in an external magnetic field acquires a magnetic moment $\mathbf{M}$. The magnitude of this magnetic moment is defined as the minus derivative of the thermodynamic potential Ω of the sample with respect to the magnetic field $\mathbf{B}$:

$$\mathbf{M} = -\frac{\partial \Omega}{\partial \mathbf{B}}\,. \tag{9.30}$$

In the case we are considering, when the sample is a one-dimensional ring, the magnetic moment is the product of the current and the area of the ring $M = IS$. Dividing the left and right sides of equation (9.30) by the area of the ring S and taking into account that the product of the magnetic field and the area is the magnetic flux $BS = \Phi$, we obtain the desired relation for the current I flowing in a ring permeated by a magnetic flux Φ:

$$I = -\frac{\partial \Omega(\Phi)}{\partial \Phi}\,. \tag{9.31}$$

The above equation is quite general and valid both for particles obeying the classical laws of motion and for quantum particles. The whole difference is concentrated in the dependence of the thermodynamic potential on the magnetic field (magnetic flux). Thus, charged quantum particles are sensitive to the Aharonov–Bohm effect, therefore the thermodynamic potential for a system of quantum particles, for example, electrons, in a one-dimensional ring depends on the magnetic flux. And the persistent current I (9.31) is different from zero.

At the same time, classical particles, for example, Brownian particles diffusing along the ring, react only to the force action of the magnetic field penetrating the ring. Therefore, in weak fields $B \ll B_c$, the thermodynamic potential for such particles does not depend on the magnetic field and the current I (9.31) carried by such particles is equal to zero.

Let us now show that for electrons in the ring, equation (9.31) is identical to equation (9.29). To do this, we write an equation for the thermodynamic potential Ω of a system of electrons with a discrete spectrum E_n in the case when an exchange of energy and particles occurs with a reservoir having a temperature T and a chemical potential μ:

$$\Omega = -k_B T \sum_n \ln\left(1 + e^{\frac{\mu - E_n}{k_B T}}\right) . \tag{9.32}$$

Substituting here the electron spectrum E_n (9.22), we obtain the dependence $\Omega(\Phi)$. Differentiating with respect to the magnetic flux according to equation (9.31), we obtain exactly equation (9.29):

$$\begin{aligned} I(\Phi) = -\frac{\partial \Omega(\Phi)}{\partial \Phi} &= k_B T \sum_n \frac{\partial}{\partial \Phi} \ln\left(1 + e^{\frac{\mu - E_n}{k_B T}}\right) = \\ &= k_B T \sum_n \left(-\frac{\partial E_n}{\partial \Phi}\right) \frac{1}{k_B T} \frac{e^{\frac{\mu - E_n}{k_B T}}}{1 + e^{\frac{\mu - E_n}{k_B T}}} = \\ &= \sum_n \left(-\frac{\partial E_n}{\partial \Phi}\right) \frac{1}{1 + e^{\frac{E_n - \mu}{k_B T}}} = \sum_n \left(-\frac{\partial E_n}{\partial \Phi}\right) f(E_n) . \end{aligned}$$

Let us emphasize that the equation (9.31) connects the current in the ring with the spectrum of electrons. Whereas the equation (9.29) is actually obtained using wave functions.

Despite the fact that the formula (9.31) is widely used in the literature, in fact, it is applicable only for simple geometry. For example, for a single ring. However, when two rings are connected to each other at one point and the magnetic flux penetrates only one of the rings, the current calculated by the formula (9.25) differs from the current calculated by the formula (9.28).

The difference in the answers is due to the fact that the use of thermodynamic relations (9.28), (9.30) and (9.31) gives the correct answer for the magnetic moment of the sample observed from large (macroscopic) distances. However, a detailed distribution of microscopic currents responsible for the magnetic moment can be obtained only with a sequential quantum-mechanical consideration based on knowledge of the wave functions. Therefore, in the case of samples with complex geometry, for the correct calculation of the persistent current, it is necessary to find the wave functions and calculate the quantum-mechanical current using equation (9.25).

In conclusion, we note that Hund in his 1938 work [16] pointed out that the properties of an electron system should oscillate with the magnetic flux. In addition, Dingle in his 1952 work [17] wrote that the equilibrium properties of an electron system should depend on the magnetic flux. However, it was only in the 1959 work of Aharonov and Bohm [10] that the physical causes of such oscillations were revealed.

Self-test questions

1. What is a persistent current?
2. Determine the spectrum of electrons in a ballistic ring without magnetic flux.
3. Calculate the current in a ring without magnetic flux.
4. Determine the spectrum of electrons in a ring with a magnetic flux.
5. What is the reason for the appearance of a persistent current?
6. Calculate the current carried by an electron in a certain quantum state in a ring with a magnetic flux.

10. Properties of a persistent current

From the equation (9.22) it is clear that the value of the energy $E_n(\Phi)$ varies monotonically with a change in the magnitude of the magnetic flux Φ. However, the properties of the entire sample (the entire electronic system of the sample), as we expect, should be periodic with respect to the magnetic flux with a period of Φ_0.

To resolve this apparent contradiction, consider the total energy E of the electrons in the sample at zero temperature T = 0 as a function of the magnetic flux Φ. To calculate the energy E, it is necessary to sum the energies of all electrons in the ring. It should be noted that the electrons occupy only such states whose energy is less than the chemical potential μ:

$$E(\Phi) = \sum_{n=-\infty}^{\infty} E_n(\Phi)\theta[\mu - E_n(\Phi)]\,,$$

where $\theta(x)$ is the Heaviside theta function, which equals unity for $x > 0$ and equals zero for $x < 0$.

It is possible to directly perform the summation in the above equation. However, we will do this later, when we calculate the magnitude of the persistent current. For now, we will limit ourselves to a qualitative analysis of the above equation and show that, indeed, the total energy E is periodic in the magnetic flux.

Fig. 10.1 shows the single-electron energy levels E_n as a function of the magnetic flux. The horizontal line in the figure indicates the level of the chemical potential μ. We know that at zero temperature all levels located below the Fermi level are filled, and all levels located above are free. From Fig. 10.1 it is clear that when the magnetic flux changes, the energy of a certain level becomes greater than the Fermi energy. The electron that occupied such a level will pass from the sample to the reservoir, and the corresponding energy level in the sample will be freed. On the other hand, there is a level whose energy

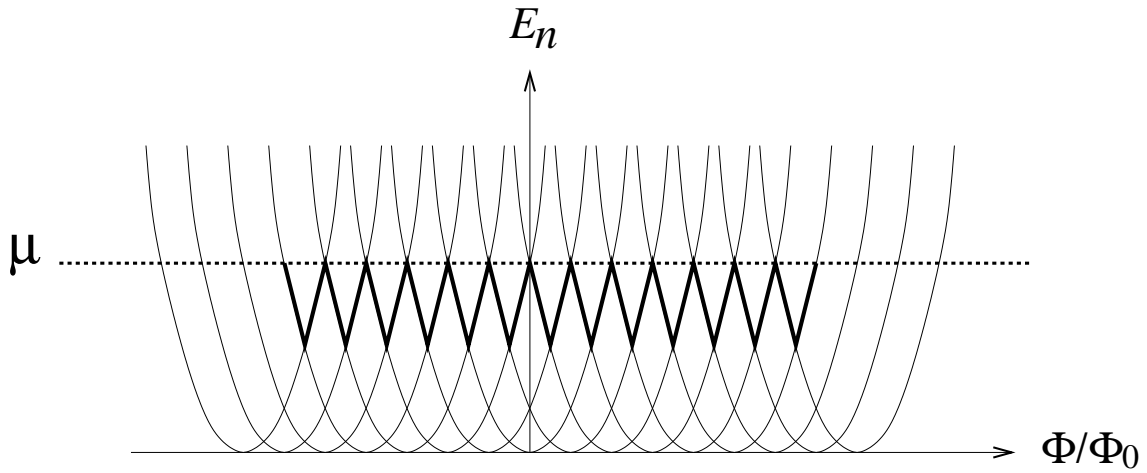

Fig. 10.1. The thick line shows the periodic change in the energy of the upper filled level when the magnetic flux magnitude Φ changes. This periodicity is the reason why the total energy of the electron system in the ring changes periodically when the magnetic flux Φ changes, despite the fact that the energy of each individual level changes monotonically with Φ. μ is the Fermi energy in the reservoir

becomes less than the Fermi energy. Such a level will be filled by an electron that has passed from the reservoir to the sample. At the same time, if we leave aside the absolute value of the numbers of filled and free levels, then the filling pattern will be repeated periodically when the magnetic flux changes by the quantum value Φ_0. That is, indeed, the energy of the entire system, which equals the sum of the energies of the filled states, is periodic in the magnetic flux with period Φ_0.

Thus, the total energy E of the system is a periodic function of the magnetic flux:

$$E(\Phi) = E(\Phi + \Phi_0)\,,$$

in the case when only those one-electron energy levels E_n that satisfy the conditions are filled in the sample

$$E_n(\Phi) < \mu\,. \tag{10.1}$$

This condition is natural for the equilibrium state. And it is this condition that leads to the fact that the internal energy of the electron system in equilibrium is periodic with respect to the magnetic flux, despite the fact that the energy of each individual single-electron level changes monotonically with a change in the magnetic flux.

It should be said that every time when the energy level crosses the Fermi level with a change in the magnetic flux Φ, it is necessary to wait for some time τ for the equilibrium filling of the levels, determined by the condition (10.1), to be established. For a ballistic ring connected to a reservoir by a point contact, characterized by a low probability of tunneling, $T \ll 1$, under the condition $E_n = \mu$, we can write $\tau \sim L/(v_F T)$. For typical values of $L \sim 10^{-6}\,\text{m}$, $v_F \sim 10^5\,\text{m/s}$, and $T = 0,01$, we obtain $\tau \sim 10^{-9}\,\text{s}$.

At the same time, with a sufficiently rapid change in the magnetic flux, the filling of the levels may not be equilibrium and the periodicity under discussion will be violated.

10.1. Analytical calculations

So, let's calculate the current I, (9.29). Since, as we expect, the persistent current is periodic with respect to the magnetic flux Φ with period Φ_0, it is convenient to represent this dependence in the form of a Fourier series. The current must become zero at $\Phi = 0$. In addition, this current must change sign when the direction of the magnetic flux changes to the opposite, since when the sign of the magnetic flux changes, the sign of the magnetic moment must change. From the above, it follows that the persistent current must be an odd function of the magnetic flux, so we can write:

$$I(\Phi) = \sum_{q=1}^{\infty} i_q \sin\left(2\pi q \frac{\Phi}{\Phi_0}\right), \tag{10.2}$$

where iq is the amplitude of the corresponding current harmonic.

In order to represent the equation (9.29) in the form of a Fourier series (10.2), we use the Poisson summation formula:

$$\sum_{n=-\infty}^{\infty} F(n) = \int_{-\infty}^{\infty} dn\, F(n) + 2\,\mathrm{Re}\left(\sum_{q=1}^{\infty}\int_{-\infty}^{\infty} dn\, F(n)\, e^{i2\pi qn}\right), \tag{10.3}$$

where $F(n)$ is an arbitrary function of an integer n. We especially emphasize that in the left-hand side n takes only integer values (discretely) while in the right-hand side n takes any real values (continuously).

As $F(n)$ we will use the product $I_n f(E_n)$ in the equation (9.29):

$$\begin{aligned} F(n) &= I_n f(E_n) \equiv \frac{eh}{m_e L^2} \frac{n - \Phi/\Phi_0}{1 + \exp\left(\dfrac{E_n - \mu}{k_B T}\right)}, \\ E_n &= \frac{h^2}{2m_e L^2}\left(n - \frac{\Phi}{\Phi_0}\right)^2. \end{aligned} \tag{10.4}$$

In this case, the equation for the current (9.29) takes the following form:

$$I(\Phi) = \int_{-\infty}^{\infty} dn\, F(n) + 2\,\mathrm{Re}\left(\sum_{q=1}^{\infty}\int_{-\infty}^{\infty} dn\, F(n)\, e^{i2\pi qn}\right). \tag{10.5}$$

First of all, let us analyze the two terms on the right side of the equation (10.5). Both of them are functions of a continuous variable n, which is integrated along the entire real axis. It can be seen from the equation (10.4) for $F(n)$ that the variable n always enters the combination $n - \Phi/\Phi_0$, so it is convenient to make the following change of variables (shift):

$$m = n - \frac{\Phi}{\Phi_0}.$$

After this replacement, the limits of integration will not change, since they are infinite, and the equation $F(m)$ will no longer depend on the magnetic flux Φ:

$$\begin{aligned} F(m) &= \frac{eh}{m_e L^2} \frac{m}{1+\exp\left(\dfrac{E_m-\mu}{k_B T}\right)}\,, \\ E_m &= \frac{h^2 m^2}{2 m_e L^2}\,. \end{aligned} \tag{10.6}$$

The magnetic flux remains only in the second term of the right-hand side in the exponential factor:

$$I(\Phi) = \int_{-\infty}^{\infty} dm\, F(m) + 2\,\mathrm{Re}\left(\sum_{q=1}^{\infty} \int_{-\infty}^{\infty} dm\, F(m)\, e^{i2\pi q m}\, e^{i2\pi q \frac{\Phi}{\Phi_0}}\right)\,. \tag{10.7}$$

Since $F(m)$ (10.6) is an odd function of m, the first integral vanishes identically. Finally, we can write

$$I(\Phi) = 2\,\mathrm{Re}\left[\sum_{q=1}^{\infty} J(q)\, e^{i2\pi q \frac{\Phi}{\Phi_0}}\right]\,, \tag{10.8}$$

where the value of $J(q)$ does not depend on the magnetic flux:

$$J(q) = \int_{-\infty}^{\infty} dm\, F(m)\, e^{i2\pi q m}\,. \tag{10.9}$$

From the equation (10.8) it is clear that, indeed, the current is periodic with respect to the magnetic flux with period Φ_0:

$$e^{i2\pi q \frac{\Phi+\Phi_0}{\Phi_0}} = e^{i2\pi q \frac{\Phi}{\Phi_0}}\, e^{i2\pi q} = e^{i2\pi q \frac{\Phi}{\Phi_0}} \times 1\,.$$

We further note that $J(q)$ is an imaginary quantity. To verify this, we consider that $F(m)$ (10.6) is an odd function of the variable m, therefore:

$$\int_{-\infty}^{\infty} dm\, F(m)\, \cos 2\pi q m \;\equiv\; 0\,,$$

$$\int_{-\infty}^{\infty} dm\, F(m)\, \sin 2\pi q m \;\neq\; 0\,.$$

As a result, the equation (10.8) for the current I will become:

$$I(\Phi) = -2\sum_{q=1}^{\infty} \mathrm{Im}\big[J(q)\big]\, \sin\left(2\pi\, q\, \frac{\Phi}{\Phi_0}\right). \tag{10.10}$$

So, we have presented the equation for the current in the form of a Fourier series. The amplitudes of the current harmonics are as follows:

$$i_q = -2\,\mathrm{Im}\big[J(q)\big]\,.$$

We see that the current is indeed an odd and periodic function of the magnetic flux Φ with period Φ_0, as we assumed.

Next, we need to calculate the value of $J(q)$. Let's take into account that only the even part of the integrand affects the value of the integral. In this case, the value of the integral over the positive half-axis of the variable m is equal to the value of the integral over the negative half-axis, so we get:

$$\begin{aligned} J(q) &= \frac{2eh}{m_e L^2} \int_0^{\infty} dm\, \frac{m\, e^{i2\pi q m}}{1 + \exp\left(\dfrac{E_m - \mu}{k_B T}\right)}\,, \\ E_m &= \frac{h^2 m^2}{2 m_e L^2}\,. \end{aligned} \tag{10.11}$$

The integrand contains an oscillating function of the variable integration. Therefore, if the remaining factors change slowly with m, the integral will be close to zero. It follows that the main contribution to the integral comes from the integration region near the Fermi energy $E_m \sim \mu$, where the Fermi distribution function changes from unity for $E_m < \mu$ to zero for $E_m > \mu$. In this region, we can use the following expansion:

$$\begin{aligned} E_m - \mu &= \frac{h^2 m^2}{2m_e L^2} - \frac{h^2 m_F^2}{2m_e L^2} = \\ &= \frac{h^2 \left(m + m_F\right)\left(m - m_F\right)}{2m_e L^2} = \Delta_F \left(m - m_F\right), \end{aligned}$$

where we assume that $m \approx m_F$ for $E_m \sim \mu$. Here Δ_F is the distance between quantum levels near the Fermi energy, and m_F is the quantity m corresponding to the Fermi energy $E_m = \mu$:

$$\begin{aligned} \Delta_F \equiv E_{m+1} - E_m &= \frac{m_F h^2}{m_e L^2} = \frac{h v_F}{L}, \\ m_F &= \sqrt{\frac{2m_e L^2 \mu}{h^2}} = \frac{L}{\lambda_F}. \end{aligned}$$

Let us introduce a new integration variable $x = \Delta_F(m - m_F)/(k_B T)$ into the equation (10.11) and write:

$$J(q) = \frac{2ehm_F}{m_e L^2} \frac{k_B T}{\Delta_F}, e^{i2\pi q m_F} \int\limits_{-\infty}^{\infty} dx \, \frac{e^{i2\pi q x \frac{k_B T}{\Delta_F}}}{1 + e^x} \left(1 + x \frac{k_B T}{\Delta_F} \frac{\lambda_F}{L}\right). \qquad (10.12)$$

In the integrand we substitute $1/m_F = \lambda_F/L$. For a not very small ring $L \gg \lambda_F$, we can consider the equation in parentheses to be equal to unity. Using the value of the integral

$$\int_{-\infty}^{\infty} dx \, \frac{e^{i\alpha x}}{1+e^{x}} = (-1)\,\frac{i\pi}{\sinh(\alpha\pi)}$$

and considering that in our case the parameter α is:

$$\alpha = 2\pi k\,\frac{k_B T}{\Delta_F}\,,$$

we get that the equation (10.12) takes the following form:

$$\mathrm{Im}\big[J(q)\big] = -\frac{2\pi e h m_F}{m_e L^2}\frac{k_B T}{\Delta_F}\frac{\cos(2\pi q m_F)}{\sinh\left(2\pi^2 q\frac{T}{\Delta_F}\right)}\,.$$

Substituting J(q) into (10.10), we find the final equation for the current:

$$\begin{aligned} I(\Phi) &= \sum_{q=1}^{\infty} i_q \sin\left(2\pi q\frac{\Phi}{\Phi_0}\right)\,, \\ i_q &= I_0\frac{2}{\pi}\frac{T}{T^*}\frac{\cos\left(2\pi q\dfrac{L}{\lambda_F}\right)}{\sinh\left(q\dfrac{T}{T^*}\right)}\,. \end{aligned} \tag{10.13}$$

We have introduced a notation for the characteristic value of persistent current:

$$I_0 = \frac{e v_F}{L}$$

and for the crossover temperature:

$$T^* = \frac{\Delta_F}{2\pi^2 k_B}\,,$$

above which the current is exponentially small.

Macroscopic limit

The magnitude of the current I decreases with increasing ring size L, so the persistent current is absent in the macroscopic limit, $L \to \infty$.

At zero temperature, the current decreases as $1/L$. However, at finite temperatures, the current decreases with increasing ring size much faster. This is due to the fact that the crossover temperature $T^*(L) \sim 1/L$ decreases with increasing L. Therefore, at a fixed temperature T, the persistent current decreases exponentially with increasing ring length, if $L \gg L^*(T)$::

$$I \sim e^{-\frac{T}{T^*}} \sim e^{-\frac{L}{L^*(T)}} ,$$

where the critical size is:

$$L^*(T) = \frac{h v_F}{2\pi^2 k_B T} .$$

Below we will estimate the values of the quantities characterizing the persistent current.

10.2. Numerical extimates

10.2.1. Current amplitude

Let us estimate the current amplitude:

$$I_0 = \frac{e v_F}{L} .$$

For a ring with size $L \sim 10^{-6}$ m and for the Fermi velocity of electrons in a $2D$ gas $v_F \sim 10^4$ m/s, we obtain:

$$I_0 \sim 10^{-9} A .$$

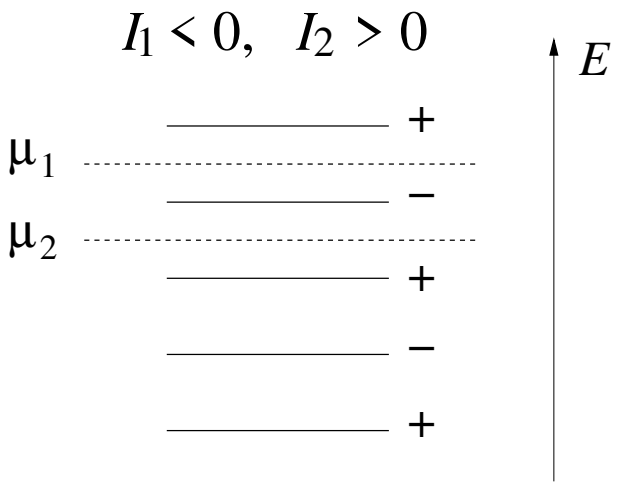

Fig. 10.2. The signs "+" and "-" indicate the direction of the currents carried by electrons at successive energy levels in a one-dimensional ballistic ring, which is penetrated by a magnetic flux $\Phi/\Phi_0 \neq 2\pi n$, $2\pi(n+0,5)$. The total current is determined by the current carried by the upper occupied level, therefore, when the Fermi energy changes from μ_1 to μ_2, the current in the ring changes direction to the opposite

From the equation for the current amplitude $I_0 = e\,v_F/L$ it follows that, in fact, the persistent current is created by a single electron with Fermi velocity, which moves along the ring. This happens because in the presence of a magnetic flux, the energy levels corresponding to the electron's clockwise and counterclockwise motion in the ring alternate, Fig. 10.2. In addition, with an increase in the energy of the level, the contribution to the current from this level increases, since the electron velocity increases. Therefore, if we consider the contribution to the current from several successive levels, we find that the contribution of each subsequent level compensates for the contribution of the previous level and adds a small amount over and above it. As a result, firstly, the current changes sign when the number of filled levels changes, that is, when the number of particles in the ring changes. This is the so-called parity effect. And, secondly, the magnitude of the total current, in fact, coincides with the magnitude of the current created by the electron in the upper filled level.

We can say that the persistent current is created by an electron moving in a circular orbit in an artificially created atom (ring). Let us compare the

magnitude of this current with the current that would be created by an electron moving in a flat circular orbit in the ground state of the hydrogen atom. However, it should be said that this example is used only for numerical comparisons, since in the hydrogen atom the electron moves in a spherical orbit and does not create an orbital magnetic moment. Thus, for the first Bohr orbit we have $R \sim 5 \times 10^{-11}\,\mathrm{m}$ and $v_1 \sim 5 \times 10^6\,\mathrm{m/s}$. As a result, we find the current

$$I_a \sim 10^{-3}\mathrm{A}\,.$$

Thus, the current in the ring is much smaller than the current in the atom:

$$\frac{I_0}{I_a} \sim 10^{-6}\,.$$

However, it is impossible to measure the electron current in an experiment. Usually, the magnetic moment created by the current $M \sim IS$ is measured, where S is the area covered by the current. Let us compare the corresponding magnetic moments:

$$M \sim IS = \frac{ev}{L}\frac{L^2}{4\pi} = \frac{ev}{4\pi}L\,.$$

We see that the value of M increases with increasing orbital size L, so the magnetic moment of the persistent current in the artificial atom (ring) turns out to be larger than the orbital magnetic moment of an electron in a regular atom:

$$\frac{M_0}{M_a} \sim \frac{I_0}{I_a}\left(\frac{L}{2\pi R}\right)^2 \sim 10\,.$$

10.2.2. Crossover temperature

Let us estimate the value T^*, which separates the region of low temperatures, $T \ll T^*$, where the persistent current does not depend on temperature,

from the region of high temperatures, $T \gg T^*$, where the persistent current is exponentially reduced. Considering that

$$\Delta_F = \frac{h v_F}{L},$$

for $L \sim 10^{-6}\,\mathrm{m}$ and $v_F \sim 10^4\,\mathrm{m/s}$ we obtain:

$$T^* = \frac{\Delta_F}{2\pi^2 k_B} \sim 25 \times 10^{-3}\,K\,.$$

The crossover temperature is quite low. Note that this temperature is actually an order of magnitude smaller than the energy level separation Δ_F.

10.3. Temperature dependence of a current

Let us analyze the dependence of the persistent current (10.13) on temperature. We will assume that the temperature remains low enough so that the state of electrons in the ring remains coherent and that the consideration based on the solution of the Schrödinger equation remains valid. That is, we will assume that one of the main conditions characteristic of mesoscopics is fulfilled, namely, that the phase failure length $L_\varphi(T)$ is much larger than the dimensions of the ring $L_\varphi(T) \gg L$. However, even under this condition, the dependence on temperature is significant, Fig. 10.3.

10.3.1. Low temperatures

At low temperatures

$$T \ll T^*$$

we can put in the equation for current (10.13)

$$\sinh\left(q\,\frac{T}{T^*}\right) \approx q\,\frac{T}{T^*}\,.$$

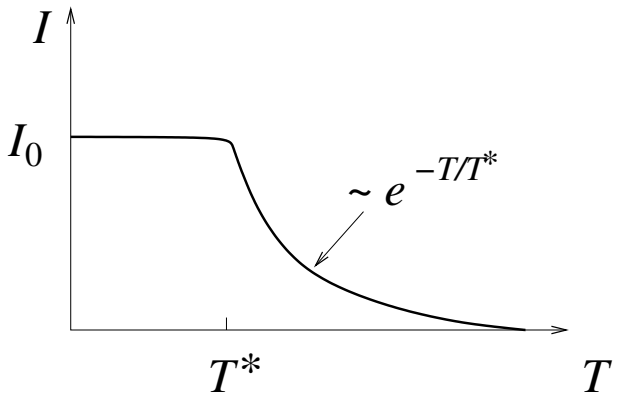

Fig. 10.3. The dependence of the persistent current on temperature T. Below the crossover temperature, $T < T^*$, the current is independent of temperature. Above the crossover temperature, $T > T^*$, the current decreases exponentially

Substituting this into (10.13), we get:

$$I(\Phi) = I_0 \frac{2}{\pi} \sum_{q=1}^{\infty} \frac{\cos\left(2\pi q \dfrac{L}{\lambda_F}\right)}{q} \sin\left(2\pi\, q \frac{\Phi}{\Phi_0}\right) . \qquad (10.14)$$

Thus, within the limits of low temperatures, the dependence $I(\Phi)$ contains various harmonics with periods Φ_0/q. The magnitude of the persistent current does not depend on temperature, but, in addition to the dependence on the magnetic flux, it also depends on the Fermi energy. The latter dependence is contained in the factor $\cos(2\pi qL/\lambda_F)$.

In the general case, at low temperatures, the dependence $I(\Phi)$ has a sawtooth shape with a period of Φ_0 (see below, Fig. 10.4 and Fig. 10.5). The jump-like change in the magnitude of the current is due to the fact that when the magnetic flux changes, one of the energy levels $E_n(\Phi)$ in the ring crosses the Fermi level, Fig. 10.1. At each such intersection, as we have already discussed earlier, the number of electrons in the ring changes by one. At the same time, the direction of the electron movement in the upper filled level changes, which changes the sign of the current to the opposite. Such a change corresponds to a jump in the dependence of the current on the magnetic flux.

At the same time, for some selected values of the chemical potential μ, the number of particles in the ring does not change when the magnetic flux changes. This is the case depicted in Fig. 10.1. The position of the chemical potential relative to the energy levels in a zero magnetic field is important. If the Fermi energy coincides with one of the energy levels or is located exactly in the middle between neighbouring doubly degenerate levels, then when the magnetic flux changes, the chemical potential level will be crossed simultaneously by two energy levels: one of them will be released, and the other will be filled with an electron. In this case, the total number of particles in the ring remains unchanged. However, since the currents carried by electrons in the intersecting levels are different, the direction of the current in the ring will also change to the opposite. In this case, the equation for the current takes the simplest form. Here, two cases are possible.

Even number of particles in a ring

If at $\Phi = 0$ the chemical potential μ coincides with one of the doubly degenerate energy levels E_{n_0} in the ring, then the total number of electrons N_e in the ring is even and does not change when the magnetic flux changes:

$$N_e = 2n_0 \,.$$

In this case, the length of the ring is a multiple of the Fermi wavelength:

$$L = n_0 \, \lambda_F \,.$$

The multiplier in the equation (10.14), which contains the ratio L/λ_F, is the same for all harmonics q:

$$\cos\left(2\pi q \frac{L}{\lambda_F}\right) = \cos(2\pi n_0 q) = 1 \,.$$

The equation for current (10.14) takes the following form:

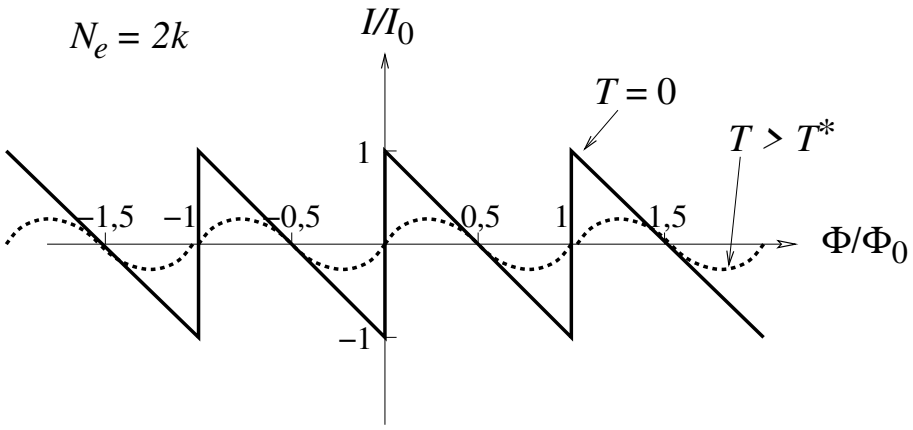

Fig. 10.4. The dependence of the persistent current I on the magnetic flux Φ for a ring with an even number of electrons $N_e = 2k$ is shown at zero temperature $T = 0$ (solid line) and at a temperature higher than the crossover temperature: $T > T^*$ (dashed line). $I_0 = ev_F/L$ is the current amplitude; $\Phi_0 = h/e$ is the magnetic flux quantum

$$I_{2N}(\Phi) = I_0 \frac{2}{\pi} \sum_{q=1}^{\infty} \frac{1}{q} \sin\left(2\pi q \frac{\Phi}{\Phi_0}\right) .$$

Applying the inverse Fourier transform to this equation, i.e., summing the series over q, we find:

$$\begin{aligned} I_{2N}(\Phi) &= -I_0 \left(2\frac{\Phi}{\Phi_0} - 1\right) , \quad 0 < \Phi < \Phi_0 , \\ I_{2N}(\Phi) &= I_{2N}(\Phi + \Phi_0) . \end{aligned} \tag{10.15}$$

The graph of this dependence is shown in Fig. 10.4, solid curve.

Odd number of particles in the ring

If at $\Phi = 0$ the chemical potential μ is exactly in the middle between the doubly degenerate energy levels E_{n_0} and E_{n_0+1}, then the total number of

electrons N_e in the ring is odd and does not change when the magnetic flux changes:

$$N_e = 2n_0 + 1\,.$$

Note that the level with $n = 0$ is nondegenerate and contains one electron, and the remaining levels are doubly degenerate. At zero temperature (the case we are considering) the levels with $n \leq n_0$ contain two electrons, and the levels with $n > n_0$ are not filled.

In this case, the ratio of the ring length to the Fermi wavelength is:

$$\frac{L}{\lambda_F} = n_0 + \frac{1}{2}\,.$$

In this case, the factor in the equation (10.14) containing this relation is:

$$\cos\left(2\pi q \frac{L}{\lambda_F}\right) = \cos\left[2\pi\left(n_0 + 0,5\right)q\right] = \cos(\pi q) = (-1)^q\,.$$

The equation for current (10.14) takes the following form:

$$I_{2N+1}(\Phi) = I_0\,\frac{2}{\pi}\sum_{q=1}^{\infty}\frac{(-1)^q}{q}\,\sin\left(2\pi q\,\frac{\Phi}{\Phi_0}\right)\,.$$

The inverse Fourier transform results in the following:

$$\begin{aligned} I_{2N+1}(\Phi) &= -2I_0\,\frac{\Phi}{\Phi_0}\,, \quad -\frac{\Phi_0}{2} < \Phi < \frac{\Phi_0}{2}\,, \\ I_{2N+1}(\Phi) &= I_{2N+1}(\Phi + \Phi_0)\,. \end{aligned} \tag{10.16}$$

The graph of this dependence is shown in Fig. 10.5.

It should be noted that the dependence (10.16) can be obtained from the

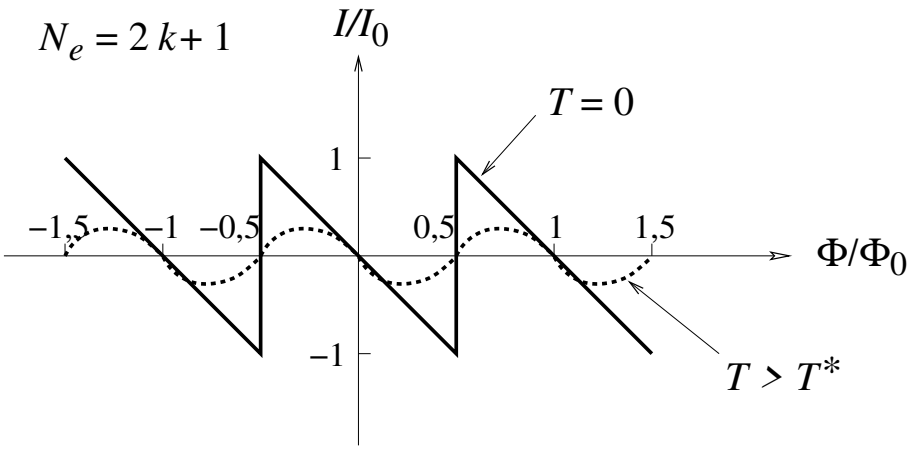

Fig. 10.5. The dependence of the persistent current I on the magnetic flux Φ for a ring with an odd number of electrons $N_e = 2k+1$. The notation is the same as in Fig. 10.4.

dependence (10.15) by shifting it by half a period:

$$I_{2N}(\Phi) = I_{2N+1}(\Phi + \Phi_0/2)\,.$$

This can be interpreted as follows. Each electron brings with it into the ring an effective magnetic flux equal to half a quantum $\Phi_0/2$, which must be added to the external magnetic flux. Two electrons make a total contribution equal to one quantum of flux, which can be ignored due to the periodicity.

10.3.2. High temperatures

Тепер розглянемо високі температури:

$$T \gg T^*\,.$$

The denominator in the equation for the amplitude of current harmonics (10.13) becomes large and increases with increasing harmonic number q:

$$\sinh\left(q\,\frac{T}{T^*}\right) \sim \frac{1}{2}\,e^{q\frac{T}{T^*}} \gg 1\,.$$

Therefore, the amplitude of the first harmonic of the current i_1 turns out to

be dominant. Therefore, the magnitude of the current decreases exponentially with increasing temperature, and the shape of the dependence of the current on the magnetic flux becomes sinusoidal:

$$I \approx I_0 \frac{4}{\pi} \frac{T}{T^*} e^{-T/T^*} \cos\left(2\pi \frac{L}{\lambda_F}\right) \sin\left(2\pi \frac{\Phi}{\Phi_0}\right) . \tag{10.17}$$

The exponential dependence on temperature and the smooth dependence on magnetic flux are a consequence of the temperature blurring of the edge of the Fermi distribution function. At high temperatures, a change in the magnetic flux does not lead to a change in the number of particles in the ring, so there are no sharp breaks in the dependence of the current on the magnetic flux. Compensation of contributions from partially filled levels leads to an exponential decrease in the current value with increasing temperature.

10.4. Parity effect

From equations (10.15) and (10.16) it is clear that the nature of the dependence of the persistent current on the magnetic flux strongly depends on the number of particles in the ring. If the number of particles in the ring is odd, then the response of the electronic system in a zero field is diamagnetic, i.e., the induced magnetic moment of the ring is opposite in sign to the applied magnetic flux. The magnitude of the diamagnetic moment is proportional to the magnetic flux and, therefore, vanishes at $\Phi \to 0$. The response of a ring with an even number of particles is paramagnetic, i.e., the induced magnetic moment of the ring coincides in sign with the applied magnetic flux. Unlike the diamagnetic moment, the magnitude of the paramagnetic moment is finite at $\Phi \to 0$.

This effect is called the parity effect. The parity effect, i.e., a significant, and moreover, periodic, change in the properties of a sample when the number of particles in it changes, is quite common in mesoscopics. A persistent current exhibits the parity effect because neighboring energy levels carry a current in the opposite direction. It should be noted that this is true only for simple geometry. In samples with a more complex shape, for example, in a ring with

a small conductor attached to it, entire groups of consecutive quantum levels carry a current in the same direction. In this case, the parity effect is modified.

In addition, we did not take into account the electron spin. If we take it into account, each energy level will be additionally doubly degenerate. In this case, for the persistent current, the number of electrons in the ring modulo 4 turns out to be significant. Only when the number of electrons in the ring changes by four does the dependence $I(\Phi)$ remain unchanged.

Self-test questions

2. How does the amplitude of the persistent current change with temperature?
3. How does the amplitude of the persistent current change with increasing ring size?
4. What is the parity effect for the persistent current?
5. What is the crossover temperature for a persistent current and what does it depend on?
6. How does the persistent current depend on the magnetic flux at low temperatures? How does the parity effect manifest itself in this case?
7. What is the peculiarity of the persistent current at high temperatures? Does the parity effect manifest itself in this case?

11. Coulomb blockade effect

Using the example of a persistent current, we have seen that the motion of a single electron can determine a completely measurable effect in mesoscopic samples. In this regard, it is natural to assume that the discreteness of the electric charge is also essential for mesoscopics. Indeed, there are conditions under which the discreteness of the charge significantly affects the properties of mesoscopic samples [31, 32, 33].

It should be said that the question of the influence of the discreteness of the charge on the properties of solids has a long history. Actually, the measurement of the electron charge itself became possible due to the fact that such an influence is significant and can be studied experimentally. Thus, as early as 1911, Milliken measured the charge of an electron by observing the motion of a suspension of microscopic oil droplets. Later, the effect of single electron tunneling on the properties of granular films was experimentally studied in the works of Giaever and Zeller (1968) [34], Lambe and Jaklevic (1969) [35], and others. It should be emphasised that, unlike the above-mentioned works, in which, in fact, a collection of small granules was studied, the mesoscopic stage of development is associated with the possibility of studying a separately taken sample, a single granule.

11.1. Charge quantisation in a small island

In order for the effect of the charge of one electron to be noticeable, it is necessary, firstly, that the energy scale associated with charging the sample with a charge of 1e be comparable to other energy scales characteristic of the given sample, for example, temperature. And, secondly, it is necessary that the sample retain its charge for a sufficiently long time. For this, the sample must be well insulated from the environment. In particular, electrical contacts must be connected to such a sample using tunnel contacts with low transparency.

Let us estimate the scale of the energy associated with a change in the sam-

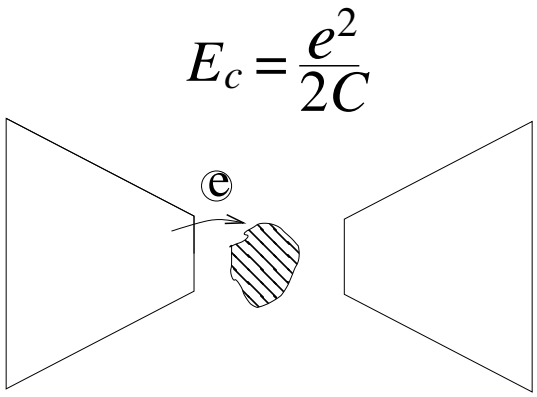

Fig. 11.1. The transfer of one electron from the reservoir to the granule changes its charge by $1e$, which is accompanied by a change in the energy of the entire system by $E_c = e^2/2C$„ where C is the electric capacitance of the granule.

ple charge by 1e, Fig. 11.1. This energy is nothing other than the electrostatic energy E_c, due to the sample's own capacitance C:

$$E_c = \frac{e^2}{2C}\,. \tag{11.1}$$

The capacitance of a spherical sample with radius R is $C = 4\pi\epsilon_0\epsilon R$, and for a sample in the form of a disk $C = 8\epsilon_0\epsilon R$. Here ϵ is the dielectric permittivity of the medium. The constant ϵ_0 is as follows: $\epsilon_0 = 8,85 \times 10^{-12}\ C^2/(Nm^2)$. For characteristics values $R \sim 10^{-6}$ m and $\epsilon \sim 10$, we obtain $C \sim 10^{-15}$ F. The corresponding electrostatic energy is:

$$E_c = \frac{(1,6 \times 10^{-19})^2}{2 \times 10^{-15} 1,38 \times 10^{-23}}\ \mathrm{C}^2/(\mathrm{F\,J/K}) \sim 1\,\mathrm{K}\,.$$

This means that when the ambient temperature is less than 1 K, the charge Q of such a sample will not fluctuate, but will be fixed. If a voltage is applied to the pellet, no current will flow, since for the current to flow, electrons must pass to the pellet. However, such a transition is impossible, since it would lead

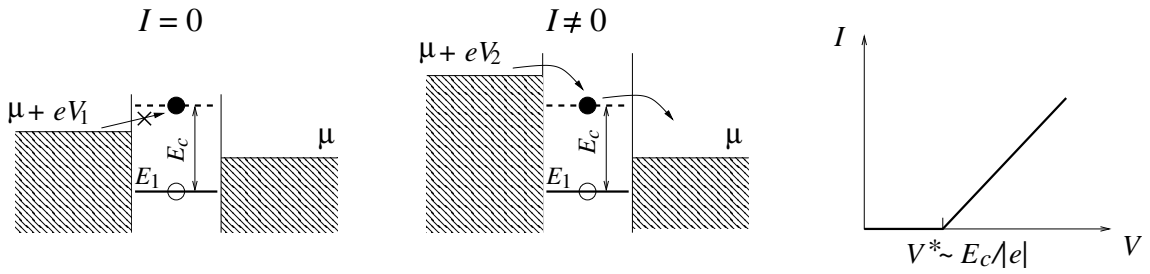

Fig. 11.2. The change in the energy of the system by E_c during the transition of the electron from the reservoir to the granule leads to the fact that the current $I \neq 0$ appears in the system only when $V > V^*$. The threshold voltage $|eV^*| \sim E_c$

to a change in the charge of the pellet. Only if a considerable voltage is applied

$$V > V^* \sim \frac{E_c}{|e|} \sim 0,8 \times 10^{-3}\ \mathrm{V}\,,$$

then the current will flow through the granule, since the source will be able to perform work against the electrostatic forces that prevent the electron from passing to the granule, Fig. 11.2. This is actually the effect of Coulomb blockade. Namely, at low temperatures the granule becomes conductive only starting from a certain threshold voltage

$$|eV^*| \sim E_c\,.$$

Next, we will analyze the requirement that the charge on the granule remains constant for a sufficiently long time. Why is this necessary? Above, we analyzed the possibility of an electron's transition to the granule, considering the electron as a classical, not a quantum particle. However, from the point of view of quantum mechanics, an electron can tunnel to the granule, stay there for some time δt, and then leave the granule. The electron can either return to the contact from which it initially tunnelled to the granule, or move to the other contact and thereby take part in the transfer of current through the granule. These are the so-called quantum fluctuations of the charge on the granule. For such virtual processes, there is no need to overcome the electrostatic barrier,

since the law of conservation of energy must be fulfilled only for the energies in the initial and final states, when the charge on the granule is absent and, accordingly, there is no electrostatic energy due to this charge. For intermediate, virtual states that exist for a short time δt, when the electron is on the granule and, as a consequence, electrostatic energy appears, the law of conservation of energy must not be fulfilled. More precisely, the law of conservation of energy is fulfilled with an accuracy of the order of δE. This quantity is related to δt by the Heisenberg uncertainty relation for energy-time:

$$\delta E \, \delta t \geq h \,, \tag{11.2}$$

where h is Planck's constant. If the energy uncertainty δE is less than the electrostatic energy E_c associated with the appearance of an electron charge on the granule,

$$\delta E \sim \frac{h}{\delta t} < E_c \,, \tag{11.3}$$

then the process of electron tunneling through the granule, in other words, the process of tunneling through a virtual electrostatic potential barrier, turns out to be impossible. If

$$\delta E \gg E_c \,,$$

then tunneling is possible.

For the occurrence of Coulomb blockade, it is necessary that the uncertainty of the energy δE be small compared to E_c. For this, it is necessary that the time δt, during which the electron is on the granule, be large. This time is in the order of magnitude equal to the time of charging or discharging the granule. It (time) is determined by the electrical characteristics - the capacitance C and the resistance of the tunnel barrier R_t between the contact (conductor) and the granule:

$$\delta t \sim R_t \, C \,.$$

Substituting this estimate into equation (11.3), we obtain a constraint on the resistance of the tunneling contact separating the granule from the environment, at which tunneling is impossible (i.e., at which $\delta E \ll E_c$):

$$R_t > \frac{h}{e^2} \approx 25,8 \times 10^3 \ \Omega \,. \tag{11.4}$$

Thus, in order for the effects associated with the discreteness of the electron charge to manifest themselves in the conductance of the granule, first, low temperatures are necessary,

$$T \ll E_c \,,$$

to avoid classical (thermal) over-barrier jumps and, secondly, considerable tunnel contact resistances to avoid jumps due to quantum tunneling,

$$\delta E \ll E_c \,.$$

Below, we will assume that both of these conditions are met, which will allow us to conduct a qualitative, semi-classical analysis of the influence of charge discreteness on the electrical conductance of the granule.

11.2. Coulomb blockade of an electron transport

Consider a granule connected by tunnel barriers to the left and right contacts. The conductance of the granule is proportional to the probability of an electron passing from the left contact to the right. In this case, this is the probability of tunneling through a double potential barrier. One potential barrier separates the granule from the left contact and the second potential barrier separates the granule from the right contact. We will assume that the granule is so small that it is necessary to take into account the quantization of the electron energy levels in the granule. In this case, we will assume that the temperature is zero.

11.2.1. Transport at resonance tunneling

First, we consider the conductance of the granule without taking into account the influence of the electrostatic energy E_c. Recall that the conductance, defined as the ratio of the current to the applied voltage at $V \to 0$, is due to the transfer of electrons with the Fermi energy through the sample. For such electrons, the tunneling probability will be maximum in the case when the Fermi level coincides with one of the quantum levels of the electrons in the granule. This corresponds to the condition of resonant tunneling. In the case of identical left and right tunneling barriers, the tunneling probability T near resonance can be represented by the following Breit–Wigner formula [7]:

$$\mathcal{T} = \frac{\Gamma^2}{\Gamma^2 + (\mu - E_0)^2}\,, \tag{11.5}$$

where Γ is the half-width of the resonance; E_0 is the value of the energy level in the granule, which is closest to the chemical potential μ of the electrons in the reservoir. The value of Γ is proportional to the probability of tunneling through a unit potential barrier.

From the equation (11.5) it is clear that the tunnel transparency $\mathcal{T}$, and with it the conductance of the granule $G = G_0\mathcal{T}$, depend on the difference $\mu - E_0$. In the general case, this difference can be arbitrary and vary from sample to sample. However, modern experimental techniques allow not only to bring the contacts to an individual granule of micron dimensions, but also to change the parameters of the granule. In particular, by using an additional metal contact that forms a capacitor with the granule, it is possible to change the potential of the granule V_g with respect to the contacts. In this case, the energy of each level in the granule will be shifted by the value eV_g, so the conductance of the granule will depend on V_g:

$$G(V_g) = G_0 \sum_n \frac{\Gamma_n^2}{\Gamma_n^2 + (\mu - E_n - eV_g)^2}\,. \tag{11.6}$$

Here, the summation is performed over all quantum levels in the granule. For each level, we have written down its Γ_n, since the tunneling probability depends on the energy and can be different for different energy levels.

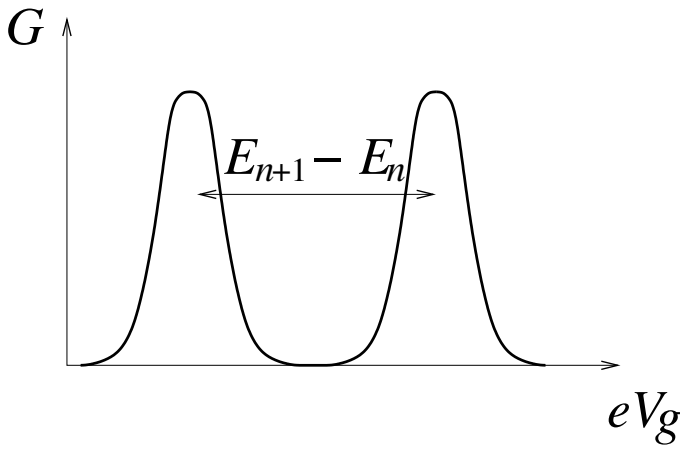

Fig. 11.3. Without taking into account the Coulomb blockade effect, the dependence of the conductance G of a sample with a discrete spectrum on the sample potential V_g at zero temperature has a resonant character. The distance between the peaks is determined by the distance between the energy levels in the sample.

Let us consider the dependence $G(V_g)$. This dependence will have the form of a set of peaks located at the following voltages:

$$eV_{g,n} = \mu - E_n \,. \tag{11.7}$$

The distance between the conductance peaks will be determined by the distance between the energy levels in the granule, Fig. 11.3.

Thus, by studying the conductance, it is possible to determine the energies of the quantum levels in the granule, i.e., to perform quantum level spectroscopy. In this case, the difference between the voltages on the screen V_g, which correspond to the peaks of the dependence $G(V_g)$, is equal to the distance between the quantum levels in the granule:

$$-(eV_{g,n+1} - eV_{g,n}) = E_{n+1} - E_n \equiv \Delta E_n \,. \tag{11.8}$$

It should also be said that to use this method, it is necessary that the temperature and voltage between the contacts are significantly smaller than the distance between the peaks ΔE_n:

$$\Delta E_n \gg k_B T|eV|\,.$$

We have described the picture of resonant tunneling without taking into account the fact that the electron charge is finite. Now we will consider how the effect of Coulomb blockade modifies the dependence of $G(V_g)$.

11.2.2. Coulomb blockade of transport

When we take into account the energy associated with the charge of the granule, we are actually taking into account the energy due to the Coulomb interaction of electrons between themselves and with other charged particles. An accurate account of these interactions requires consideration of the many-particle Schrödinger equation and is a rather difficult task. At least, it can be argued that in this case the single-particle energy levels E_n calculated in the model of non-interacting electrons that we have used so far cannot be used to adequately characterise the transport properties.

However, there is an approximation that has proven itself well. It consists in the fact that the influence of electrostatic interaction is taken into account by introducing additional energy, which depends on the total number of electrons in the granule. In this model, the energies of single-particle levels depend on the number of electrons N_e in the granule. This dependence is defined as follows. Let $E_n(N_e)$ be the single-particle energy levels in a granule with N_e excess electrons. Excess electrons are those electrons whose charge is not compensated by the charge of the granule ions. Then the energy levels in a granule with $N_e + 1$ electron will be defined by the following equation:

$$E_n(N_e + 1) = E_n(N_e) + E_c(N_e + 1) - E_c(N_e)\,. \tag{11.9}$$

Here, the electrostatic energy E_c of the system depends on the charge of the

granule, i.e., on the number of electrons Ne in the granule, and on the potential V_g of the granule, which can be changed using a metal screen:

$$E_c(N_e) = \frac{(eN_e)^2}{2C} + eN_eV_g\,. \tag{11.10}$$

Substituting this equation into the equation (11.9), we obtain

$$E_n(N_e+1) = E_n(N_e) + \frac{e^2}{C}(N_e+1/2) + eV_g\,. \tag{11.11}$$

Let us consider how the presence of electrostatic energy changes the conditions for the resonant transfer of electrons through the granule. Let the voltage on the screen V_g correspond to the resonance condition, (11.7), without taking into account the electrostatic energy $eV_{g,n} = \mu - E_n$. What will happen in this case? It seems that the electron should move to the granule and fill the level E_n. But this does not happen. Why? Because when the electron moves to the granule, the electrostatic energy $E_c \sim e^2/(2C)$ will arise, which will shift the position of the energy levels in the granule relative to the chemical potential and, thereby, violate the resonance condition. It follows that the correct resonance condition must take into account the change in the electrostatic energy of the system when the number of electrons on the granule changes. Considering the above, the condition for resonant tunneling in the presence of the Coulomb blockade effect is the following

$$E_n(N_e+1) = \mu\,. \tag{11.12}$$

Using the equations (11.9) and (11.11), we obtain:

$$E_n(N_e) + \frac{e^2}{C}(N_e+1/2) + eV_{g,n} = \mu\,. \tag{11.13}$$

Thus, the value of the voltage on the screen at which the conductance of the granule has a resonant peak will be as follows:

$$-eV_{g,n} = E_n(N_e) - \mu + \frac{e^2}{C}(N_e + 1/2)\,. \tag{11.14}$$

The following resonance will occur if the voltage across the screen is:

$$-eV_{g,n+1} = E_{n+1}(N_e + 1) - \mu + \frac{e^2}{C}(N_e + 3/2)\,. \tag{11.15}$$

Note that the number of electrons in the granule has changed after the previous resonance and is equal to $N_e + 1$. The distance between the resonance peaks in the $G(V_g)$ dependence will be as follows:

$$-(eV_{g,n+1} - eV_{g,n}) = E_{n+1}(N_e + 1) - E_n(N_e) + \frac{e^2}{C}\,. \tag{11.16}$$

Comparing the equation (11.16) with the equation (11.8), we see that taking into account the electrostatic energy changes the distance between the peaks. If the electric capacitance C is sufficiently small and, accordingly, the electrostatic capacitance e^2/C is sufficiently large, then the distance between the conductance peaks does not depend on the location of the energy levels E_n of the electrons in the granule and is determined only by the electrostatic energy E_c, Fig. 11.4.

Thus, depending on the ratio between ΔE_n and $E_c = e^2/(2C)$, the study of resonant tunneling allows either to investigate the quantum energy levels of the electrons in the granule, or to measure the electric capacitance of the granule:

$$-(eV_{g,n+1} - eV_{g,n}) = \begin{cases} E_{n+1} - E_n & C \to \infty\,, \\ \dfrac{e^2}{C}, & C \to 0\,. \end{cases} \tag{11.17}$$

Let us compare ΔE_n (when $E_n \sim \mu$) and E_c for a two-dimensional disk-shaped granule with diameter L:

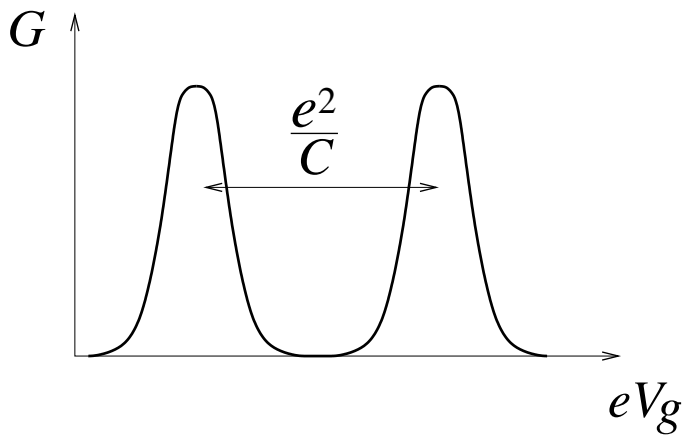

Fig. 11.4. For samples with a small size and, accordingly, a small electric capacitance $C \to 0$, the change in the electrostatic energy $E_c \sim e^2/C$, which is associated with the change in the sample charge during the tunneling of a single electron, becomes significant and, in fact, replaces the energy due to spatial quantization. For such samples, the effect of Coulomb blockade leads to the fact that the distance between the positions of the resonances in the dependence $G(V_g)$ is determined by the energy E_c

$$\Delta E_n = \frac{h^2}{4\pi m^* L^2}\,,$$

$$E_c = \frac{e^2}{C} = \frac{e^2}{4\epsilon\epsilon_0 L}\,.$$

We see that as the granule size decreases, the distance between quantum levels ΔE_n grows faster than the electrostatic energy E_c. The energies ΔE_n and E_c become of the same order for such a length:

$$L_c \sim \frac{h^2\epsilon\epsilon_0}{\pi m^* e^2} = 7,9 \times 10^{-9}\,\mathrm{m}\,,$$

where we set $\epsilon = 10$ $m^* = 0,067\, m_e$.

In sufficiently small granules, for which $L < L_c$, the electrostatic energy E_c can be ignored. Note that the value of L_c is still larger than atomic dimensions $\sim 10^{-10}$ m, at which this approximation loses its meaning.

In granules of larger dimensions, for which $L > L_c$, the electrostatic energy exceeds the spatial quantization energy, and therefore it is the value of E_c that determines the experimentally measured dependence of the conductance G on the voltage on the barrier V_g. However, even in this case, the position of the quantum levels E_n can be determined from the experimental data. For this purpose, as follows from the equation (11.16), it is necessary to study the violation of equidistance in the position of the peaks on the graph of the dependence of the sample conductance on the potential V_g.

Self-test questions

1. What is the Coulomb blockade effect?
2. How does the magnitude of the electrostatic energy change when the size of the sample decreases?
3. What conditions are necessary to create the Coulomb blockade effect?
4. Describe the mechanism of current flow through a sample with a small electrical capacitance.
5. What is the difference between current flow during resonant tunneling and when the Coulomb blockade effect exists?

References

[1] Imry Y. Physics of mesoscopic systems / Y. Imry. In: Directions in Condensed Matter Physics, G. Grinstein and G. Mazenco (Eds.).– Singapore: World Scientific, 1986.– P. 101–163. 6, 35, 58

[2] Imry Y. Introduction to Mesoscopic Physics / Y. Imry.– New York Oxford: Oxford University Press, 2002. 6

[3] van Kampen N. G. In: Statistical Physics, Proceedings of the IUPAP International Conference, L. Pel and Szepflanszy (Eds.).– Amsterdam: North-Holland, 1976. 9

[4] Yanson I.K. Atlas of microcontact spectra of electron-phonon interaction in metals / I.K. Yanson, A.V. Khotkevich. – K.: Naukova Dumka, 1986.– 144 p. 17

[5] Omelyanchuk A. N. On the theory of nonlinear effects in the electrical conductivity of metal bridges / A. N. Omelyanchuk, I. O. Kulik, R. I. Shekhter // Letters to JETP.– 1977.– V. 25, N 10.– p 465–469. 17

[6] Landau L. D. Statistical Physics. Part 1 / L. D. Landau, E. M. Lifshitz. – M.: Nauka, GRFML, 1976.– 583 p. 33, 35

[7] Landau L. D. Quantum Mechanics. Non-relativistic Theory / L. D. Landau, E. M. Lifshitz. – M.: GIFML, 1963.– 702 p. 74, 89, 133, 166

[8] Aprikosov A. A. Fundamentals of the theory of metals / A. A. Aprikosov. - M.: Nauka, GRFML, 1987.– 520 p. 40, 45, 122

[9] Landauer R. Electrical resistance of disordered one-dimensionaled lattices / R. Landauer // Phil. Mag.– 1970.– V. 21.– P. 863. 47

[10] Aharonov Y. Significance of electromagnetic potentials in the quantum theory / Y. Aharonov, D. Bohm // Phys. Rev.– 1959.–V.115.–P. 485–491. 59, 141

[11] Chambers R. G. Shift of an electron interference pattern by enclosed magnetic flux / R.G. Chambers // Phys.Rev.Lett.– 1960.– V. 5.– P. 3–5. 62

[12] Little W. A. Observation of quantum periodicity in the transition temperature of a superconducting cylinder / W. A. Little, R. D. Parks // Phys. Rev. Lett.– 1962.– V. 9.– P. 9–12. 66

[13] London F. Superfluids. Volume 1 / F. London.– N.Y.: John Wiley and Sons, 1950. 66

[14] Altshuler B. L. Aharonov–Bohm effect in disordered wires days / B. L. Altshuler, A. G. Aronov, B. Z. Spivak // Letters to JETP.– 1981.– V. 33, N 2.– p. 101–103. 66

[15] Sharvin D. Yu. Quantization of magnetic flux in a cylindrical film of normal metal / D. Yu. Sharvin, Yu. V. Sharvin // Letters to JETP.– 1981.– V. 34, N 5.– p. 285–288. 66

[16] Hund F. Rechnungen über das magnetische Verhalten von kleinen Metallstücken bei tiefen Temperaturen / F. Hund // Annalen der Physik (Leipzig).– 1938.– V. 424, N 1–2.– P. 102–114. 66, 141

[17] Dingle R. B. Some Magnetic Properties of Metals. IV. Properties of Small Systems of Electrons / R. B. Dingle // Proceedings of the Royal Society of London. Series A, Mathematical and Physical Sciences.– 1952.– V. 212, N 1108.– P. 47. 66, 141

[18] Büttiker M. Quantum oscillations in one-dimensional normal-metal rings / M. Büttiker, Y. Imry, M. Ya. Azbel // Phys. Rev. A.– 1984.– V. 30.– P. 1982–1989. 66

[19] Webb R. A. Observation of h/e Aharonov–Bohm Oscillations in Normal-Metal Rings / R. A. Webb, S. Washburn, C. P. Umbach, R. B. Laibowitz // Phys. Rev. Lett.– 1985.– V. 54, N 25.– P. 2696–2699. 67

[20] Chandrasekhar V. Observation of Aharonov–Bohm Electron Interference Effects with Periods h/e and h/2e in Individual Micron-Size, Normal-Metal

Rings / V. Chandrasekhar, M. J. Rook, S. Wind, D. E. Prober // Phys. Rev. Lett.– 1985.– V. 55, N 15.– P. 1610–1613. 67

[21] Griffith J. S. A free-electron theory of conjugated molecules. Part 1.– Polycyclic hydrocarbons, // Trans. Faraday. Soc.– 1953.– V. 49.– P. 345–351. 77

[22] Ford C. J. B. Gated asymmetric rings as tunable electron interferometers / C. J. B. Ford, A. B. Fowler, J. M. Hong, C. M. Knoedler, S. I. Laux, J. J. Wainer, S. Washburn // Surf. Science.– 1990.– V. 229.– P. 307–317. 83

[23] Büttiker M. Generalized many-channel conductance formula with application to small rings / M. Büttiker, Y. Imry, R. Landauer, S. Pinhas // Phys. Rev. B.– 1985.– V. 31, N 10.– P. 6207–6215. 108

[24] Wharam D. A. One-dimensional transport and the quantization of the ballistic resistance / D. A. Wharam, T. J. Thornton, R. Newbury, M. Pepper, H. Ahmed, J. E. F. Frost, D. G. Hasko, D. C. Peacock, D. A. Ritchie, G. A. C. Jones // J. Phys. C.: Solid State Phys.– 1988.– V. 21, N 8.– P. L209–L214. 121

[25] van Wees B. J. Quantized Conductance of Point Contacts in a Two-Dimensional Electron Gas / B. J. van Wees, H. van Houten, C. W. J. Beenakker, J. G. Williamson, L. P. Kouwenhoven, D. van der Marel, C. T. Foxon // Phys. Rev. Lett.– 1988.– V. 60, N 9.– P. 848–850. 121

[26] Kulik I. O. Quantization of flux in normal metal / I. O. Kulik // Letters to JETP.– 1970.– V. 11, N 8.– p. 407–410. 124

[27] Büttiker M. Josephson behavior in small normal one-dimensional ring / M. Büttiker, Y. Imry, R. Landauer // Phys. Lett. A.– 1983.– V. 96, N 7.– P. 365–367. 124

[28] Levy L. P. Magnetization of mesoscopic cooper rings: evidence for persistent currents / L. P. Levy, G. Dolan, J. Dunsmuir, H. Bouchiat // Phys. Rev. Lett.– 1990.– V. 64, N 17.– P. 2074–2077. 124

[29] Chandrasekhar V. Magnetic response of a single, isolated gold loop / V. Chandrasekhar, R. A. Webb, M. J. Brady, M. B. Ketchen, W. J. Gallagher, A. Kleinsasser // Phys. Rev. Lett.– 1991.– V. 67, N 25.– P. 3578–3581. 124

[30] Mailly D. Experimental observation of persistent currents in a GaAs–AlGaAs single loop / D. Mailly, C. Chapelier, A. Benoit // Phys. Rev. Lett.– 1993.– V. 70, N 13.– P. 2020–2023. 124

[31] Kulik I. O. Kinetic phenomena and effects of charge discreteness in a granular medium / I. O. Kulik, R. I. Shekhter // JETP.– 1975.– V. 68, N 2.– p. 623–640. 161

[32] Averin D. V. Single electronics: a correlated transfer of single electrons and Cooper pairs in system of small tunnel junctions / D. V. Averin, K. K. Likharev // in Mesoscopic Phenomena in Solids, B. Altshuler, P. A. Lee, R. A. Webb (Eds.), Elsevier, Amsterdam.– 1991.– P. 173–272. 161

[33] Kastner M. A. The single-electron transistor / M. A. Kastner // Rev. Mod. Phys.– 1992.– V. 64, N 3.– P. 849–858. 161

[34] Giaever I. Superconductivity of Small Tin Particles Measured by Tunneling / I. Giaever, H. R. Zeller // Phys. Rev. Lett.– 1968.– V. 20, N 26.– P. 1504–1507. 161

[35] Lambe J. Charge-Quantization Studies Using a Tunnel Capacitor / J. Lambe, R. C. Jaclevic // Phys. Rev. Lett.– 1969.– V. 22, N 25.– P. 1371–1375. 161